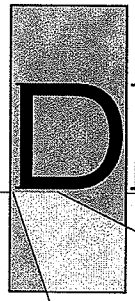

Innovations Deserving
Exploratory Analysis Programs

Highway IDEA Program

Liquefaction Mitigation Using Vertical Composite Drains: Full Scale Testing

Final Report for Highway IDEA Project 94

Prepared by:
Kyle M. Rollins, Brigham Young University, Provo, UT

February 2004

TRANSPORTATION RESEARCH BOARD
OF THE NATIONAL ACADEMIES

INNOVATIONS DESERVING EXPLORATORY ANALYSIS (IDEA) PROGRAMS
MANAGED BY THE TRANSPORTATION RESEARCH BOARD (TRB)

This NCHRP-IDEA investigation was completed as part of the National Cooperative Highway Research Program (NCHRP). The NCHRP-IDEA program is one of the four IDEA programs managed by the Transportation Research Board (TRB) to foster innovations in highway and intermodal surface transportation systems. The other three IDEA program areas are Transit-IDEA, which focuses on products and results for transit practice, in support of the Transit Cooperative Research Program (TCRP), Safety-IDEA, which focuses on motor carrier safety practice, in support of the Federal Motor Carrier Safety Administration and Federal Railroad Administration, and High Speed Rail-IDEA (HSR), which focuses on products and results for high speed rail practice, in support of the Federal Railroad Administration. The four IDEA program areas are integrated to promote the development and testing of nontraditional and innovative concepts, methods, and technologies for surface transportation systems.

For information on the IDEA Program contact IDEA Program, Transportation Research Board, 500 5th Street, N.W., Washington, D.C. 20001 (phone: 202/334-1461, fax: 202/334-3471, http://www.nationalacademies.org/trb/idea)

The project that is the subject of this contractor-authored report was a part of the Innovations Deserving Exploratory Analysis (IDEA) Programs, which are managed by the Transportation Research Board (TRB) with the approval of the Governing Board of the National Research Council. The members of the oversight committee that monitored the project and reviewed the report were chosen for their special competencies and with regard for appropriate balance. The views expressed in this report are those of the contractor who conducted the investigation documented in this report and do not necessarily reflect those of the Transportation Research Board, the National Research Council, or the sponsors of the IDEA Programs. This document has not been edited by TRB.

The Transportation Research Board of the National Academies, the National Research Council, and the organizations that sponsor the IDEA Programs do not endorse products or manufacturers. Trade or manufacturers' names appear herein solely because they are considered essential to the object of the investigation.

ABSTRACT

Liquefaction has typically been mitigated by in-situ densification; however, this is often time-consuming and expensive. In addition, in-situ densification is difficult to accomplish when sands contain fines. Vertical composite earthquake (EQ) drains offer the possibility of preventing liquefaction and associated settlement while reducing the cost and time required for treatment. To evaluate the behavior of these drains under full-scale conditions, controlled blasting techniques were employed to liquefy loose sand at a test site in Vancouver, British Columbia. The soil profile contained a liquefiable clean sand layer from 6 to 13 m below the ground surface.

A blast liquefaction test was first performed on an untreated site and then the same explosive charge sequence was used on two sites treated with earthquake drains. At one drain test area, drains were installed with a pipe mandrel in a manner to effect as little soil densification as possible. At a second area, drains were installed with a finned mandrel using high vibration designed to produce soil densification. Very little settlement was produced in the first area, but significant settlement (volumetric strains of 2.5%) was produced in the second area. Although settlement clearly showed densification, CPT soundings conducted 3 to 5 days after drain installation showed a 30 to 50% decrease in cone tip resistance.

Although the EQ Drains were insufficient to prevent initial liquefaction during the rapid loading produced by the blasts, the measured rate of dissipation was significantly greater at both drain test areas than in the untreated area. Dissipation rates were similar for both areas treated with drains. Despite the high pore pressures, the blast induced settlement in the first drain test area was only 60% of that in the untreated area. CPT soundings conducted over a two month period after blasting showed a 20 point increase in relative density for the layer where drains were installed with high vibration while a 10 point increase was produced where drains were installed with low vibration. This result indicates that both blast treatment and drain installation can produce significant increases in density.

With minor modifications in the input parameters, computer analyses performed using FEQDrain were successful in matching measured pore pressure and settlement response during the blasting. These calibrated models were then used to model response to a variety of earthquake events. The results indicate that the drains can prevent liquefaction and excessive settlement when drain diameter and spacing are properly designed for the expected earthquakes.

TABLE OF CONTENTS

ACKNOWLEDGEMENTS

Funding for this study was provided by a grant from the National Cooperative Highway Research Program-Ideas Deserving Exploratory Analysis (NCHRP-IDEA) program as project 94. This support is gratefully acknowledged. The conclusions from this study do not necessarily reflect the views of the sponsors.

We express our appreciation to the British Columbia Ministry of Transportation for allowing us to use the Vancouver test site. Nilex, Inc. donated all equipment, personnel and materials necessary to install the drains at the test site which made this project possible. Advanced Drainage Systems, Inc. donated the EQ-Drain pipes installed at the two test areas. ConeTec, Inc. provided equipment and personnel necessary to perform CPT soundings and install pore pressure transducers. In addition, they donated CPT time for performing post-blast soundings. These donations and contributions made this project feasible.

Prof. John Howie from the Civil Engineering Dept. at the University of British Columbia performed seismic cone testing at the site and supplied shear wave velocity profiles.

Dr. Blair Gohl of Pacific Geodynamics, Inc. provided data for the untreated test area at the Vancouver test site which provided a baseline for comparison of the drain behavior. This information is gratefully acknowledged. David Anderson, Civil & Environmental Engineering Department Technician at Brigham Young University, provided technical support and data acquisition services for this study and his vital contribution is appreciated.

LIST OF FIGURES

LIST OF TABLES

1.0 INTRODUCTION

One of the most destructive effects of earthquakes is the phenomenon known as liquefaction. When liquefaction occurs in loose saturated sands, the soil loses shear strength and temporarily acts as a liquid. Such temporary loss of shear strength can have catastrophic effects on earthworks or structures founded on these deposits. Liquefaction has resulted in significant damage to transportation systems in nearly every major earthquake event. For example, liquefaction resulted in nearly $1 billion worth of damage during the 1964 Niigata Japan earthquake (NRC, 1985), $99 million damage in the 1989 Loma Prieta earthquake (Holzer, 1998), and over $11.8 billion in damage just to ports and wharf facilities in the 1995 Kobe earthquake (EQE,1995).

Typically, liquefaction hazards have been mitigated by densifying the soil in-situ using techniques such as vibro-compaction, deep soil mixing, dynamic compaction, or explosives. While these techniques have generally proven effective in clean sands, they are not successful for sands with higher fines contents. In addition, these conventional methods are relatively costly and time-consuming. In an era when transportation construction budgets are becoming increasingly tight and projects are increasingly placed on fast-track schedules, innovative alternative solutions are required to deal with liquefaction hazards.

An alternative to densifying the sand is to provide drainage so that the excess pore water pressures generated by the earthquake shaking are rapidly dissipated thereby preventing liquefaction from occurring. The concept of using vertical gravel drains for liquefaction mitigation was pioneered by Seed and Booker (1977) who developed design charts that could be used to determine drain diameter and spacing. Improved curves which account for head losses were developed by Onoue (1988). Although gravel drains or stone columns have been utilized at many sites for liquefaction mitigation, most designers have relied on the densification provided by the stone column installation rather than the drainage. Some investigators suspect that significant settlement might still occur even if drainage prevents liquefaction. In addition, investigators have found that sand infiltration can reduce the hydraulic conductivity and flow capacity of gravel drains in practice relative to lab values (Boulanger et al, 1997).

One recent innovation for providing drainage is the Earthquake Drain (EQ-Drain) EQ Drains are vertical, slotted plastic drain pipes 75 to 150 mm in diameter. These drains are installed with a vibrating steel mandrel in much the same way that pre-fabricated vertical drains

(PVDs) are installed for consolidation of clays. The drains are typically placed in a triangular grid pattern at center-to-center spacings of 1 to 2 m depending on the permeability of the soil to be treated. In contrast to conventional PVDs, which have limited flow capacity (2.83×10^{-5} m^3/sec, for a gradient of 0.25), a 100 mm diameter drain can carry very large flow volumes (0.093 $m^{3/}$sec) sufficient to relieve water pressure in sands. This flow volume is more than 10 times greater than that provided by a 1 m diameter stone column (6.51×10^{-3} m^3/sec). Filter fabric tubes are placed around the drains to prevent infiltration of silt and sand. These vertical drains can be installed more rapidly and at a fraction of the cost of stone columns. For example, for a 12 m-thick layer, treatment with stone columns would typically cost \$107/m^2 of surface area and vibro-compaction would cost \$75/m^2, while the drains only cost \$48/m^2 (Nilex, 2002). In addition, the drains can be installed in about one-third to one-half of the time required to treat a profile using conventional means.

Although EQ-Drains have already been used at a few sites in the US, no installation has experienced an earthquake and this lack of field performance data is a major impediment to expanding the use of this technique. In addition, there is very little data available to indicate what degree of densification would be produced during drain installation and how this would improve overall performance. If field tests can prove the effectiveness of the drainage technique, significant time and cost savings can be achieved for both new construction and for retrofit situations. Drains could potentially be used to prevent liquefaction in sands with high fine contents which cannot be improved with conventional techniques; however, drain spacing would have to be closer than for clean sands. Drains could be placed in zones around deep foundations to prevent liquefaction and loss of skin friction or under shallow foundations to improve bearing capacity. Drains could also be placed in sections of a slope to prevent sliding or within loose backfill behind a quay wall to limit lateral movements.

Equipment for installing the drains can be easily developed with minor modifications to equipment that is already widely used by geotechnical specialty contractors. Therefore, the implementation of the method would be relatively simple once it is proven effective. In addition, simplified equations (Onuye, 1988) and computer programs (Pestana et al, 1997) are available to aid designers in selecting drain diameters and spacings if they can be validated by field performance testing.

1.1 INVESTIGATIVE APPROACH

As with all new techniques, full-scale verification of the theoretical principles involved is required before the method can be reliably used in practice. In the present case, verification is especially difficult because of problems in simulating large-scale earthquake effects. Rather than instrumenting a field site and waiting for an earthquake to test the drain behavior, we have used controlled blasting techniques to produce liquefaction under field conditions and compared behavior with and without vertical drains. The tests were carried out at site near the south portal of the Massey Tunnel which passes under the Fraser River in Vancouver, British Columbia, Canada as shown in Fig. 1. This site is within 220 meters of a Canadian Liquefaction experiment (CANLEX) test site where significant geotechnical investigations had previously been performed (Wride et al, 2000). The soil profile at this site contained a relatively uniform layer of saturated liquefiable clean sand located between 6 and 14 m below the ground surface suitable for the test program.

This test program had the following basic objectives:

1. To evaluate the ability of vertical drains to dissipate excess pore pressures and reduce liquefaction-induced settlement under full-scale conditions.
2. To distinguish improvement due to densification versus drainage.
3. To provide case histories that can be used to validate computer models for assessing the influence of drainage on liquefaction potential.

To accomplish these objectives, a blast liquefaction test was first performed on an untreated site and then the same explosive charge sequence was used on two sites treated with earthquake drains. At one drain test area, drains were installed with a pipe mandrel in a manner to effect as little soil densification as possible and at the second area, drains were installed with a vibrating mandrel designed to produce soil densification. Soil subsidence from drain installation at each area was measured. Cone penetration test (CPT) soundings were performed at each area before drain installation and immediately after installation. Data collected during the blasts included pore pressure response, settlement, and dynamic soil response. Additional CPT tests have been performed periodically at both EQ Drain blast sites since the blasts. This report provides details on geotechnical site characterization, EQ Drain test layout, drain installation procedures, results of the blast testing, analysis of the test data, and preliminary conclusions.

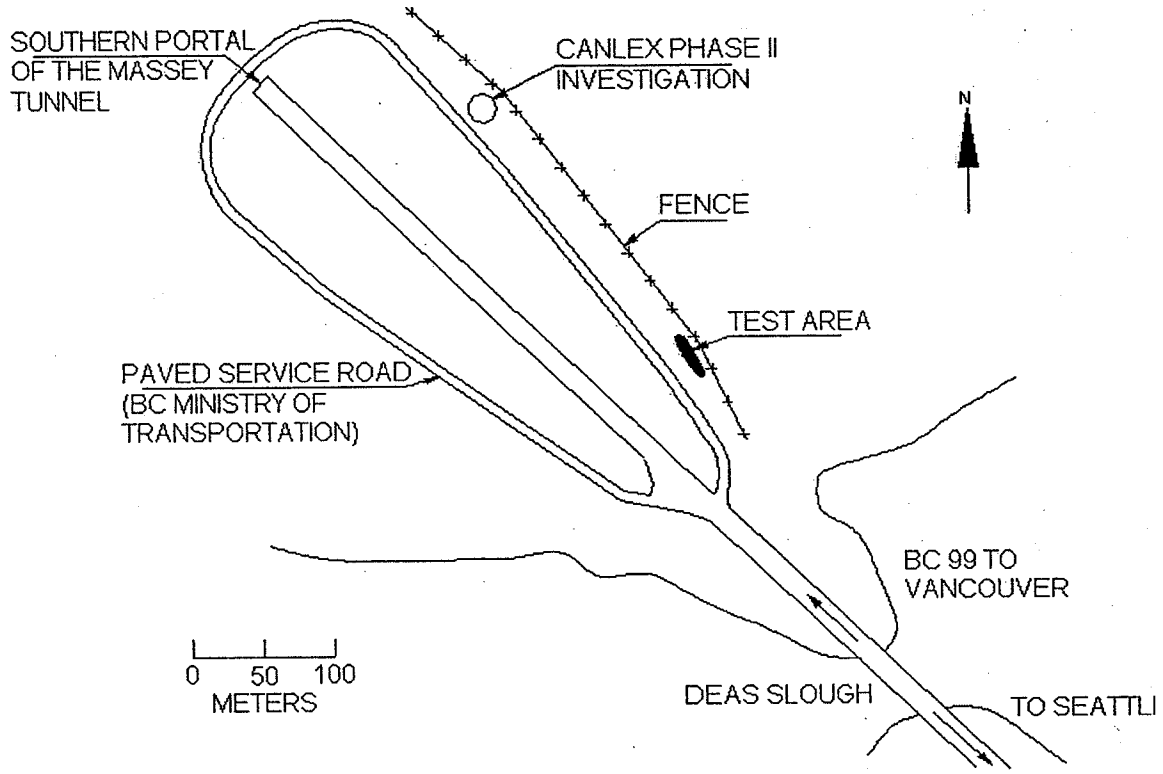

Figure 1 General location of the test area south of the Massey Tunnel Portal and CANLEX liquefaction research site near Vancouver, BC, Canada.

2.0 GEOTECHNICAL SITE CHARACTERIZATION

The site is located at the south end of the George Massey Tunnel on Deas Island along the eastern side of the right-of-way of Highway 99 as shown in Fig. 1. The centers of four blast areas (two used by Pacific Geodynamics for BC Ministry of Transportation tests and two for EQ Drain tests) lie between two BC Hydro power-line poles located along the fence bounding the east side of the site, as shown on Figure 2. The area is relatively flat lying and grass covered. The site is located approximately 220 m south of a test site used in the Canadian Liquefaction Experiment (CANLEX) as described by Wride (2000). The CANLEX site was extensively characterized using electronic cone penetration testing, standard penetration testing; shear wave logging and undisturbed soil sampling. The CANLEX information was used to provide a preliminary assessment of the stratigraphy at the blast sites, which was confirmed by subsequent cone penetration testing (Gohl, 2002).

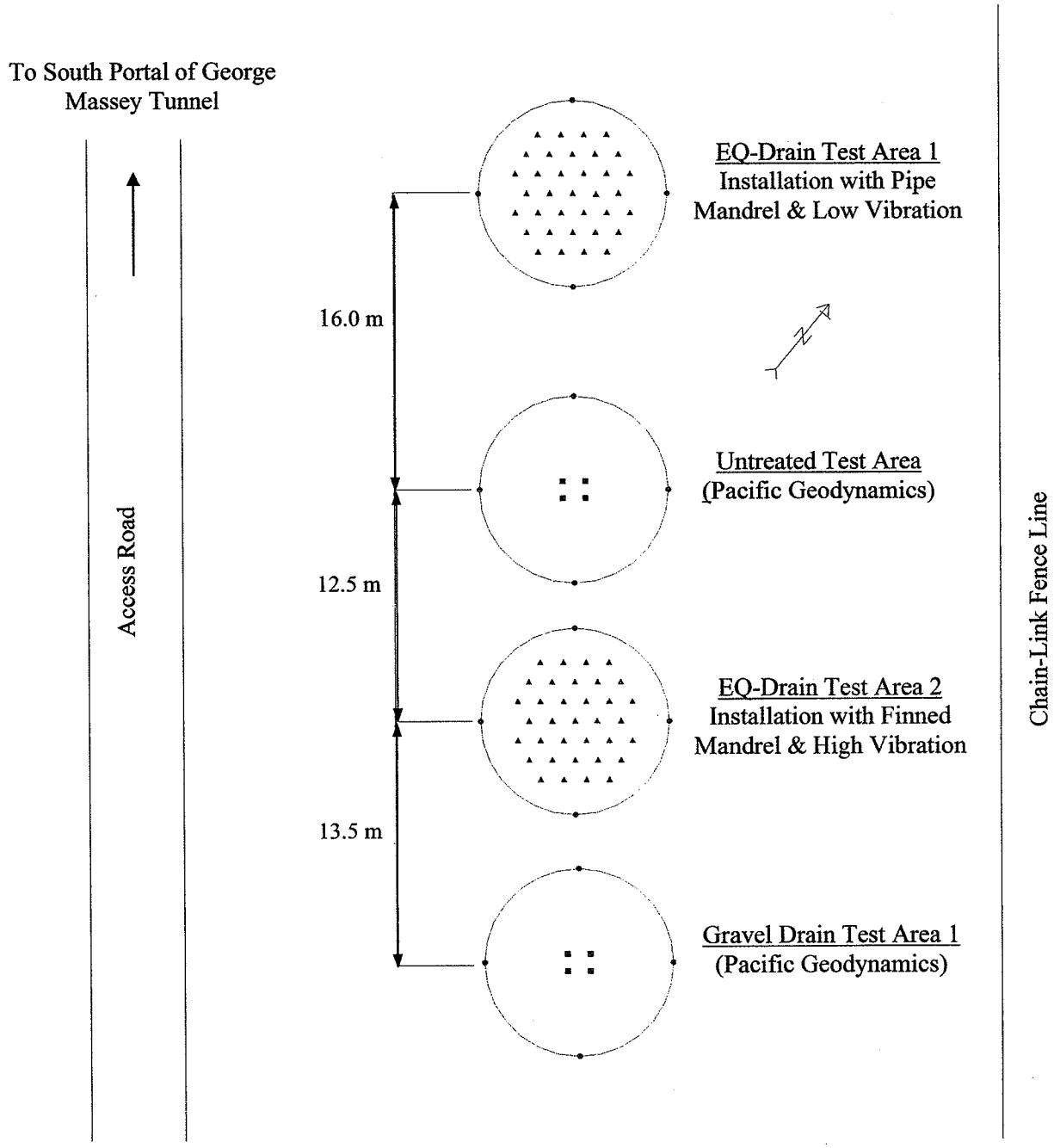

Figure 2 Location of blast liquefaction test areas at Vancouver, BC test site.

The soils in the upper 25 m of the site generally consist of naturally deposited alluvial sands that are approximately 200 years old (Mónahan et al, 1995). Geotechnical investigations consisted of cone penetration testing (CPT), shear wave velocity logging, and permeability testing. In

addition, some geotechnical properties could be approximated from previous testing at the adjacent CANLEX site.

2.1 CPT TESTING

Prior to drain installation at the test site, CPT soundings were performed using an electronic piezocone at the center of each test site in general accordance with ASTM D-3441. Results from the CPT soundings for the untreated area and the two drain test areas are shown in Figs. 3 through 5, respectively. CPT results consisted of cone tip resistance (q_c), friction ratio (f_r), and pore water pressure (u) recorded at 0.05 m depth intervals. Data for the CPT at the untreated test site was provided by Gohl (2002). Based on correlations developed by Robertson et al (1986) the soil behavior profile was interpreted at each site. The profile at all three sites is generally fairly similar and consists of a surface layer of sand to silty sand to an average depth of about 3 m, underlain by a layer of sand silt or silt from a depth of 3 to approximately 6 m. This silt layer is in turn underlain by a relatively clean sand layer from 6 to 15 m. This lower clean sand layer, particularly from 6 to 13 m in depth, was considered to be liquefiable and was the focus of the current study. Within this layer, the average cone tip resistance was typically about 6 MPa with a friction ratio of about 0.5%. Cone soundings at the CANLEX site indicate that the sand layer below 15 m becomes considerably denser.

The relative density, D_r, was estimated based on the CPT cone resistance using the equation

$$D_r = \left[\frac{\left(\frac{q_{c1}}{p_a} \right)}{305} \right]^{0.5} \qquad (1)$$

developed by Kulhawy and Mayne (1990) where p_a is atmospheric pressure and the sand is assumed to be normally consolidated and moderately compressible. The relative density computed using this equation is also shown as a function of depth for each site in Figs. 3 through 5. In the clean sand layer the relative density is typically between 40 and 45% and is relatively uniform with depth.

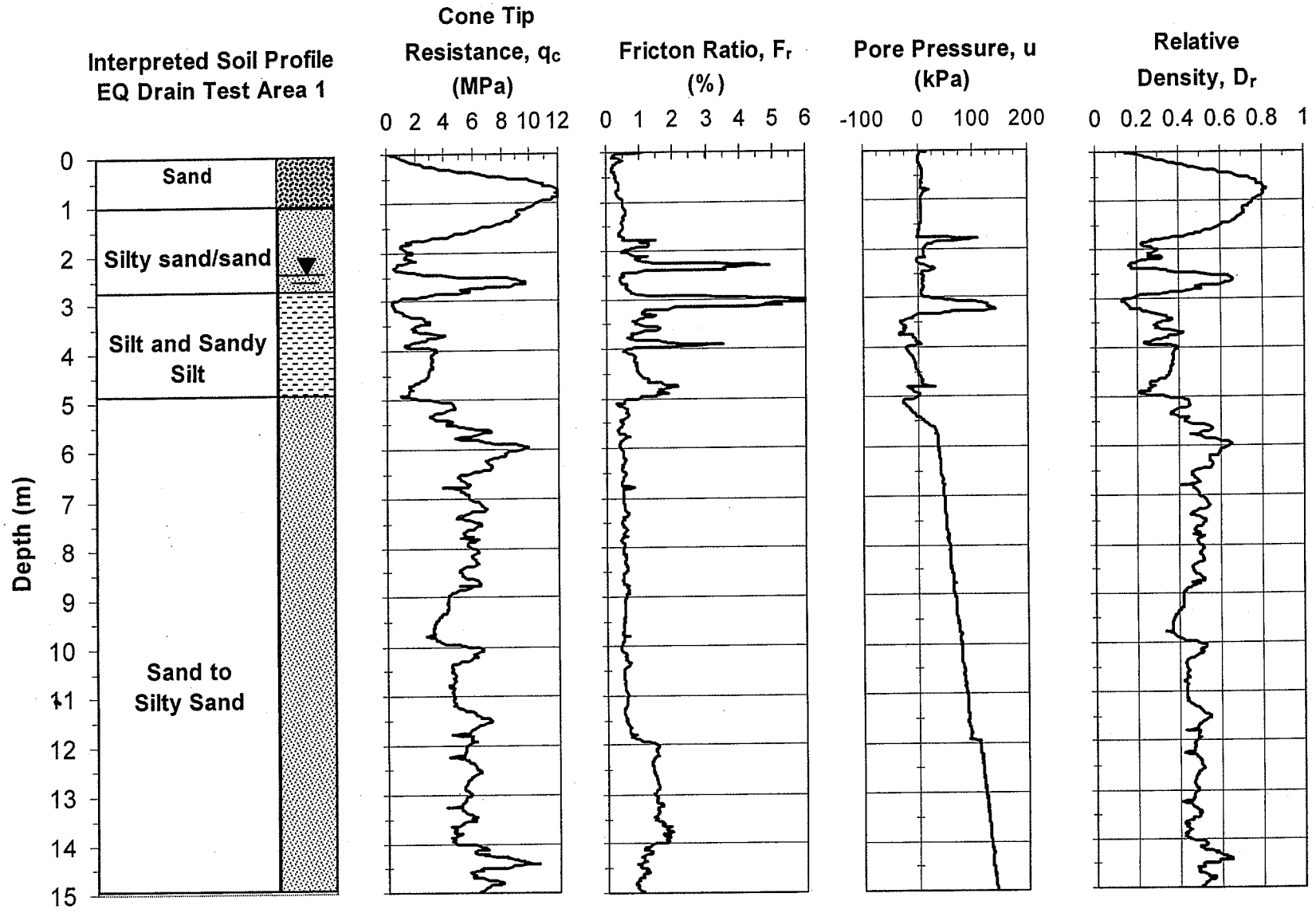

Figure 3 Results of CPT sounding at Untreated Test Area in Vancouver, BC along with interpreted soil profile and relative density profile (Gohl, 2002)

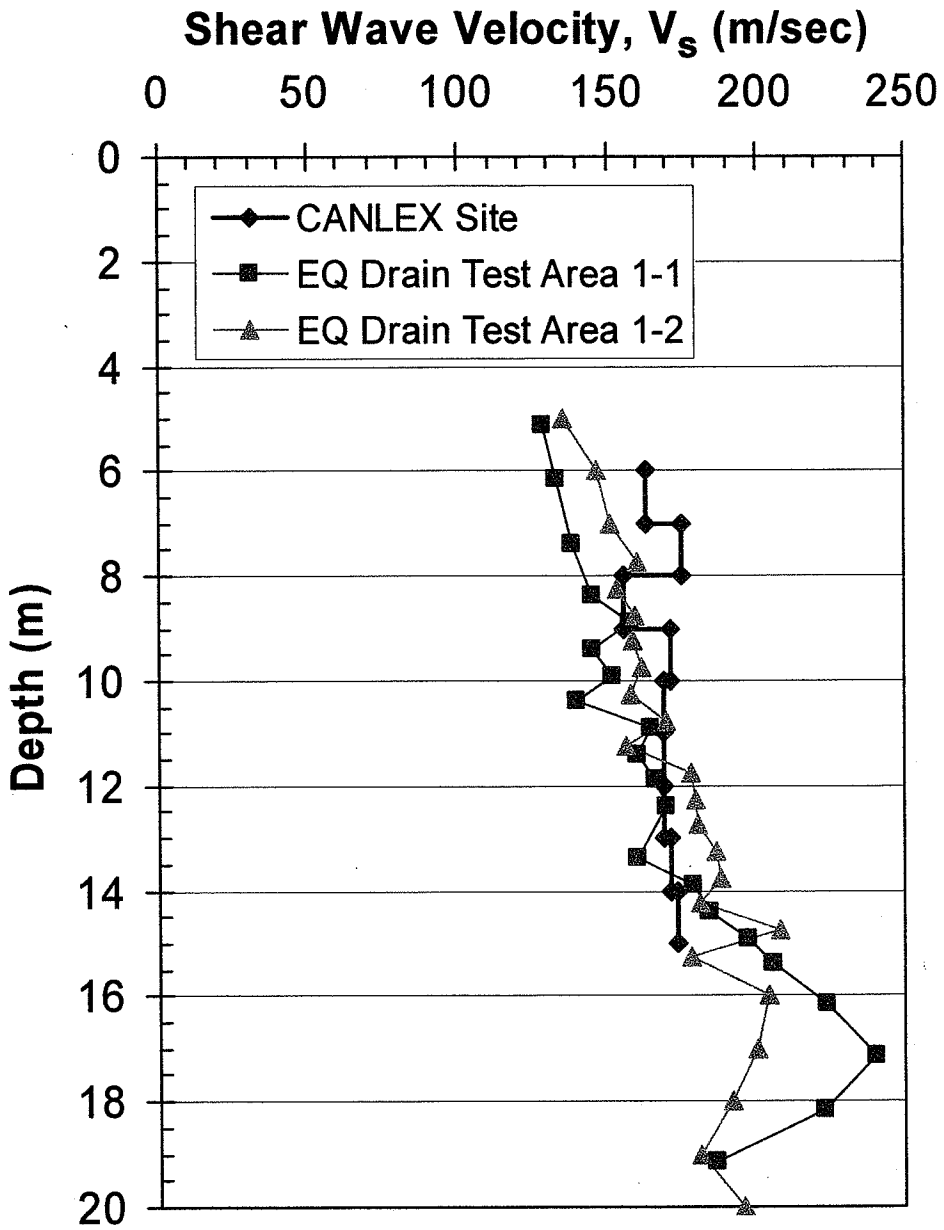

Figure 7 Measured shear wave velocity (V_s) as a function of depth (Howie, Personal Communication, 2002) along with data from adjacent CANLEX site (Wride et al, 2000).

was measured using a pressure gauge. These values were then used to compute the hydraulic conductivity. This test provided an indication of the variation of k_h with depth.

In addition to the packer tests, drawdown tests were also performed by pumping at one drain location and measuring the drawdown at two adjacent drains. The flow rate at the pumped drain was measured with a flow meter and the drawdown in the adjacent drains was measured using an electronic water level sensor. This test provides an overall average k_h within the pervious segment of the drain below the water table. A more detailed description of the test procedures and results are provided in the Appendix.

The k_h computed from the packer tests and the drawdown test are plotted as a function of depth in Fig. 8. The results from the packer tests suggest that k_h increases gradually with depth from a low of about $8x10^{-3}$ cm/sec at a depth of 4 m to a high of about $5x10^{-2}$ cm/sec at a depth of 11.5 m. The k_h in EQD Test Area 2 (finned-mandrel, high vibration) is somewhat higher than that in Area 1, which does not seem reasonable since the sand would likely be denser. However, the difference is relatively small and may be attributable to natural soil variation and measurement uncertainties. The k_h computed from the drawdown tests ($8x10^{-3}$ cm/sec) is somewhat lower than that from the packers test but certainly with the typical range of variation expected for hydraulic conductivity measurements.

The hydraulic conductivity interpreted from a CPT sounding performed at the CANLEX site by Conetec, Inc. (Weller, 2003, Personal Communication) is also shown in Fig. 8 for comparison purposes. The agreement between the k_h values obtained by the two methods is relatively good. The largest discrepancy occurs within the sandy silt layer, which appears to be a little thicker and to have a somewhat lower k based on the CPT sounding, than measured at the drain test site. The profile interpreted from the CPT sounding also indicates the presence of a few silt or sandy silt lenses within the clean sand layer with permeability coefficients which are two orders of magnitude lower than that in the clean sand. These thin, low permeability layers do not significantly affect the equivalent horizontal permeability of the layer; therefore, they do not show up in the test results from the borehole packer tests.

Overall, the results from the packer tests, drawdown test and CPT sounding are relatively consistent and provide relatively tight constraints on the values which should be used in the subsequent analyses.

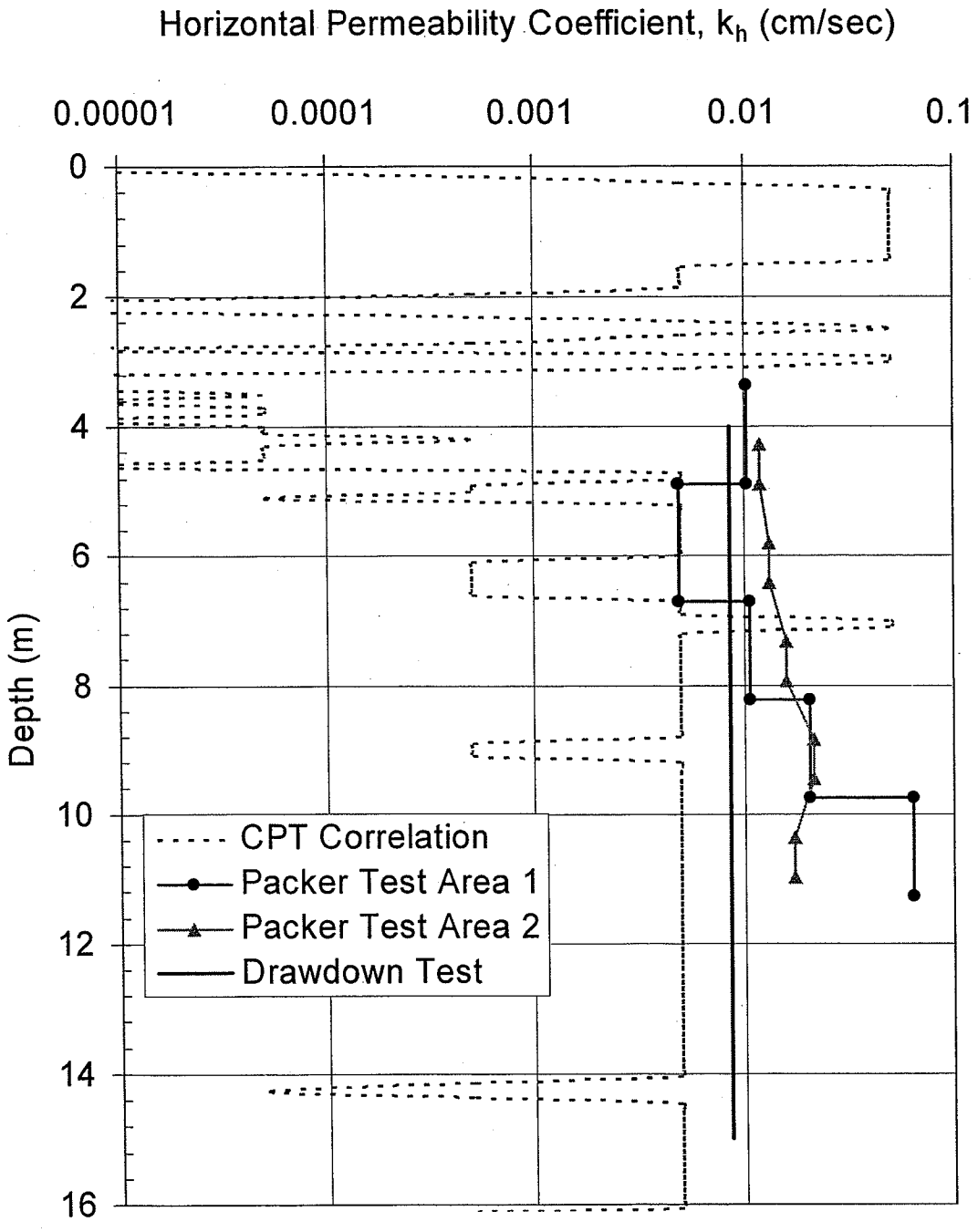

Figure 8 Horizontal hydraulic conductivity (k_h) as a function of depth measured in packer tests and drawdown tests along with values interpreted from CPT soundings at the adjacent CANLEX site (Weller, 2003, Personal Communication).

2.4 DATA FROM OTHER INVESTIGATIONS

Typical grain size distribution curve boundaries for Fraser River sands are shown in Fig. 9 based on work reported by Gohl (2002). Based on these curves the sands are poorly graded clean to silty fine sands and classify as SP or SP-SM materials according to the Unified Soil Classification System.

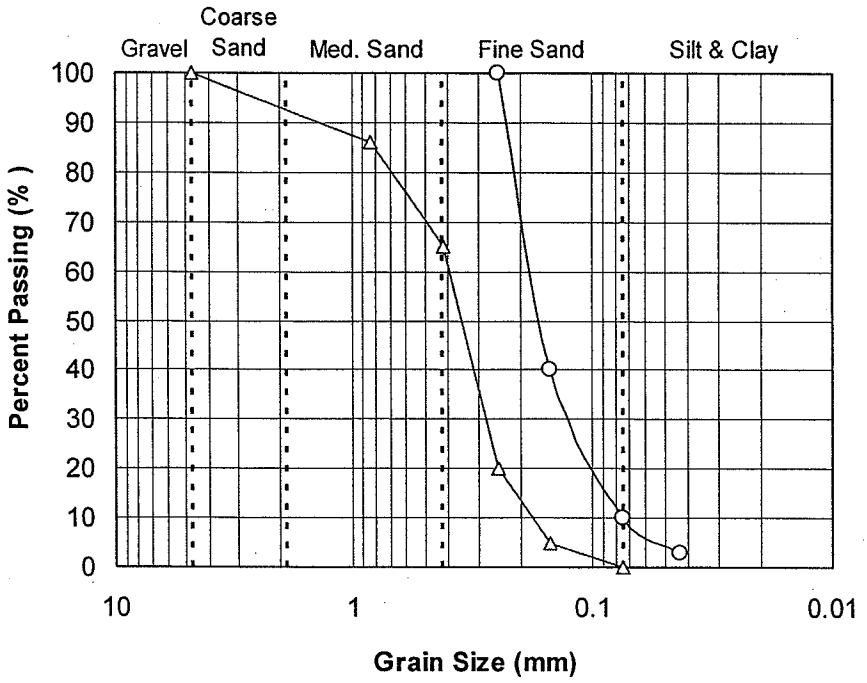

Figure 9 Typical grain size distribution curve boundaries for Fraser River Sand.

During the CANLEX investigations, site specific correlations were developed between CPT q_c and $(N_1)_{60}$ values. The average $q_c/(N_1)_{60}$ ratio was determined to be 0.58 with a standard deviation of 0.17 (Wride et al, 2000). Based on an average q_c value of about 6 MPa in the clean sand layer at the EQ-Drain test areas, the $(N_1)_{60}$ value might range from a minimum of 8 to a maximum of 14 with an average of 10.3. Therefore, the sand layer would clearly be susceptible to liquefaction based on the SPT blowcount. An $(N_1)_{60}$ value greater than about 25 or 30 would be necessary to make the sand immune to liquefaction.

Based on pressuremeter tests at the CANLEX site, the average at-rest earth pressure coefficient (K_o) in the clean sand layer was determined to be 0.40. In addition, the in-place void ratio (e_o) was estimated to be approximately 1.0 based on a number of in-situ tests (Wride et al, 2000) although the scatter ranged from 0.8 to 1.2.

3.0 EQ DRAIN PROPERTIES AND INSTALLATION

As indicated previously, one objective of the EQ Drain tests was to further define the relative effect of drainage and densification on liquefaction mitigation. To this end, two test blast areas were considered; one testing vertical drains installed with as little densification of the soil as possible (EQD Test Area 1), and the second with drains installed by a method that also densified the soil (EQD Test Area 2). As shown in Figs. 10 and 11, the drain layout at each site consisted of 35 drains arranged in a triangular pattern with a center-to-center spacing of 1.22 m.

3.1 DRAIN AND FILTER PROPERTIES

The corrugated (ADS) drain pipes used in the study had an inside diameter of 10.2 cm and a flow area of 81.7 cm^2. The corrugations on the drains were 9.5 mm deep, so the outside diameter was 12.07 cm. Three horizontal slots, approximately 25 mm long, were cut into each corrugation. This gave the drains an orifice area of 40.2 cm^2/m of length. The drain pipes were wrapped with a geosynthetic fabric (model SB-252) manufactured by Synthetic Industries. The fabric was a polypropylene spunbond material with an apparent opening size (AOS) of 50 microns. The fabric was folded over and stapled at the base to prevent infiltration of sand. The grab tensile strength based on ASTM D-4632 was 40 lbs in the machine direction and 50 lbs in the cross machine direction. Anchor plates consisting of 150 mm x 150 mm x 12.5 mm steel plate were attached to the bottom of each drain that was pre-cut to length of 13.4 m. Photos of the drain pipe, fabric and anchor plates are shown in Fig 12.

3.2 DRAIN INSTALLATION

3.2.1 Low Vibration Installation

The drains were "bottom loaded" into the mandrel by attaching a light rope to the top end of the drain. The rope extended up into the mandrel and fed out of the mandrel over a pulley positioned within the mandrel wall just below the vibrator clamp. One workman on the ground pulled the drains up into the mandrel with this rope, while another guided the drain into the bottom of the mandrel. The drains were pulled up tight, so that the anchor plate covered the bottom of the mandrel. The drains were installed to a design depth of 12.8 m using a thick-

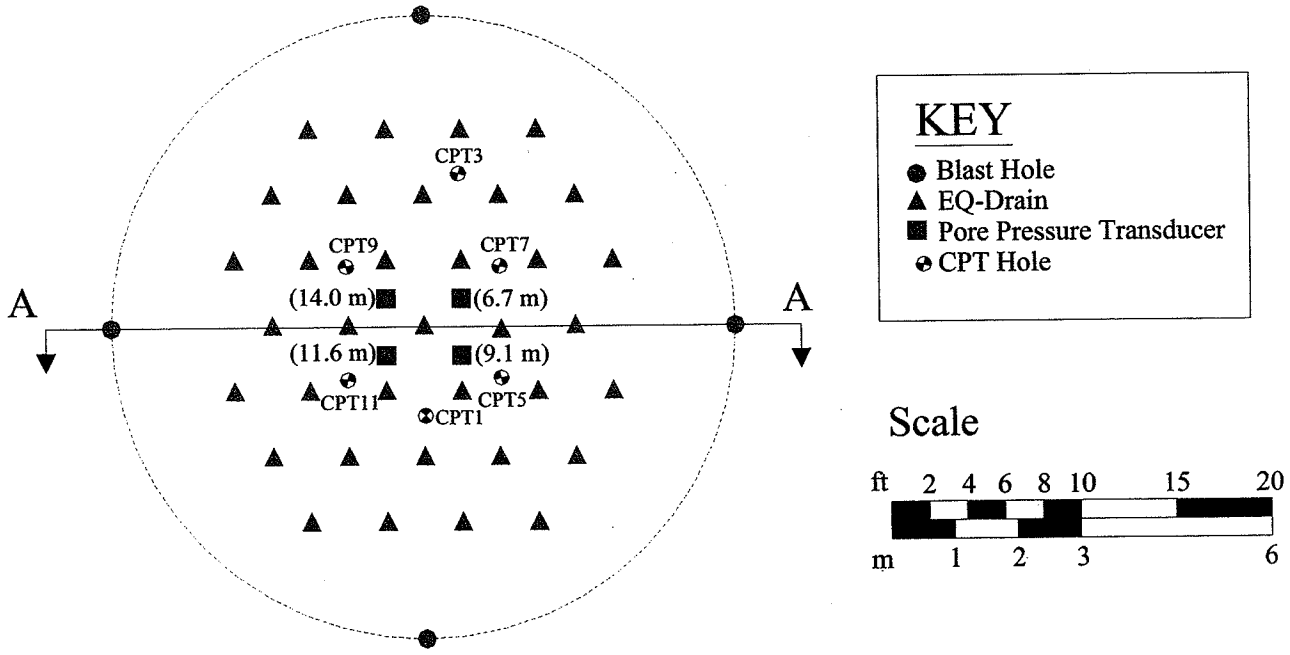

Fig. 10 Layout of EQ Drains and blast holes at Test Area 1 along with locations of CPT holes and piezometers. Depths of piezometers are shown in parenthesis.

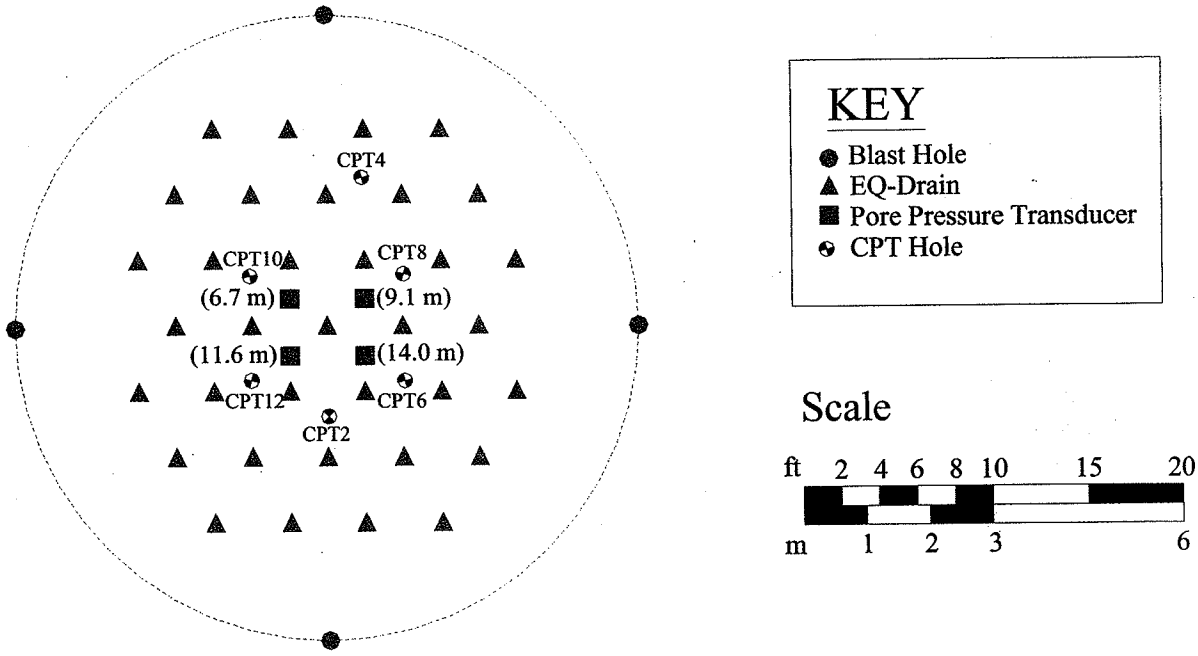

Fig. 11 Layout of EQ Drains and blast holes at Test Area 2 along with locations of CPT holes and piezometers. Depths of piezometers are shown in parenthesis.

(a)

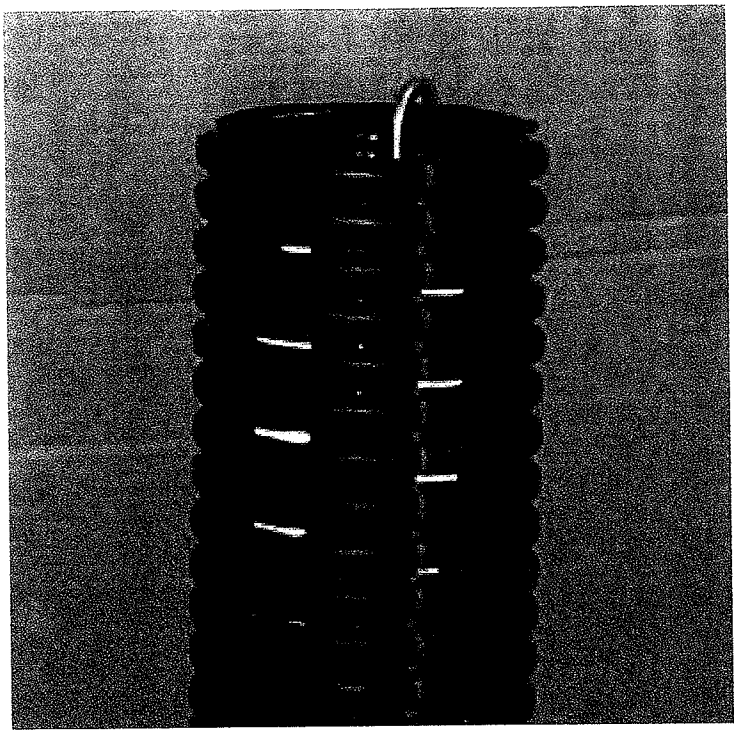

(b)

Figure 12 (a) EQ Drain without filter fabric showing slots illuminated by light inside pipe and (b) EQ Drain with filter fabric and anchor plate at the end.

walled pipe mandrel clamped to an ICE Model 44 vibratory hammer (500 N-m energy) suspended from a 70-ton mobile crane as shown in Fig. 13 and 14.

The drains were held in position with the anchor plate firmly against and covering the bottom of the mandrel, while the crane positioned the mandrel over drain locations. The mandrel was then lowered until the mandrel rested on the ground at the desired location. The vibrator was turned on at the lowest amplitude and the mandrel was allowed to penetrate into the ground to the desired depth of installation. After reaching the desired depth the mandrel was withdrawn, leaving the drain in place.

A problem was initially encountered with the drain pulling out of the hole for some distance as the mandrel was withdrawn. This appeared to be caused by the anchor plate pulling loose from the drain. The problem was remedied by attaching the anchor plates more securely to the drain pipes.

3.2.2 High Vibration Installation

In Test Area 2, the goal was to densify the soil while installing the drains using more conventional procedures. The equipment and procedures used in Test Area 2 were identical to those used in Test Area 1 except for two differences. First, during insertion, the vibratory hammer was operated at the highest level. Second, the installation mandrel was fitted with three symmetrically-spaced "fins", as shown in Figure 15, to transmit vibration to the soil during installation. A typical drain was placed to a depth of 12.8 m in approximately 3 minutes.

Normal production installation rigs utilize a "fixed-lead" system to hold and guide the mandrel vertically during penetration. The "free hanging" system was used in this case to minimize complications with moving a production rig into Canada, and to reduce mobilization costs. This procedure made it somewhat more difficult to control the verticality of the drain.
During installation, some difficulties were encountered with sand infiltration in some of the drains. Further investigation suggests that the pressure of the liquefied sand at the base of the drain pipe was exceeding the strength of the staples or ripping the fabric and allowing sand to flow inward. The filter fabric had been exposed to sunlight for several months prior which likely decreased the tear strength. In two projects, subsequent to this IDEAS study, a stronger fabric or a plastic cap has been used at the base of the drain pipe and this problem has not reoccurred.

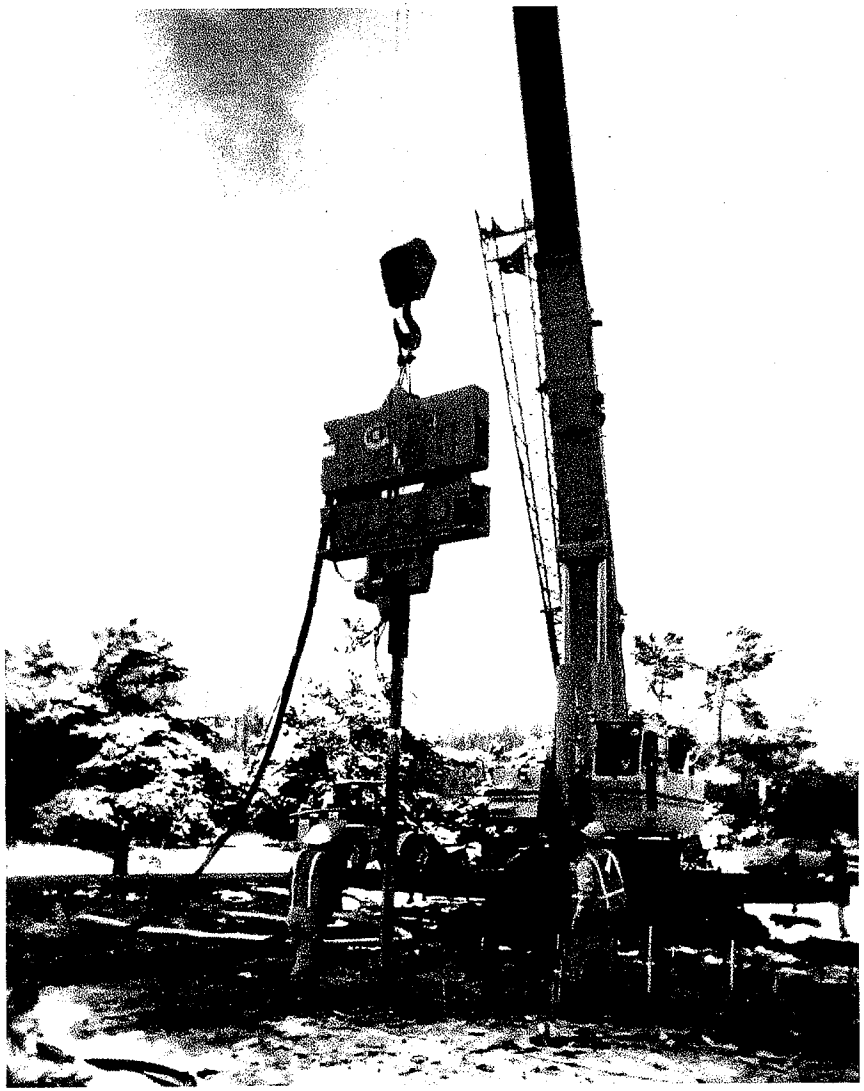

Figure 13 Photo showing installation of EQ Drain using pipe mandrel with vibratory hammer and minimum vibration.

Figure 14 EQ Drain with anchor plate being inserted into pipe mandrel in preparation of installation.

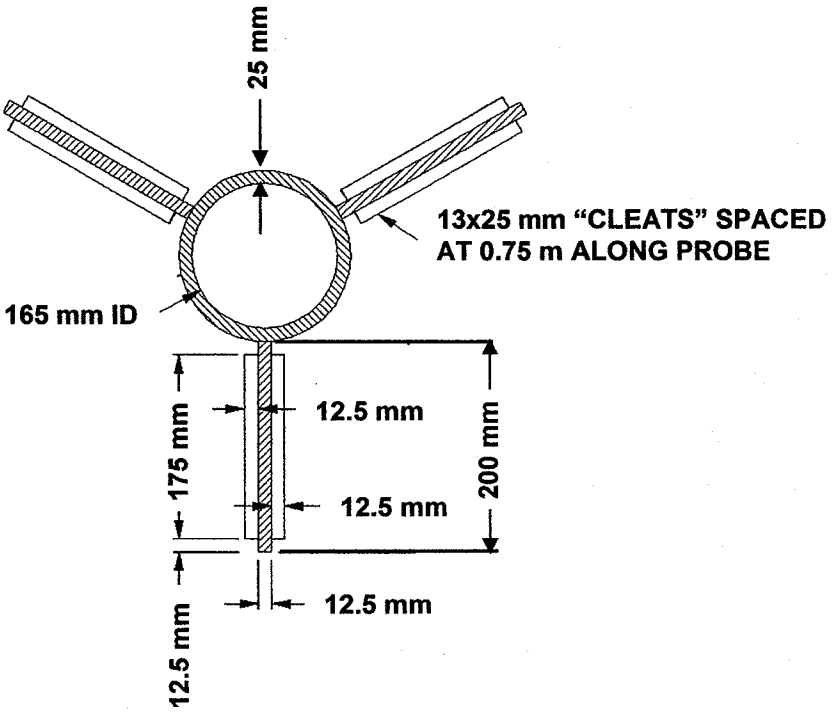

Figure 15 Dimensions and layout of finned mandrel along with photo of the mandrel in the field.

3.3 INSTALLATION-INDUCED PORE PRESSURE GENERATION

3.3.1 Pore water pressure monitoring instrumentation

At each EQ Drain test area, four piezometers were installed at a distance of 0.61 m from the center drain as shown in Figs. 10 and 11 prior to drain installation. This was done so that installation induced pore pressures could be measured. The piezometers were installed at depths of 6.7, 9.1, 11.6, and 14.0 m below the ground surface. A summary of the piezometer number, location, and depth is provided in Table 1 along with the initial vertical effective stress.

The piezometers consisted of electrical pore pressure transducers mounted inside a nylon cone tip with ports open to the surrounding ground water. A schematic drawing of the transducer and cone tip housing is provided in Fig. 16. The transducers were piezoresistive sensors specially designed to resist a transient blast pressure of up to 41.4 MPa (6000 psi) and then record the residual pore pressure to an accuracy of ± 0.7 kPa (± 0.1 psi) The pore water pressure was recorded using a laptop based computer data acquisition system at a sampling rate of 10 Hz during drain installation.

At the drain test areas a new approach was used to install the piezometers. The cone tip was pushed the entire depth and bentonite was injected into the holes as the cone rod was extracted to keep the hole open. Steel cables extending to the ground surface were attached to each piezometer so that it could be extracted after testing. Unfortunately, only about half of the piezometers could be recovered using this approach. Photos of the CPT rig installing the piezometers are shown in Fig. 17.

Table 1 Summary of piezometer location and properties at EQ Drain test areas.

Location	Depth (m)	Vertical Effective Stress, σ'_o (kPa)	Piezometer Number
EQD Test Area 1	6.7	84.6	PPT 751
EQD Test Area 1	9.1	103.4	PPT 604
EQD Test Area 1	11.6	123.8	PPT 605
EQD Test Area 1	14.0	142.8	PPT 698
EQD Test Area 2	6.7	84.6	PPT 308
EQD Test Area 2	9.1	103.4	PPT 606
EQD Test Area 2	11.6	123.8	PPT 611
EQD Test Area 2	14.0	142.8	PPT 607

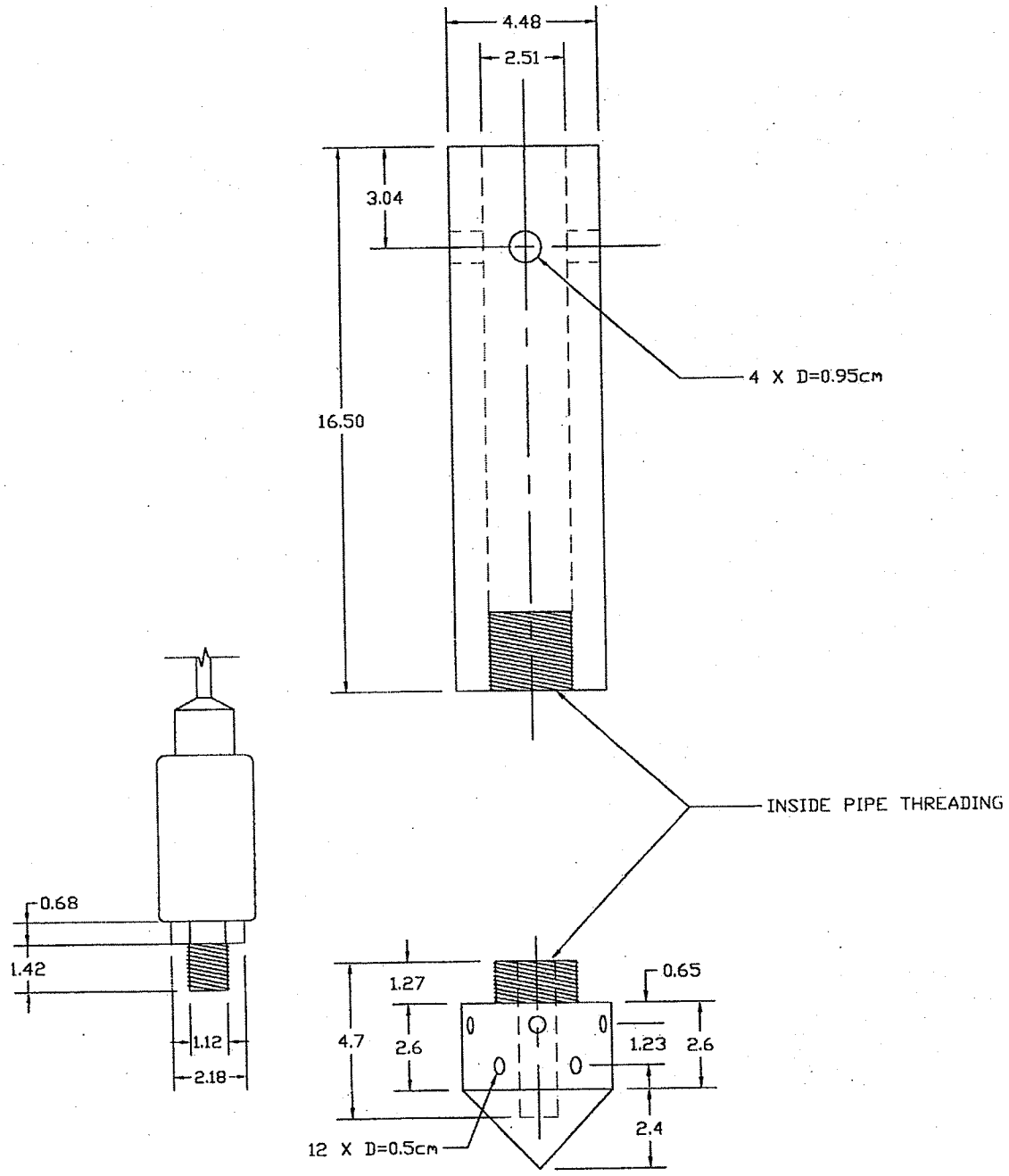

Figure 16 Schematic drawing of pore pressure transducer and nylon cone tip housing.

(a)

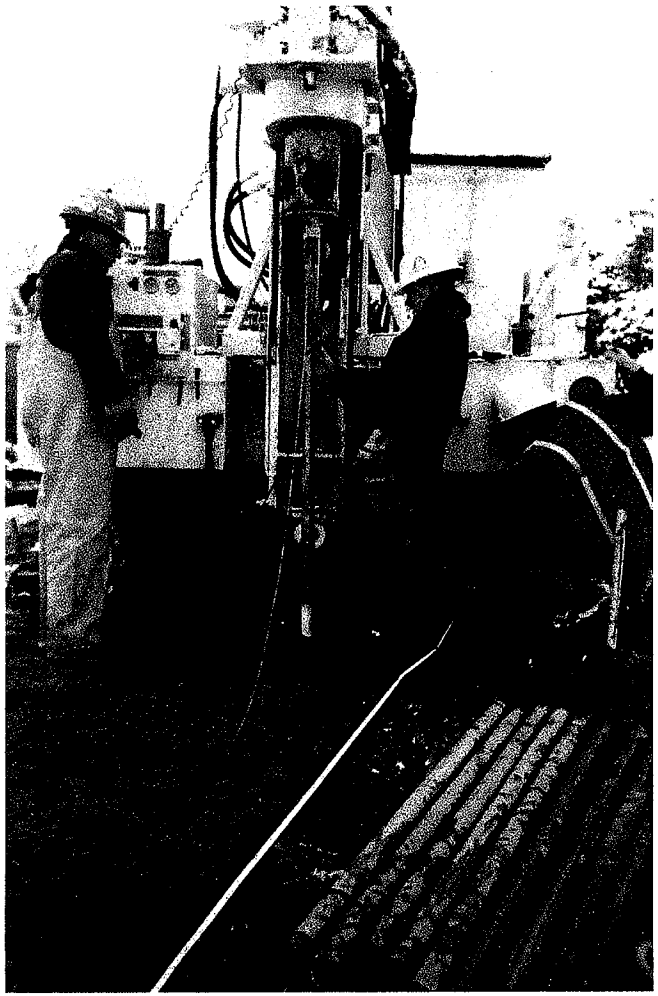

(b)

Figure 17 Photos of piezometer installation using Conetec CPT rig.

3.3.2 Pore water pressure response

Time histories of pore water pressure measured during the installation of the drains in the two test areas are shown in Fig. 18. For EQD Test Area 1 (pipe mandrel, low vibration) drains were installed beginning at the southwest side of the cluster and progressing toward the northeast side. For EQD Test Area 2 (finned mandrel, high vibration) the drains were installed beginning from the center of the cluster. Time constraints prevented measurement of pore pressure for all the drains.

As the mandrel moved downward and past a given piezometer, the pressure peaked and then dropped off. The amplitude of peaks in the pore pressure typically decreased with depth. In addition to the peaks, there was also a gradual increase in the residual pressure as the installation process continued across the site.

To facilitate comparisons, the excess pore pressure produced by the installation was normalized by the vertical effective stress at each piezometer location (see Table 1) to compute the excess pore pressure ratio ($R_u=\Delta u/\sigma'_o$). An excess pore pressure ratio of 1.0 indicates liquefaction The vertical effective stresses were computed to be 84.6, 103.4, 123.8, and 142.8 kPa for depths of 6.7, 9.1, 11.6 and 14 m depths, respectively. This assumes a unit weight of 19 kN/m^3 from 0 to 2.6 m, an effective unit weight of 8.7 kN/m^3 from 2.6 to 6 m, and an effective unit weight of 8 kN/m^3 from 6 to 15 m. To prevent damage to the piezometers during drain installation using the "hanging-lead" approach adopted at the test area, no piezometer was closer than 0.6 m to the mandrel.

Fig. 19 presents a plot of the maximum excess pore pressure ratio as a function of depth for the two drain test areas. Although liquefaction (R_u=1.0) may potentially be induced immediately adjacent to the mandrel, the maximum measured R_u at a distance of 0.6 m did not exceed 0.24. As expected, the maximum R_u values are typically higher for the area where the finned mandrel was used with higher vibration levels. In addition, the maximum R_u value decreases with depth in both cases, which suggests that it is more difficult to generate pore pressure as the vertical stress in the ground increases but the vibrational energy of the hammer remains constant.

(a)

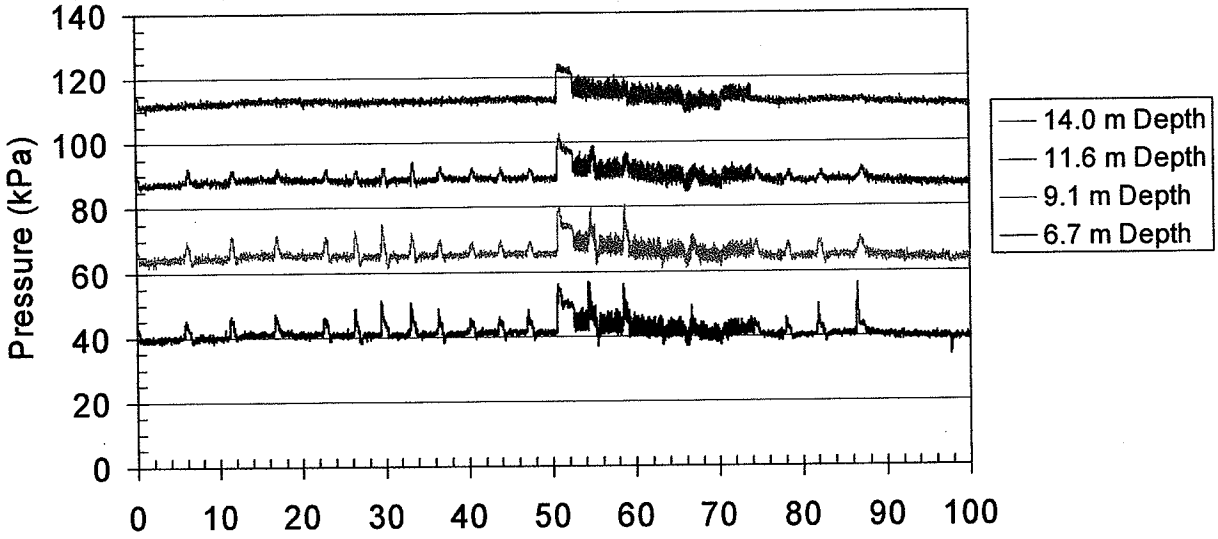

(b)

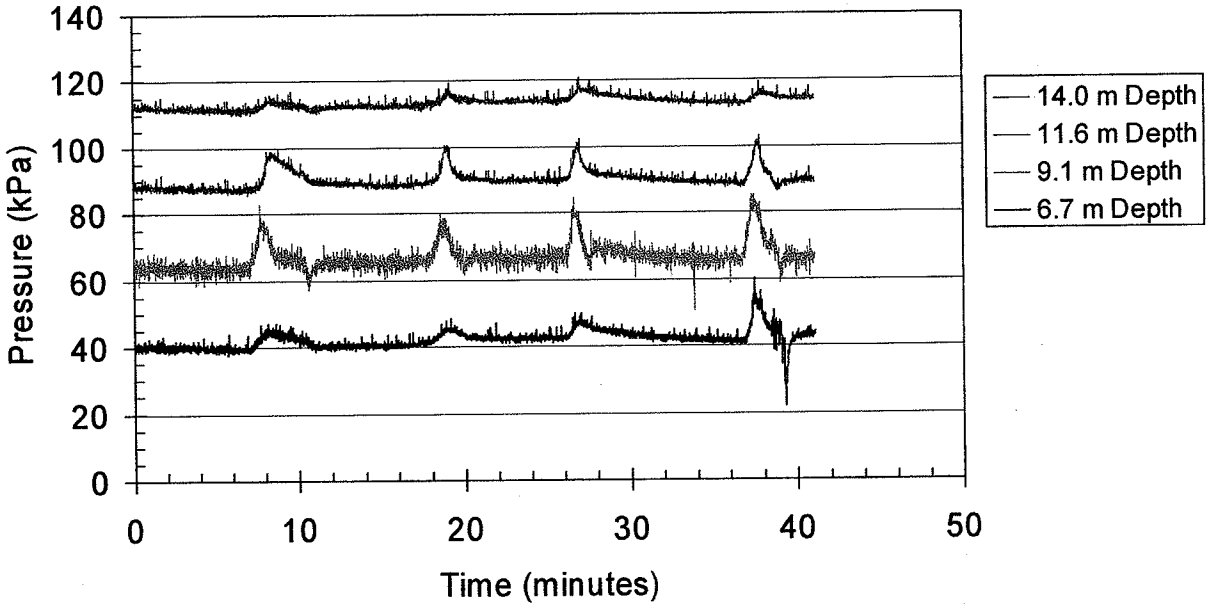

Figure 18 Time histories of pore water pressure during installation of EQ Drains at (a) test area 1 (pipe mandrel, low vibration) and (b) test area 2 (finned mandrel, high vibration).

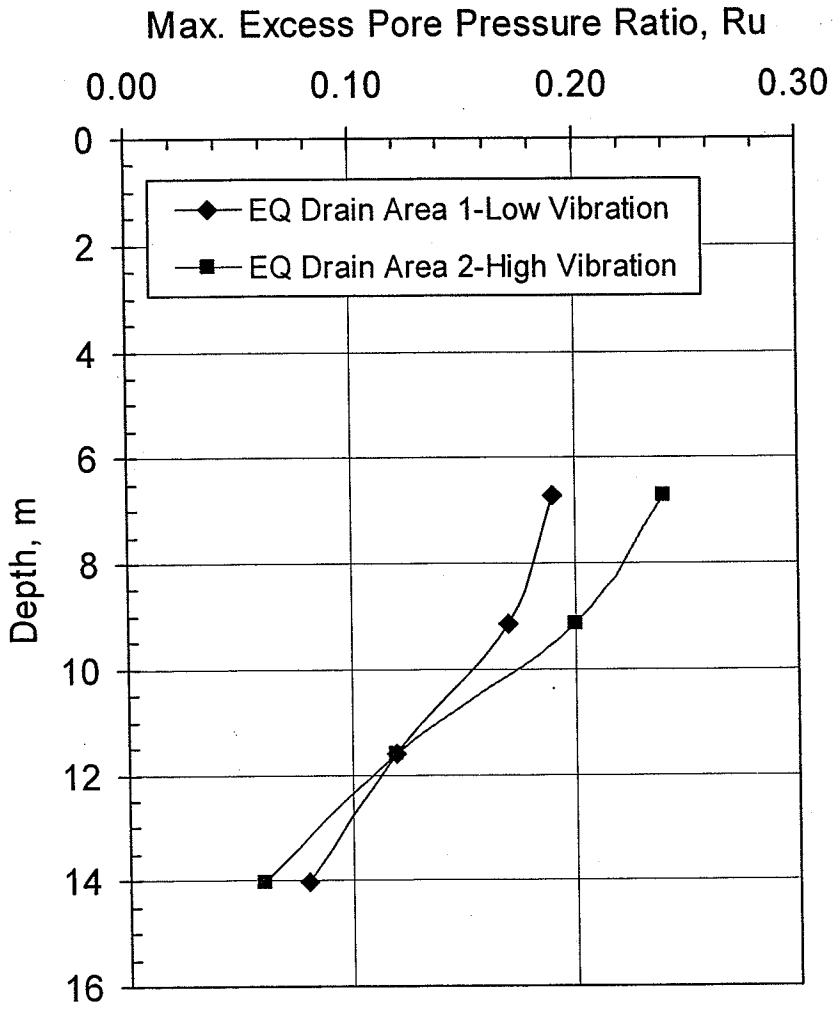

Figure 19 Maximum excess pore pressure ratio (R_u) as a function of depth for both EQ Drain test areas based on measurements during drain installation.

3.4 INSTALLATION-INDUCED VIBRATION

3.4.1 Vibration monitoring

Vibration monitoring was performed using two three-component blast seismographs. The seismographs were placed at various distances from the vibrating probe during installation. The seismographs measured velocity time histories for each component and peak displacement and acceleration were determined from the velocity time histories.

3.4.2 Measured vibration and correlation equations

Peak particle velocity (PPV) was measured as a function of time while a number of drains were installed. In general, PPV tended to decrease as the mandrel depth increased. The predominant frequency of the maximum velocity was typically between 25 and 50 Hz. The maximum PPV for each drain installation is plotted as a function of distance from the mandrel in Fig. 20. Based on the field data, the PPV (mm/sec) can be estimated using the equation

$$PPV = 78.2x^{-1.32} \qquad (2)$$

where x is the distance to the mandrel in meters. This best-fit equation has an r^2 value of 0.96, which indicates good correlation. Vibrations are typically limited to 25 mm/sec to prevent cracking to adjacent structures. If this criterion is used, the data indicate that drains should be installed no closer than about two meters from an adjacent structure.

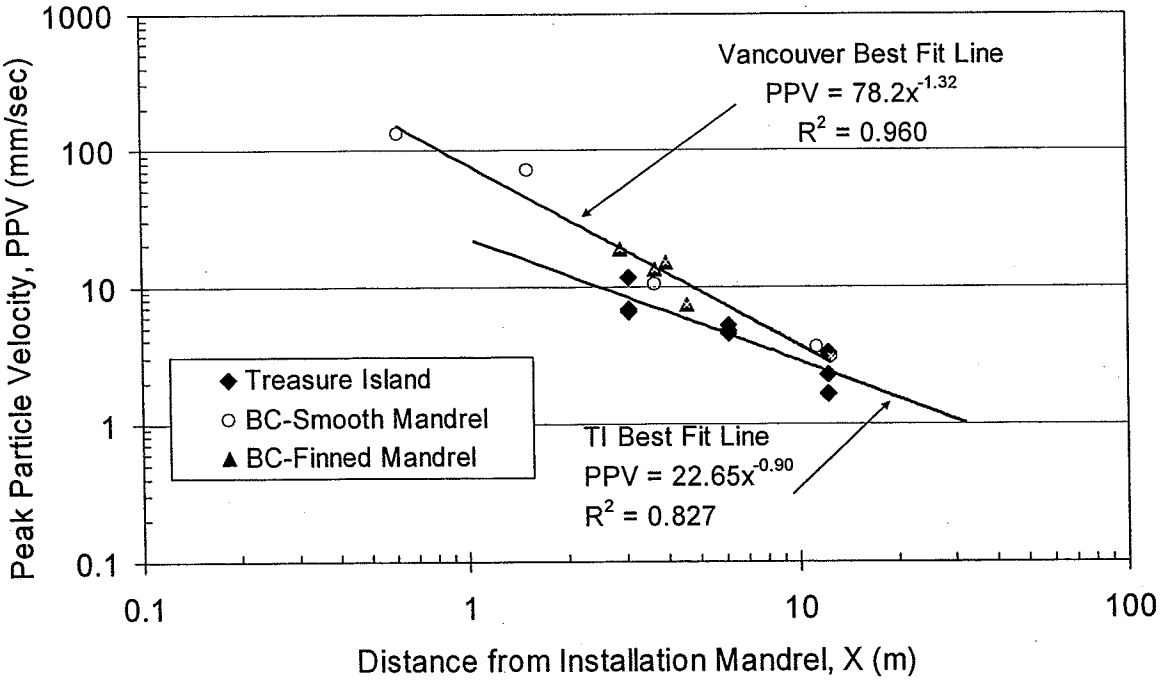

Figure 20 Variation of peak particle velocity as a function of distance from the installation mandrel.

Similar PPV data from the Treasure Island test site are also shown in Fig. 20. The best fit line using only the Treasure Island data is somewhat flatter than that for the Vancouver data. This likely occurs because the vibratory hammer used in Vancouver produced four times the energy as that used at Treasure Island. However, when the entire data set is observed together, the data points appear to be relatively consistent and the equation based on the Vancouver data set would not greatly overestimate the measured PPV at Treasure Island.

3.5 INSTALLATION-INDUCED SETTLEMENT

3.5.1 Settlement monitoring instrumentation

The change in elevation around each drain cluster was determined using a survey level before and after installation. The elevation was typically measured along eight rays spaced at 45 degree angles from the center drains. Measurement points along these rays were at 0.61-meter intervals for the first 3.66 meters, and then at 1.22-meter intervals to 14.6 meters for the EQD test areas. In some cases, obstructions prevented measurements at each point along each array.

3.5.2 Results of settlement surveys

Contours of the installation induced settlement at EQD Test Areas 1 and 2 are shown in Figs. 21 and 22, respectively. The location of the outer edge of the drain cluster is also shown with a dashed white line to provide perspective. The greatest settlement generally occurred near the center of the drain cluster and the settlement contours were typically concentric about the center. The settlement in EQD Test Area 2 was clearly much greater than in Area 1.

Fig. 23 provides a plot of the average installation-induced settlement vs. radial distance from the center of the tests area for both EQ Drain test areas. Nearly 350 mm of settlement occurred at the center of EQD Test Area 2 where the finned-mandrel was used with high vibration to install the drains. This settlement decreased to about 50 mm at the periphery of the drain cluster. This differential settlement is likely due to arching against the surrounding untreated soil. In contrast, the maximum settlement was only 100 mm at the center of EQD Test Area 1 where drains were installed with a smooth pipe mandrel and low vibration. For the soil conditions at this test site, the finned mandrel installation produced 250% more settlement than the pipe mandrel installation.

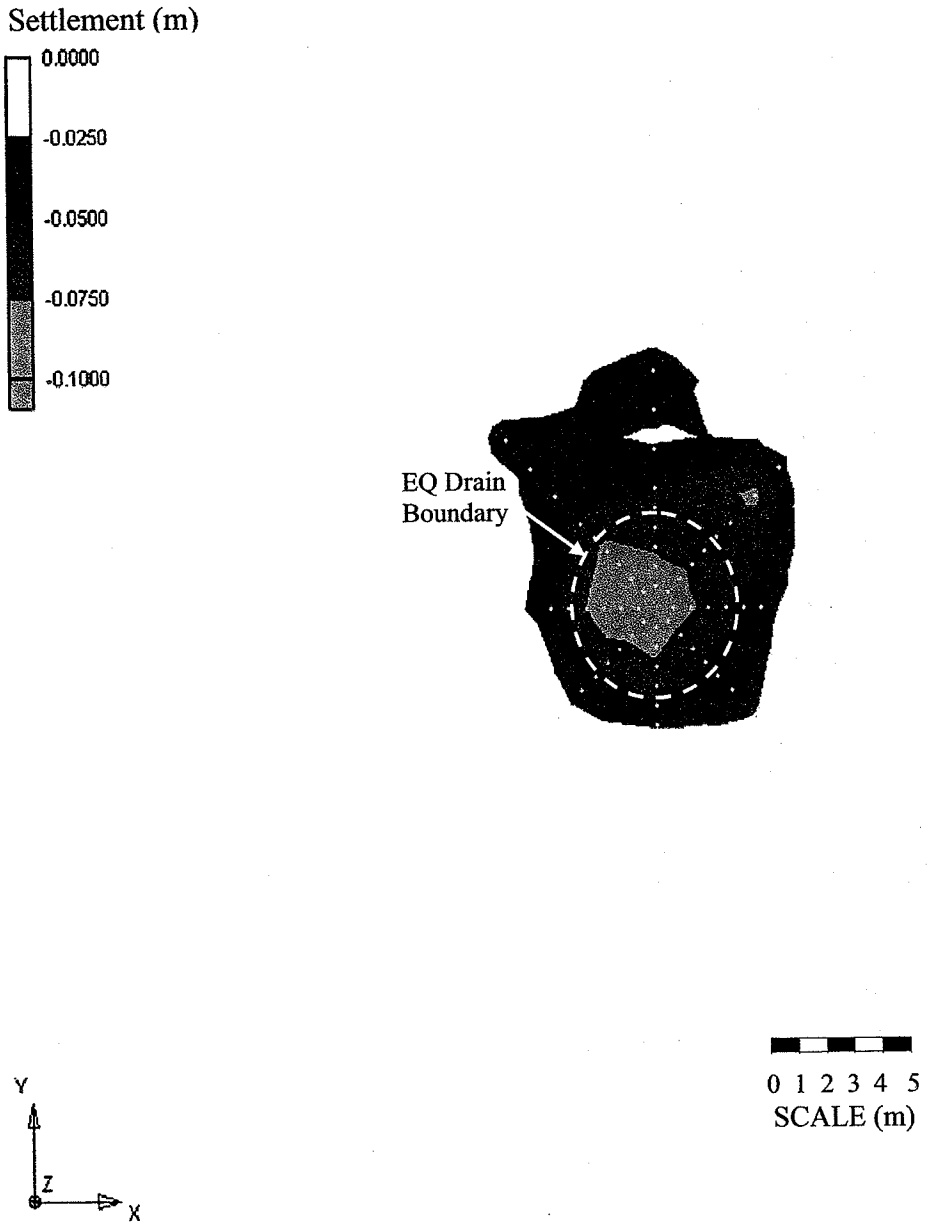

Figure 21 Contours of settlement (in meters) due to drain installation at EQ Drain Test Area 1 using a pipe mandrel and low vibration. Survey marker locations are shown along with the boundary of the zone treated with EQ Drains.

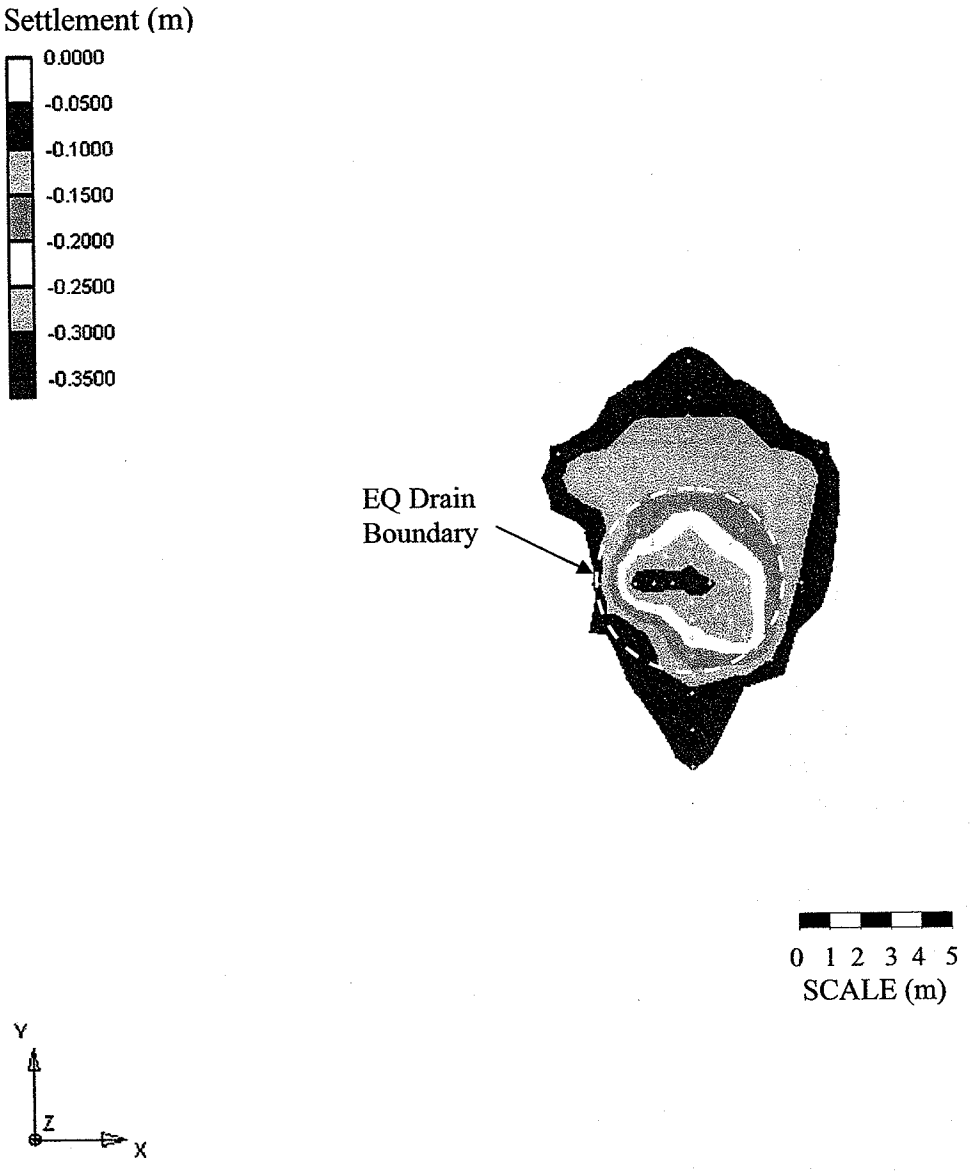

Figure 22 Contours of settlement (in meters) due to drain installation at EQ Drain Test Area 2 using a finned mandrel and high vibration. Survey marker locations are shown along with the boundary of the zone treated with EQ Drains.

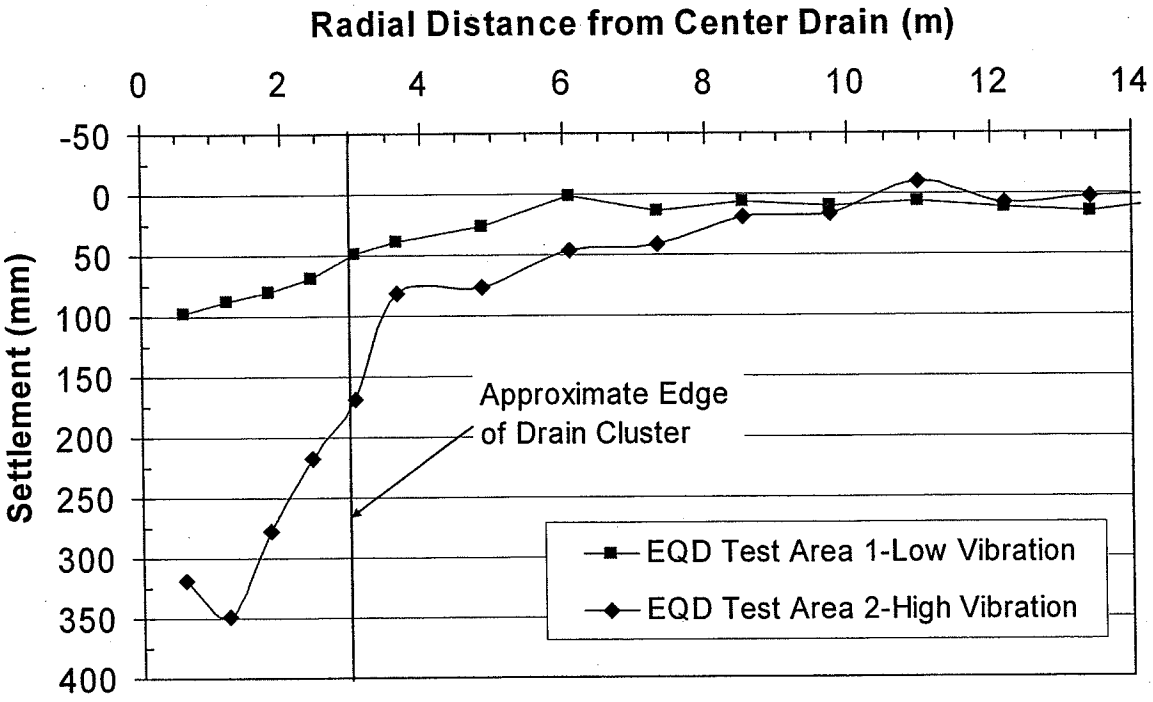

Figure 23 Average installation-induced settlement for EQD Test Area 1 (low-vibration and pipe mandrel) and EQD Test Area 2 (high-vibration and finned mandrel) as a function of distance from the center drain.

Assuming that the settlement occurred entirely within the loose sand layer from 6 to 13 m below the ground, the installation induced volumetric strain would be 1.4 and 5% for EQD Test Areas 1 and 2, respectively. Sondex measurements, described subsequently for the untreated test area, suggest that only about half of the total settlement in the profile was coming from the clean sand layer. Based on this assessment, the volumetric strain would be 0.7 and 2.5% for EQD Test Areas 1 and 2, respectively. The settlement basin produced by the drain installation was not backfilled prior to the blast to facilitate direct settlement measurements.

3.6 POST-INSTALLATION CPT TESTING

CPT tests were performed at both EQ Drain test areas within 3 to 5 days of the drain installation. Plots of pre- and post-installation cone tip resistance for each drain test site are presented in Fig. 24 for comparison. Despite the settlement data showing that the

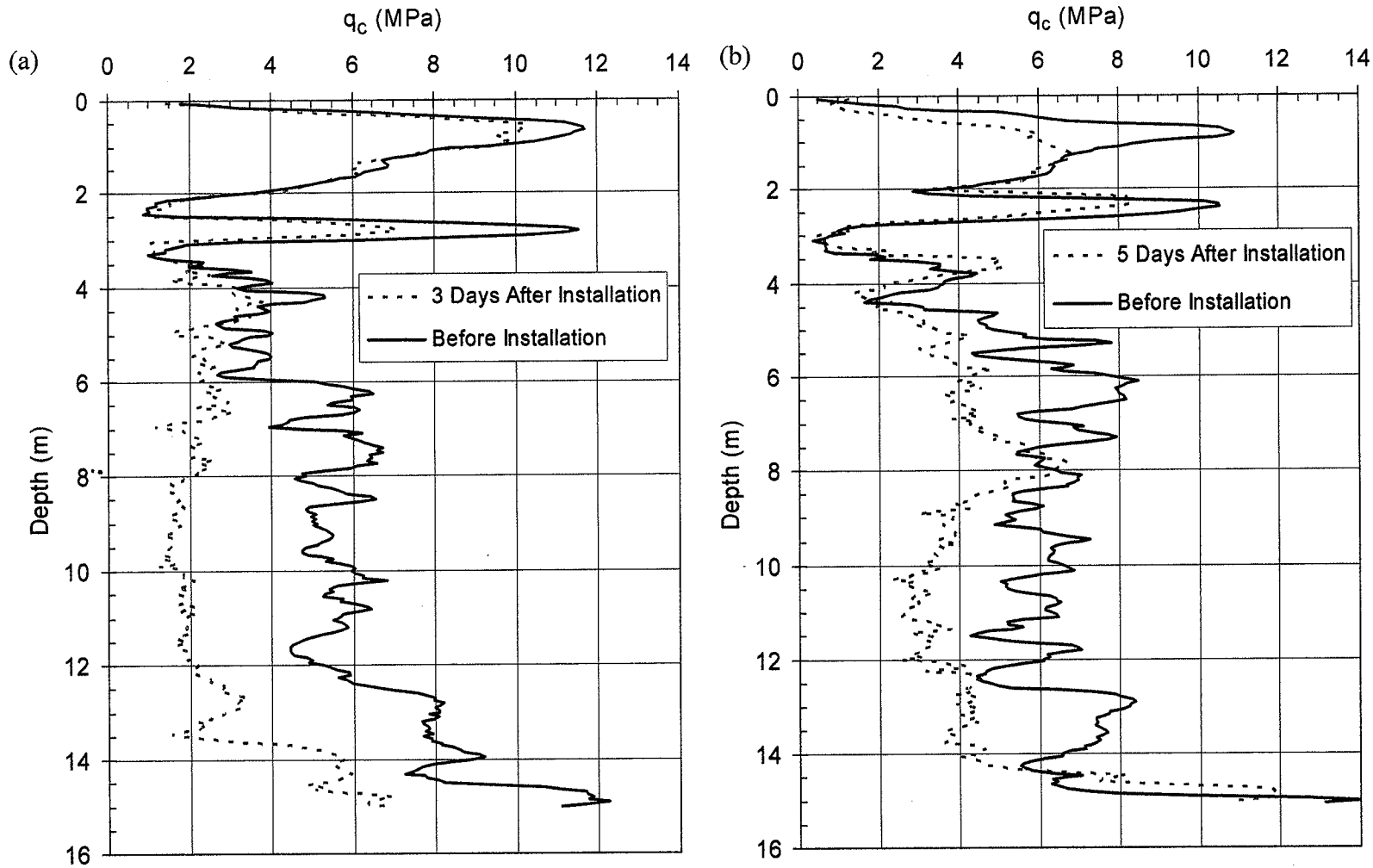

Figure 24 Plots of CPT cone resistance versus depth before and after installation of EQ Drains at (a) Test Area 1 (pipe mandrel, low vibration) and Test Area 2 (finned mandrel, high vibration

drain installation clearly increased the sand density, the cone tip resistance decreased in the sand layer for both installation techniques. The decrease was greatest (more than 50%) for the site where installation was performed with minimum vibration treatment. In this case, the reduction in resistance produced by the installation was not counteracted by the increase in density due to vibration that apparently occurred at EQD Test Area 2 where maximum vibration was used.

4.0 BLAST TESTING AT UNTREATED AREA

The blast testing in the untreated test area was carried out by Pacific Geodynamics, Inc. under contract with the BC Ministry of Transportation. These tests served as a baseline for comparison with blast tests at a site treated with gravel drains. Gohl (2002) provides additional details of the blast testing at the gravel drain test site. By collaborating with Pacific Geodynamic on this project, the data for the untreated test site could also be used as the baseline for comparison with the EQ Drain test areas. A summary of the blast testing procedure and the results of the testing at the untreated test area are provided in this section of the report.

4.1 BLAST DESIGN

The main criteria used in the selection of explosive charge weights were:

1. To keep the peak particle velocities at sensitive locations near the blast to less than 50 mm/sec.
2. To ensure that the ground settlements did not adversely impact nearby BC Hydro power line poles.
3. To keep peak dynamic blast pressures below the maximum tolerable level of 41 MPa (6000 psi) at piezometer locations.
4. To provide a reasonably broad zone of liquefaction.
5. To limit dynamic pressures at the gravel drains to prevent damage to the central PVC pipe.

At the start of testing, a series of single blast hole detonations was carried out in the untreated test area to confirm the blast design. A brief summary of the single blast hole tests is provided below.

For Test Blast 1, charges were loaded in blast hole A-1 as shown in Fig 25 Explosive charge weights (Trade name *Dynoseis*) of 4, 3, and 2 kg were centered at depths of 14.5, 11.4 and 8.5 meters below the ground surface, respectively. The explosives were placed in water-filled blast holes with gravel stemming between charges.

The charges were detonated sequentially at 0.5 second intervals. The blasting produced excessive pressure and destroyed piezometer HP-2. In addition, SP-1 was sheared off at a depth of 8 m.

For Test Blast 2, charges were loaded in blast hole B-1 as shown in Fig. 25. Explosive charge weights (Trade name *Dyno-Xtra*) of 3.6, 2.7, and 1.8 kg were centered at depths of 14.1, 11.1 and 7.9 meters below the ground surface, respectively. The explosives were once again loaded in a water-filled blast hole with gravel stemming between charges. Based on the results of the testing, the dynamic peak pressures were found to be too high to be safely withstood at several piezometers locations.

For Tests Blast 3, charges were loaded in blast hole C-1 as shown in Fig. 25. Explosive charge masses (Trade name *Dyno-Xtra*) of 2.7, 1.8, 1.8 and 1.8 kg were centered at 15.5, 12.3, 9.1 and 6.1 m below the ground surface, respectively. The explosives were placed after dewatering the blast hole and placing gravel stemming between charges. The dewatering process significantly reduced the transient blast pressures at the piezometers levels without reducing the development of excess pore pressures. Based on this series of trial detonations, it was determined that the main criteria were best achieved using four decks of *DYNO-XTRA* explosives with charge weights of 2.7, 1.8, 1.8, and 1.8 kg centered at depths of approximately 14, 11, 8, and 5 m, respectively.

Finally, Test Blast 4 was carried out following Test Blasts 1 through 3 in the Untreated Test Area. The test holes were arranged in a diamond configuration (holes D-1 through D-4 on Figure 25) and each blast hole was 5 m from the center of the test area. Electrical blasting caps were used to initiate detonation with the timing of the firing of each cap controlled using an electrical timing board. The explosives were fired in each blast hole using a "bottom-up" detonation sequence with a delay of approximately 0.5 seconds between firing successive charges in the blast holes. The blast hole detonation sequence was: east hole, north hole, west hole, south hole.

4.2 PORE PRESSURE RESPONSE FOR UNTREATED AREA

4.2.1 Pore Pressure Monitoring

To provide some redundancy and evaluate consistency in the measurements at the untreated test site, two piezometers were installed at a depth of 8.2 m and two piezometers were installed at a depth of 12.5 m. Details regarding the piezometers are summarized in Table 2. The transducers in the piezometers were supplied by the same manufacturer as those installed at the EQ-Drain Test Areas and were capable of withstanding 41.4 MPa transient blast pressures while recording the residual excess pore pressure to an accuracy of ± 0.7 MPa. The same nylon cone housing was also used for the untreated test site; however, the installation process was somewhat different.

Rather than inserting the cone tip using a CPT rig as was done at the EQ Drain test areas, a 125 to 150 mm diameter bore hole was drilled to a depth about 0.3 m above the desired piezometer depth. The drill hole was then filled with relatively thick bentonite slurry. Finally, the piezometers was inserted through the slurry and pushed the last 0.3 m into the sand with the drill rods. This is the same procedure that was employed previously for the Treasure Island testing, but the piezometers were placed much deeper at the Vancouver test site. This procedure was successful in inserting the piezometers without causing any damage to the lead wires or the transducers. In addition, wire cables were attached to each piezometer and following the testing each piezometer was easily pulled out of the soil so that they could be reused in the future.

Table 2 Summary of piezometer locations and properties at untreated test area.

Location	Depth (m)	Vertical Effective Stress, σ'_o (kPa)	Piezometer Number
Untreated Area	8.2	87.5	P-1
Untreated Area	8.2	89.9	P-2
Untreated Area	12.5	124.9	P-3
Untreated Area	12.5	123.30	P-6

4.2.2 Pore pressure response

Following the detonation of the blast charges, sand boils were observed at the center of the test area and water rose significantly in a standpipe suggesting that liquefaction had been produced. The excess pore pressure (Δu) measured by the piezometers was divided by the vertical effective stress (σ'_o) at each piezometer depth to obtain the excess pore pressure ratio (R_u). An R_u of 1.0 indicates complete liquefaction. The vertical effective stress was calculated assuming a moist unit weight of 19 kN/m^3 above the water table at 2.6 m, a buoyant or effective unit weight of 8 kN/m^3 in the silt to silty sand layer between 2.6 and 6 m depth, and a buoyant unit weight of 8.7 kN/m^3 in the loose sand between 6 and 13 m. The computed vertical effective stresses at each piezometer location are summarized in Table 2.

The measured excess pore pressure ratio versus time curves for each of the four piezometers are presented in Fig. 26. A comparison of the curves at the same depths indicates that the pore pressure response is consistent and reproducible. The R_u time

histories at the 8.2 m depth are significantly different than those at the 12.5 m depth. At 8.2 m the R_u values remain relatively constant for several minutes before decreasing whereas the R_u values at 12.5 m depth begin to decrease almost immediately after the end of the blast. This difference in response is likely due to the flow of water as the excess pore pressures dissipate upward. Although the R_u is about the same at both depths, the hydraulic head is greater at the lower depth than at the shallow depth; therefore upward flow would occur. As the water flows upward, it would likely be trapped by the silt layer above the clean sand layer and the R_u would remain higher for a longer time. This is apparently what occurred at this test area.

Fig. 27 presents a more detailed view of the generation of the excess pore pressure ratio with each charge detonation. After each charge is detonated, there appears to be a transient increase and decrease in the R_u value followed by a net increase in the residual excess pore pressure ratio. A review of the data in Fig. 27 suggests that the residual excess pore pressure reaches a value between 0.8 and 0.9 after approximately four blast detonations. Subsequent charge detonations appear to maintain the R_u or increase it only slightly.

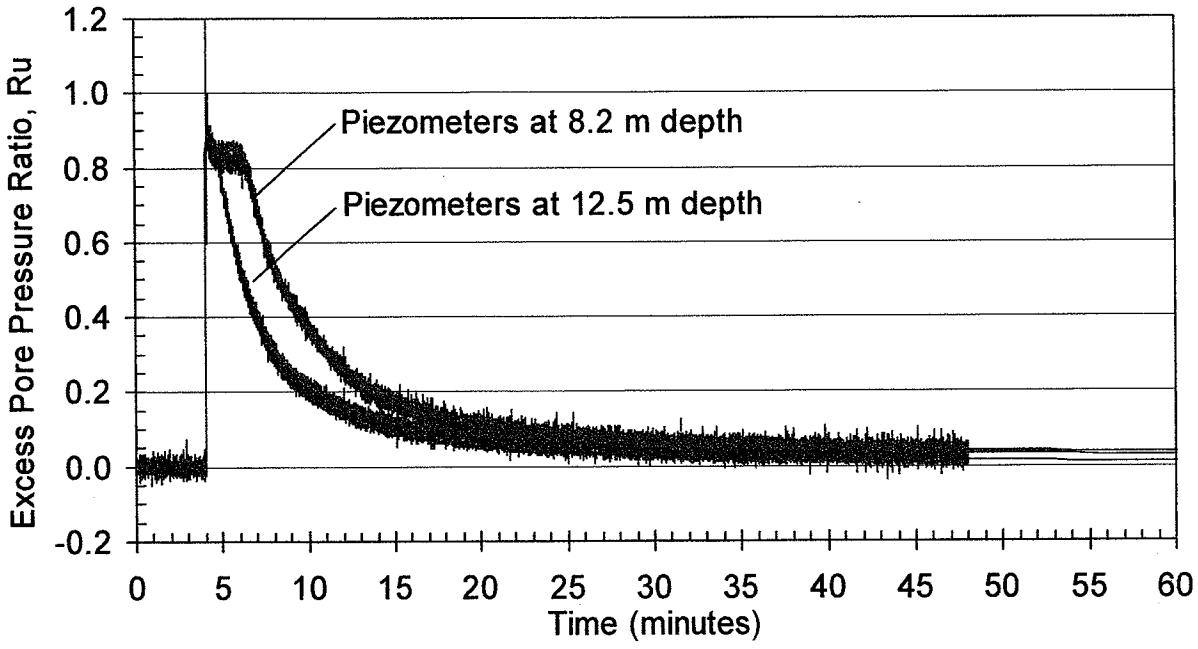

Figure 26 Excess pore pressure ratio versus time curves for two piezometers at 8.2 m depth and two piezometers at 12.5 m depth in the untreated test area.

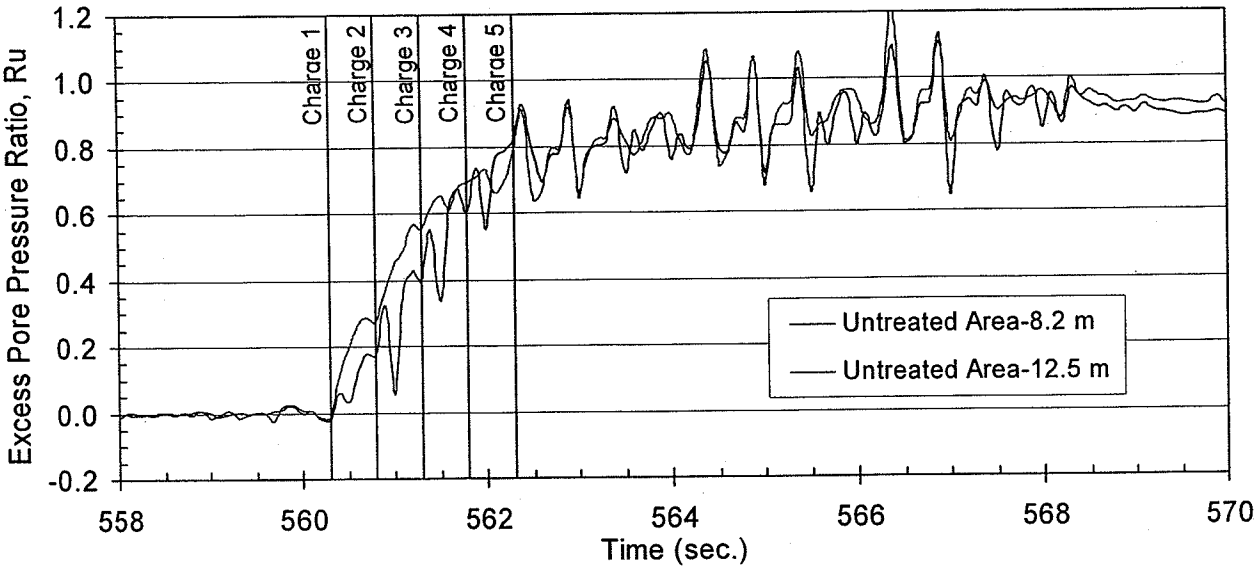

Figure 27 Generation of excess pore pressure ratio (R_u) as a function of time during the detonation of explosive charges.

4.3 BLAST INDUCED SETTLEMENT

The settlement produced by Test Blast 4 (a four-hole blast) was determined by measuring the change in elevation with a survey level along a series of rays extending from the center of the test area. The change in elevation was measured at approximately 45 locations within the blast area at distances of up to 20 m from the center of the blast area. A contour drawing of the settlement produced by the blasting is shown in Fig. 28. and the average settlement as a function of distance from the center is shown in Fig. 29. In general, the blasting caused a bowl-shaped depression centered at the mid-point of the area of blasting. For Test Blast 4 a maximum settlement of 500 mm occurred in the center and settlements of more than 1 cm, considered to be the accuracy of the settlement survey, extended up to 20 m from the center of the blast area.

Settlement was also measured as a function of depth using a "Sondex tube" placed near the center of the untreated test area. A Sondex tube consists of a flexible vacuum hose which contains a series of magnetic rings spaced initially at approximately 1.5 m intervals down the length of the hose. Each sondex tube, containing a weight at the

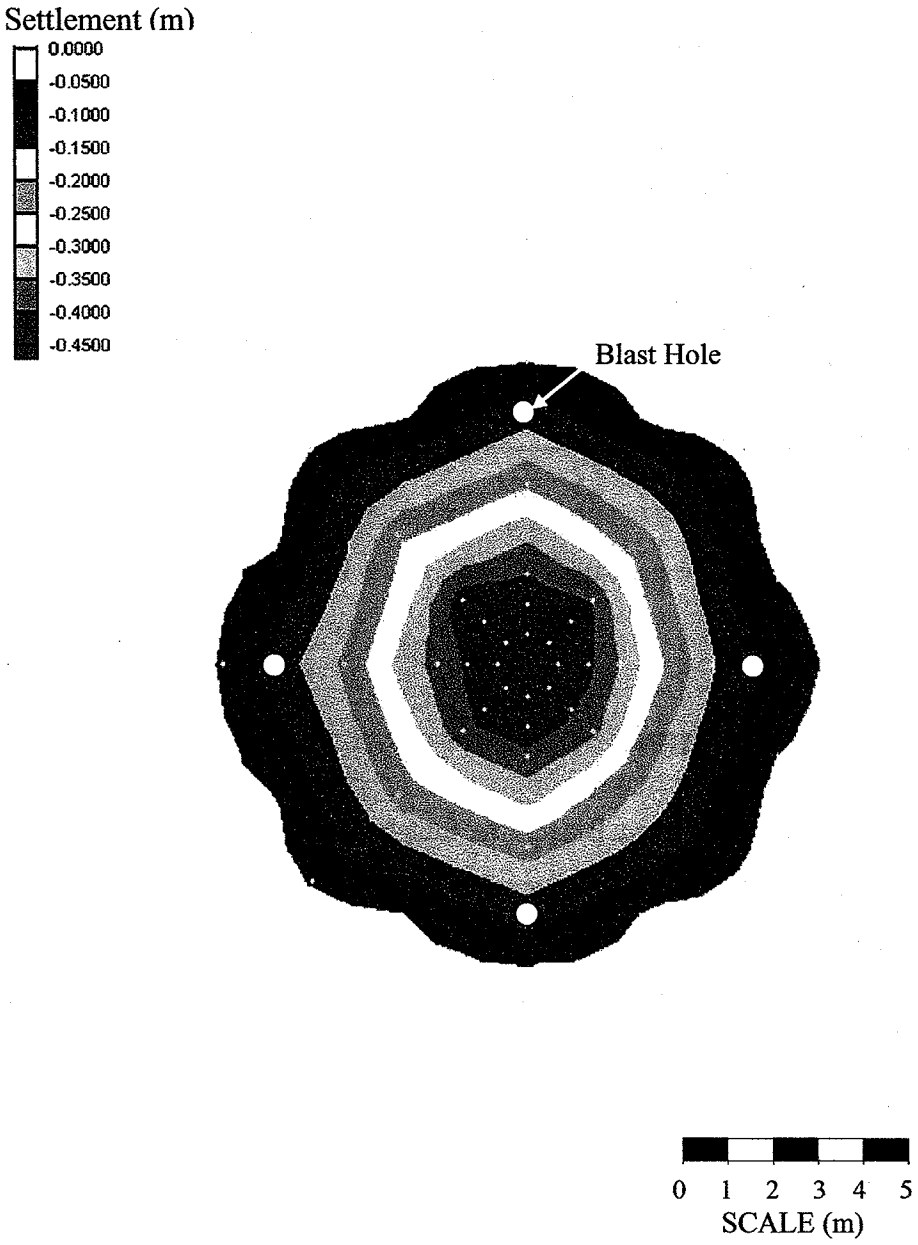

Figure 28 Contours of settlement due to blasting at Untreated Test Area.

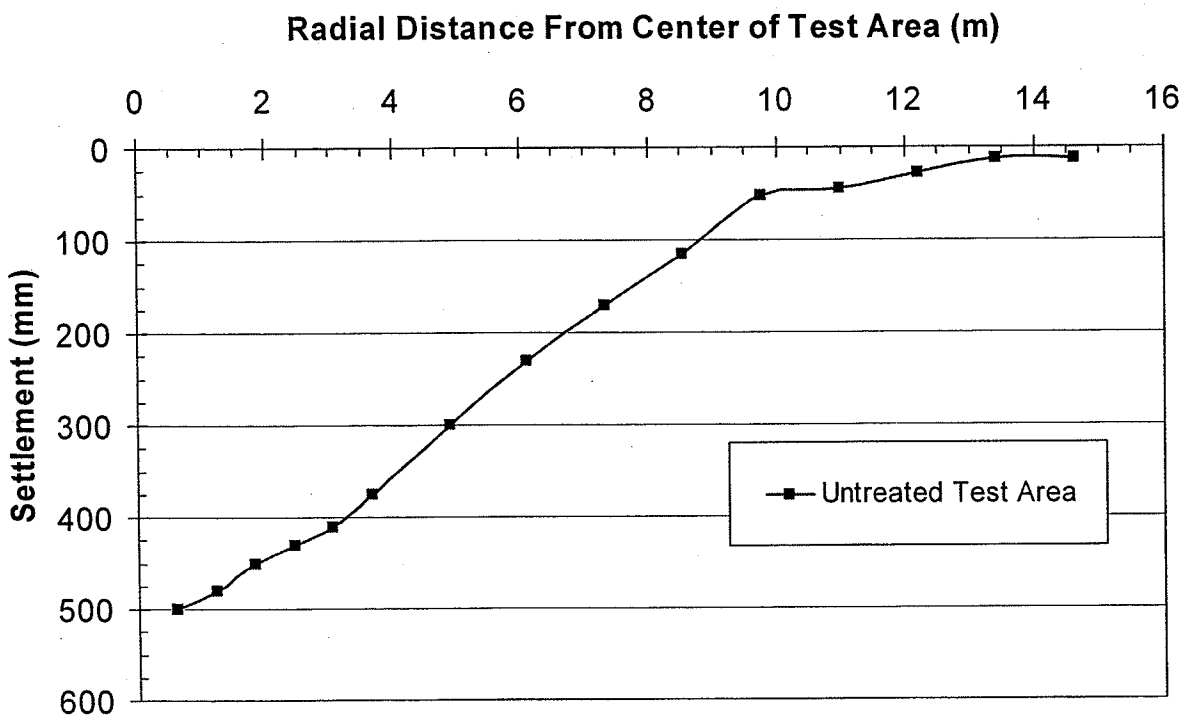

Figure 29 Average settlement blast induced settlement versus radial distance from the center of the test area for the untreated test area.

end of the tube, was installed down a drill hole advanced to a depth of 18.7 m. The annulus between the mudded drill hole wall and the Sondex tube was then backfilled with a granular material to provide contact between the tube and the external soil mass. Following the blasting, the flexible Sondex tube adjusts to accommodate the settlement of the surrounding ground. In principle, the ground settlement versus depth can then be estimated by tracking the change in position of each ring before and after the blasting.

The settlement as a function of depth below the ground surface obtained from the Sondex tube measurement is presented in Fig. 30 (Gohl, 2002). Based on the data in Fig. 30 the settlement in the loose sand layer from 6 to 13 m is about 54% of the total ground surface settlement. Therefore, the volumetric strain in the clean sand layer due to Test Blast 4 was about 3.8%.

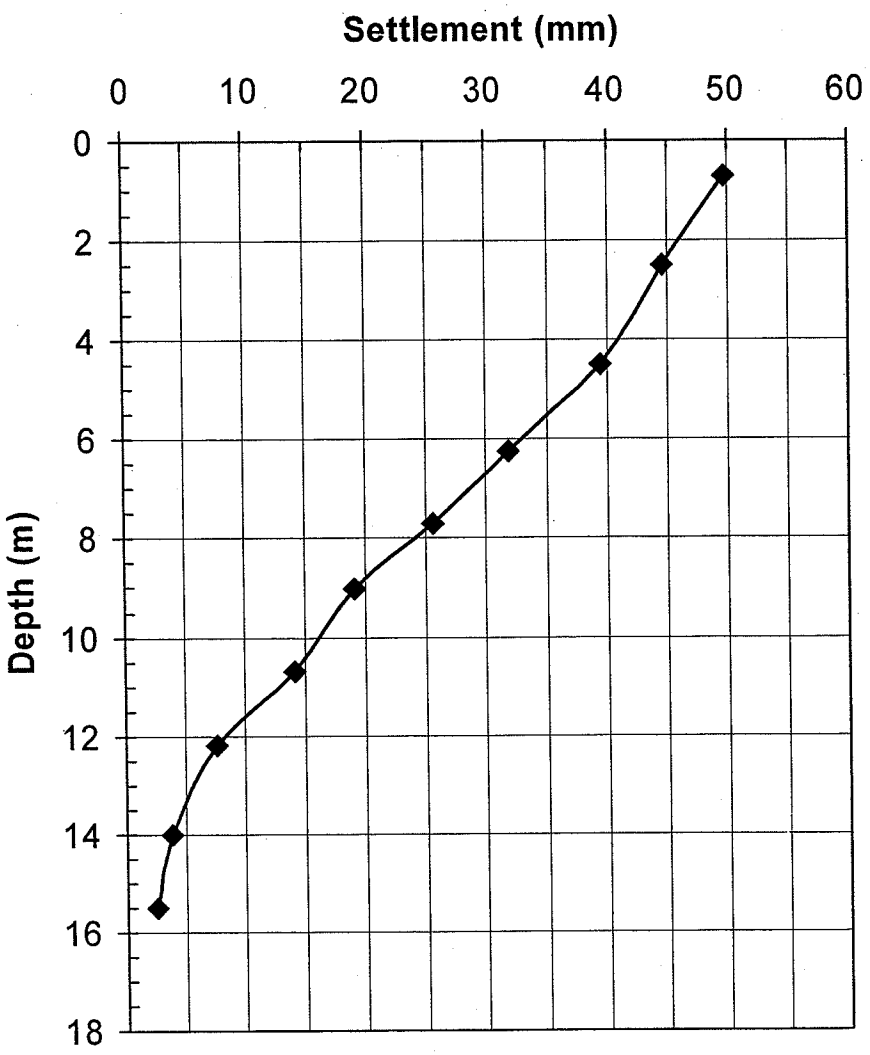

Figure 30 Settlement as a function of depth below the ground surface at the untreated test area (After Gohl, 2002).

5.0 BLAST TESTING AT EQ DRAIN TEST AREAS

5.1 TEST LAYOUT AND INSTRUMENTATION

Blast tests were performed at EQD Test Areas 1 and 2 approximately one week after the drains were installed. The blast sequence used was essentially the same as that employed previously in the tests at the untreated site. Four explosive charges were detonated in each of four holes located at 90 degree intervals around a circle with a radius of 5 m from the center of the drain cluster as shown previously in Fig. 10. In each hole, charge weights of 3.0, 1.8, 1.8 and 1.8 kg were centered at depths of approximately 14,

11, 8, and 5 m, respectively with gravel stemming between each charge. A profile view of the test area showing the charge locations in relation to the drains and piezometers is provided in Fig.31 The water in the PVC pipe was pumped prior to placing the charges and stemming. The charges were detonated one at a time from the bottom up with delays of 0.5 seconds between charges. Therefore, the total blast sequence took about 7.5 seconds. At both sites, large volumes of water began flowing from the drains within about 2 to 3 seconds after the initial charge detonation suggesting that liquefaction, or at least significant excess pore pressures, had been produced.

5.2 PORE PRESSURE RESPONSE

During each EQ Drain test blast, four piezometers pushed into the soil profile were monitored within the test area under consideration. These measurements were made to allow a comparison with pore pressure response in the untreated test area. These piezometers were placed at 6.7, 9.1, 11.6, and 14.0 below the ground as shown in Fig. 31. In addition, two piezometers were placed at depths of 6.7 and 11.6 m within two drains. These measurements were made to evaluate the response of the water in the drain relative to that in the soil between the drains. Finally, four piezometers were monitored at the other EQ Drain test area and four piezometers installed by Pacific Geodynamics (Gohl, 2002) at the gravel drain test area were also monitored. (P-1 @ 8.2 m, P-2@ 12.5 m, P-3 @ 8.2 m and P-6 @ 12.5 m) These measurements were made so that the variation in induced pore pressure response could be evaluated as a function of distance.

Unfortunately, two of the piezometers within each EQD test area, which had been providing reliable data during the installation process, failed prior to the completion of all the blast testing. We suspect that the waterproof cable was damaged by the cone rods during installation and water eventually made its way down the cable and into the strain gauge in the transducer causing it to fail.

Shortly after the first four charges were detonated at each drain test site, water began rapidly flowing out of the drains indicating that high pore pressures had been produced. The measured pore pressure time histories also indicated that liquefaction was produced in about three or four stress cycles produced by the blasting. The large blast

Section A-A

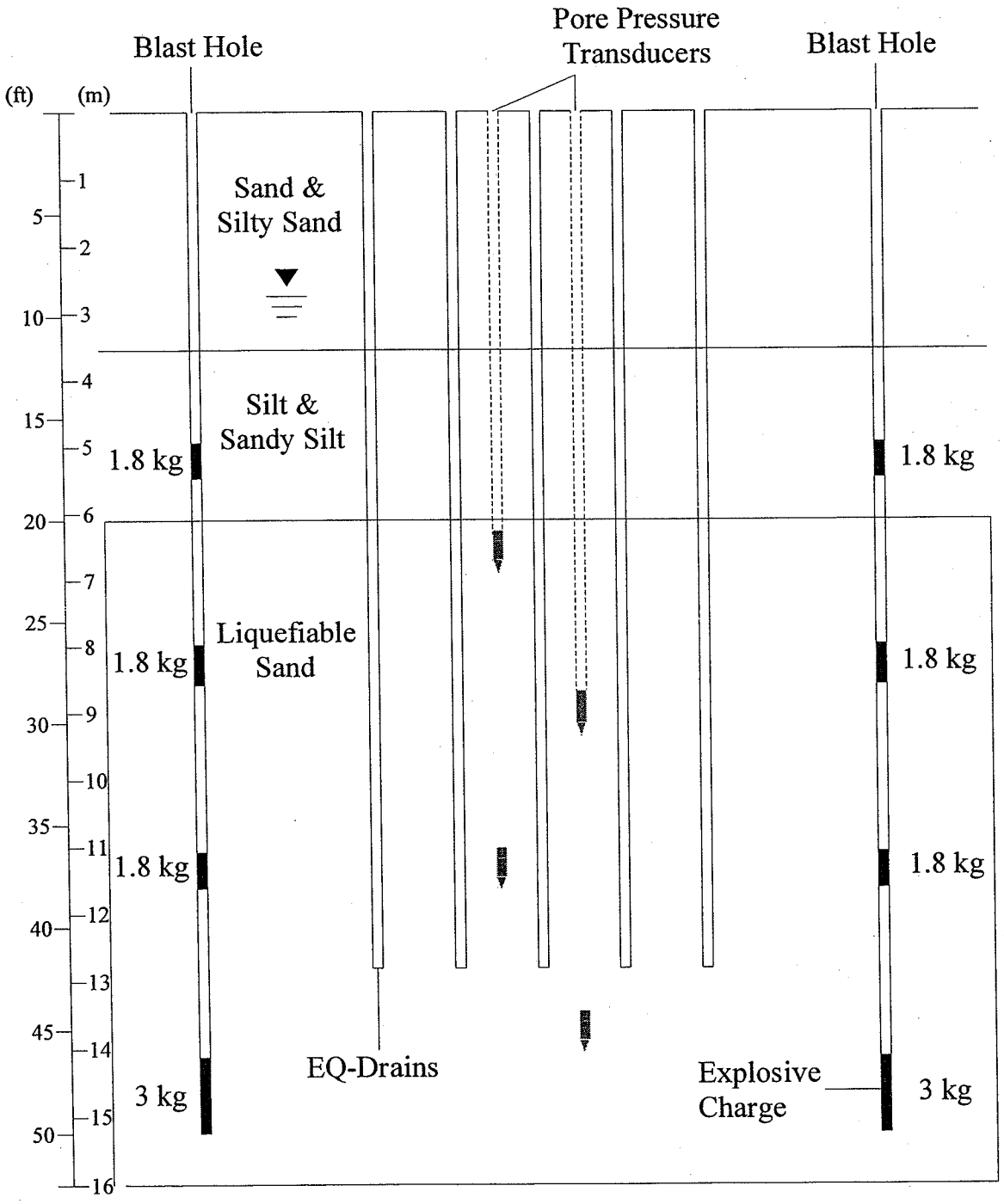

Figure 31 Section AA (see Fig. 10) through center of EQ Drain Test Area showing location of explosive charges in relation to EQ Drains, piezometers, and soil conditions.

charges and the low liquefaction resistance of the sand combined to produce the rapid liquefaction.

In some cases, the water flowing from the drains was dirty indicating that sand was moving into the drain likely at tears in the fabric at the base of the drain as discussed previously. Measurements after testing did not show any buildup of sand in the drains.

R_u versus time curves for piezometers at 6.7 and 11.6 m depths in EQ Drain Test Area 2 (high vibration) are compared with curves from piezometers at similar depths in the untreated test area in Fig. 32. In addition, R_u versus time curves are provided for the transducers positioned inside the drains themselves. Although the EQ Drains were insufficient to prevent initial liquefaction, the rate of dissipation at both depths was significantly greater in the drain test area than in the untreated area. This clearly indicates that the drains were performing their function. The R_u values in the drains themselves also rose following blasting due to water flowing out of the drains and ponding in the settlement basin above the ground surface. The R_u values in the drains remained constant after water reached the top of the settlement basin and began flowing out.

Once the R_u in the ground dropped below the R_u in the drain, the drains no longer provided any benefit and the dissipation rate became essentially equal to that of the untreated soil. At this point, water in the drain began flowing out into the unsaturated soil above the static water table. Fortunately, at this time the drains had already reduced the R_u values to relatively safe levels (between 0.2 and 0.4). Eventually, the ponded surface water flowed back down the drains and the static water level was re-established.

R_u time histories measured by the four piezometers located in the gravel test area during the test blast in EQD Test Area 2 are shown in Fig. 33 (b). On average, these piezometers were located 8.9 m from the nearest blast hole. Peak R_u values were between 0.45 and 0.60. R_u time histories for the four piezometers located in EQD Test Area 1 due to the test blast in EQD Test Area 2 are shown in Fig. 33. On average, these piezometers were located 23.9 m from the nearest blast hole. Peak R_u values for three of the piezometers were approximately 0.1, but one piezometers recorded a peak residual R_u value of 0.34. These data are used subsequently to develop R_u versus scaled distance plots.

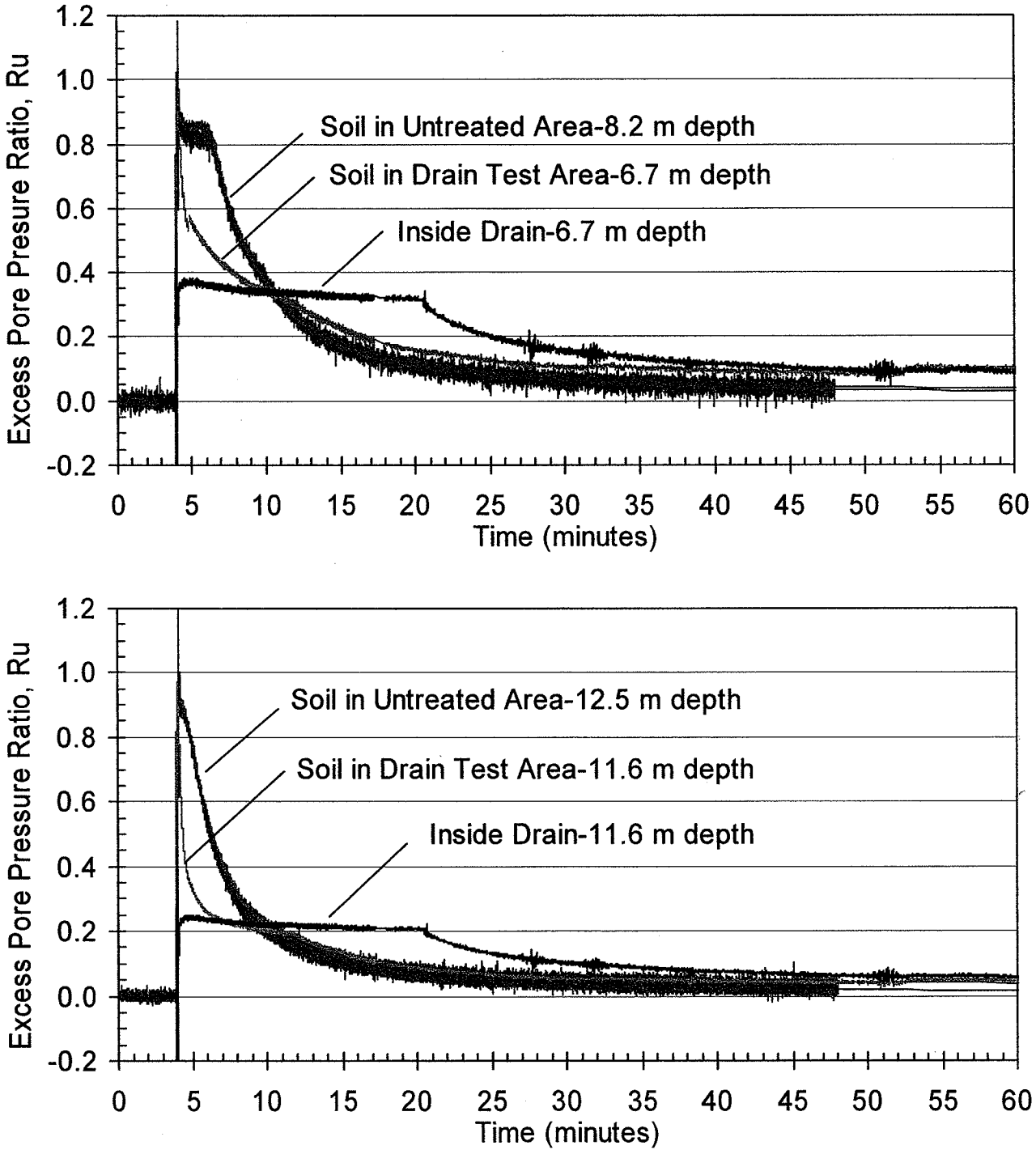

Figure 32 Excess pore pressure ratio time histories for piezometers in the soil and inside a drain at EQ Drain Test Area 2 during test blast. Time histories for piezometers at similar depths in soil at the untreated test area are shown for comparison purposes.

(a)

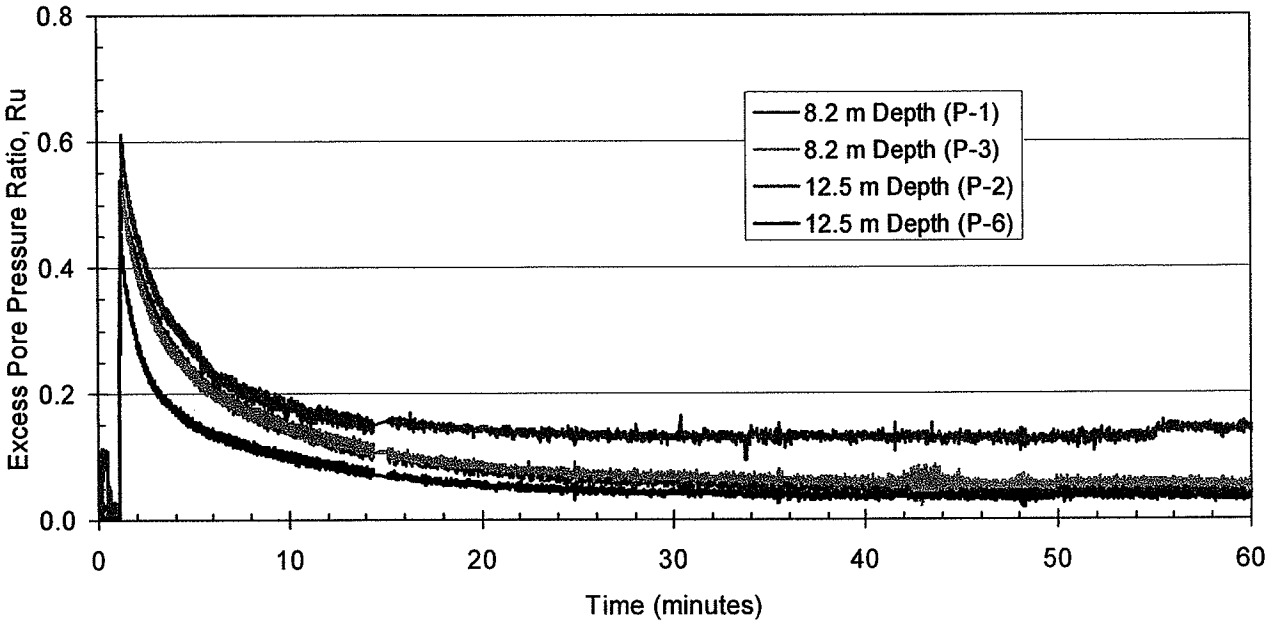

(b)

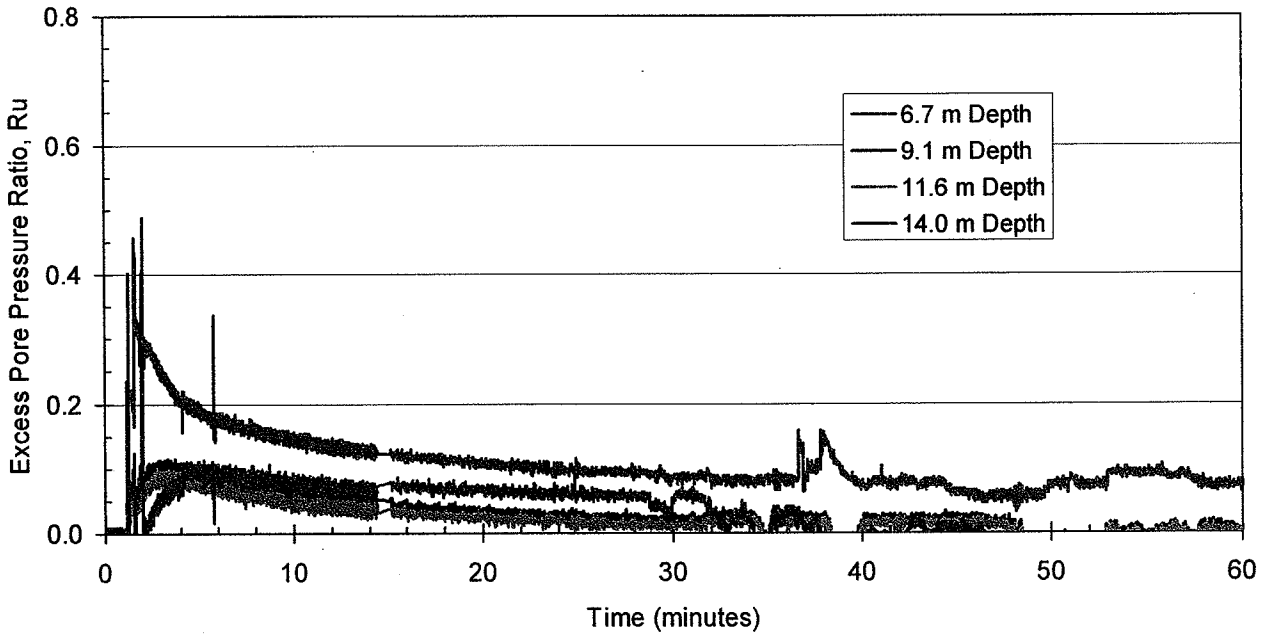

Figure 33 Excess pore pressure ratio time histories measured at (a) the gravel drain test area and (b) EQ Test Area 1 due to the blast at EQ Drain Test Area 2.

R_u versus time curves for piezometers at 9.1 and 12.5 m depths in EQ Drain Test Area 1 (low vibration) are compared with curves from piezometers at similar depths in the untreated test area in Fig. 34. Although transducers were positioned inside the drains themselves at the same elevations as those in the soil, the force of the water erupting from the drains was sufficient to push the transducers up and out of the drains. Once again, the EQ Drains were insufficient to prevent large increases in R_u; however, the peak values were reduced somewhat. In addition, the rate of dissipation at both depths was significantly greater in the drain test area than in the untreated area. Because this test area was not significantly densified during drain installation, these findings suggest that the improvement in dissipation rate is associated with drainage rather than reductions in soil compressibility produced by densification. This indicates that the drainage alone can provide significant benefits in terms of excess pore pressure reduction.

The rate of dissipation slowed considerably after R_u dropped to between 0.4 and 0.2 at the two depths. Based on the measurements at EQD Test Area 2, this is likely the point at which the head in the soil dropped below that in the drain so that dissipation was controlled by the dissipation rate of the soil alone.

R_u time histories recorded by the two functioning piezometers located in EQD Test Area 2 due to the test blast in EQD Test Area 1 are shown in Fig. 35(a). On average, these piezometers were located 23.9 m from the nearest blast hole. Peak R_u values were between 0.11 and 0.18. R_u time histories measured by the four piezometers located in the gravel test area during the test blast in EQD Test Area 1 are shown in Fig. 35 (b). On average, these piezometers were located 37 m from the nearest blast hole. Peak Ru values were relatively small ranging from 0.05 to 0.09. These data are used subsequently to develop R_u versus scaled distance plots.

The peak residual R_u values produced by the explosive charges detonated during this testing program are plotted against the scaled distance in Fig. 36. In this case, the scaled distance is the horizontal distance from the blast hole in meters divided by the cube root of charge weight in kilograms. An average charge weight of 2 kg was used for the Vancouver tests. A linear relationship between R_u and scaled distance proposed by Studer and Kok (1980) is also presented in Fig. 36 along with data from previous blast-induced liquefaction studies at Treasure Island in San Francisco Bay and Charleston,

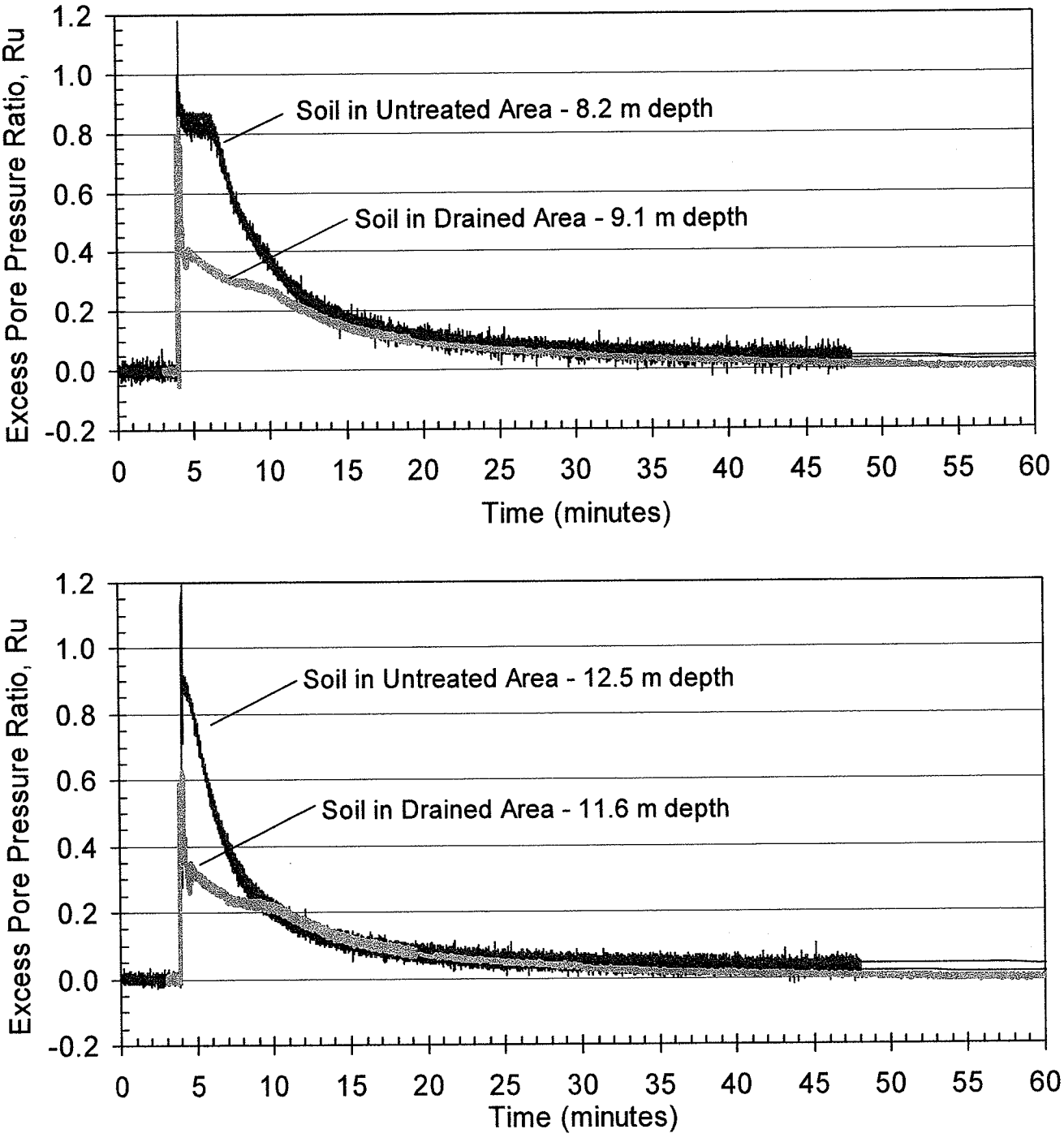

Figure 34 Excess pore pressure ratio time histories for piezometers in the soil and the drain at EQ Drain Test Area 1 during test blast. Time histories for piezometers at similar depths in soil at the untreated test area are also shown for comparison purposes.

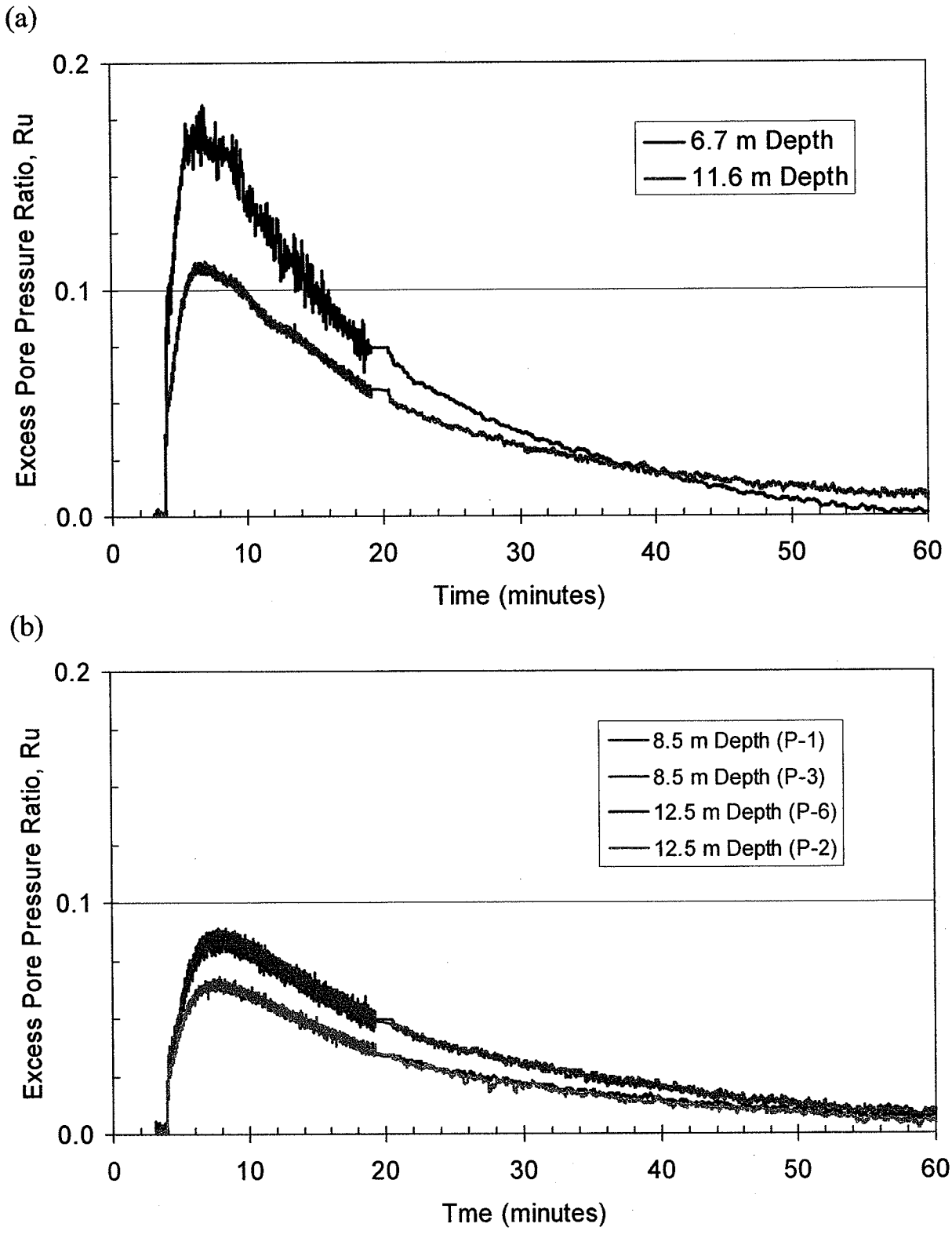

Figure 35 Excess pore pressure ratio time histories measured at (a) EQ Drain Test Area 2 and (b) the untreated test area due to the blast at EQ Drain Test Area 1.

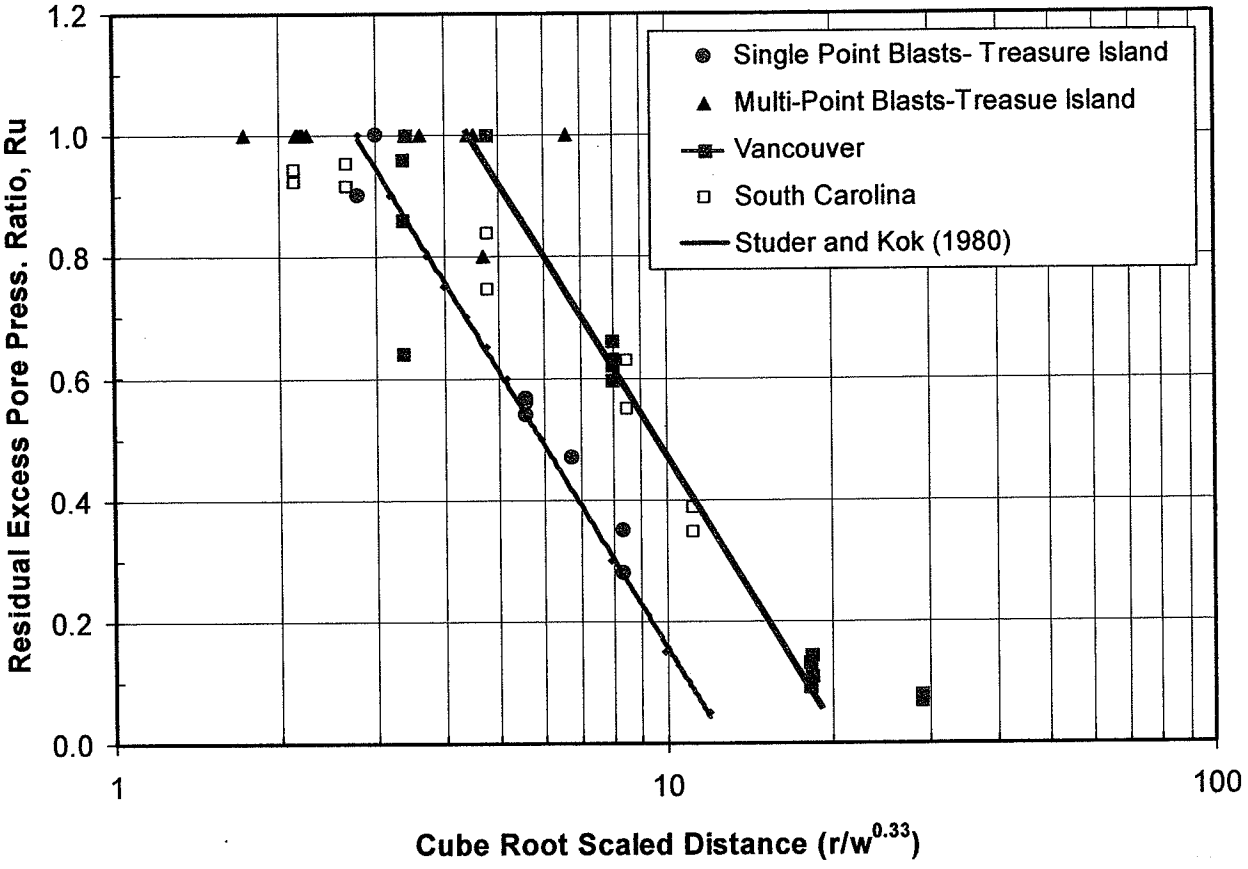

Figure 36 Measured residual excess pore pressure ratio (R_u) as a function of cube root scale distanced ($r/w^{0.33}$) from blast tests at Vancouver, Treasure Island (Rollins et al, 2000), and South Carolina along with mean curve proposed by Studer and Kok (1980) based on single point blasts.

South Carolina. The measured R_u values from the Vancouver tests typically lie significantly above the line proposed by Studer and Kok (1980). Based on previous experience, this is likely due to the fact that multiple blasts were detonated at each hole producing multiple stress cycles. The cumulative effect was to increase the R_u above what would occur for a single charge detonation with the same mass. Previous studies at Treasure Island showed excellent agreement with the Studer and Kok (1980) relationship when single charges were used, but the equation underestimated R_u values when multiple blasts were used. Based on the available data from the Vancouver study, a line roughly parallel to that proposed by Studer and Kok has been developed as shown in Fig. 36. The relationship suggests liquefaction extended 5.5 m beyond the blast holes during the tests. This relationship also yields reasonable estimates of R_u produced at other test sites

5.3 BLAST INDUCED VIBRATION

Ground velocity time histories were recorded by a number of three-component blast seismographs placed at various distances from the explosive charge during each blast. The highest particle velocity in any of the three component directions was then selected as the peak particle velocity (PPV) at that location. The PPV is typically plotted as a function of the scaled distance. The scaled distance in this case is the horizontal distance to the blast hole divided by the square root of the charge mass. This approach is used to normalize for the effect of charge mass so that log-log linear plots can be obtained. The average charge mass of 2 kg was used in normalizing the PPV data.

Fig. 37 presents the peak particle velocity as a function of distance for both EQ Drain test sites along with similar data from the Treasure Island blast testing (Rollins et al, 2000). The data points from Treasure Island are generally consistent with those from

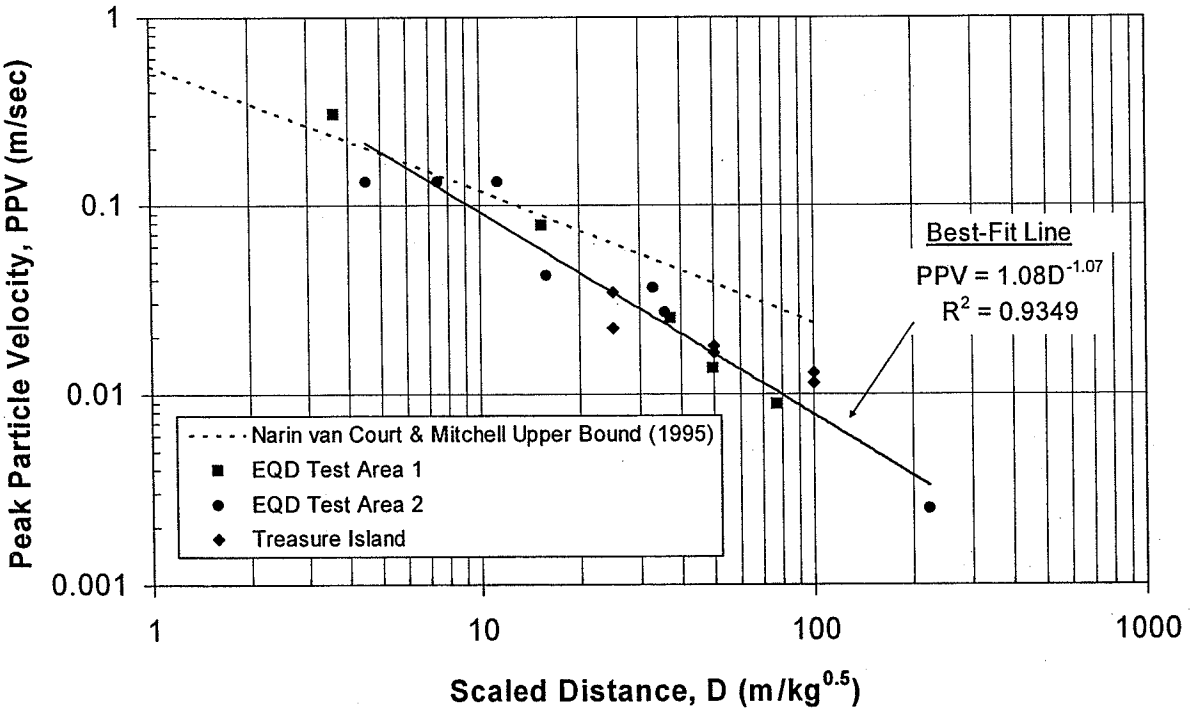

Figure 37 Measured peak particle velocity (PPV) as a function of scaled distance from blast charge for both EQ Drain test areas in Vancouver, BC along with data from testing at Treasure Island.

the Vancouver testing. The data points generally fall below the upper bound defined by data from Narin van Court and Mitchell (1995). Based on the Vancouver data only, the best fit equation for PPV in units of m/sec is

$$PPV = 1.08\ D^{-1.07} \qquad (3)$$

where D is the scaled distance in units of $m/(kg^{0.5})$.

5.4 BLAST INDUCED SETTLEMENT

Before and after each blast, an elevation survey was performed on the points along the rays extending from the center of the drain cluster to evaluate the liquefaction-induced settlement. Post-blast surveys were conducted within about an hour after the blast and then again 18 to 24 hours after the blast. The surveys consistently indicated that essentially all of the settlement occurred within 1 hour after the blast; therefore, the settlement data presented will only involve these data. Contour plots of the settlement around both EQ drain tests areas are presented in Figs. 38 and 39 along with the boundary of the EQ Drains and blast holes locations. Once again, the settlement was greatest at the center of the test area and the settlement contours generally appeared to be concentric about the center of the test area.

Figure 40 presents a plot of the average settlement versus distance from the center of the test area resulting from blasting in EQD Test Area 1 and 2 in comparison with the settlement at the untreated site as measured by Pacific Geodynamics (Blair, 2002). Despite the fact that liquefaction occurred at all three sites, the installation of the drains clearly decreased the measured settlement. For example, at EQD Test Area 2, where high vibration was used during installation, the maximum settlement was 0.2 m less or only 60% of that in the untreated area. Previously, the drain installation in this area had produced more than 0.3 m of settlement. The maximum settlement for Test Area 2 (Finned Mandrel, high vibration) was 0.1 m less or 25% lower than that in EQD Test Area 1 (Pipe mandrel, low vibration). The difference in installation induced settlements at the two tests areas was over 0.2 m.

The general shape of the settlement versus distance curves is also quite different for the area treated with drains relative to the untreated site. For the EQD sites, the

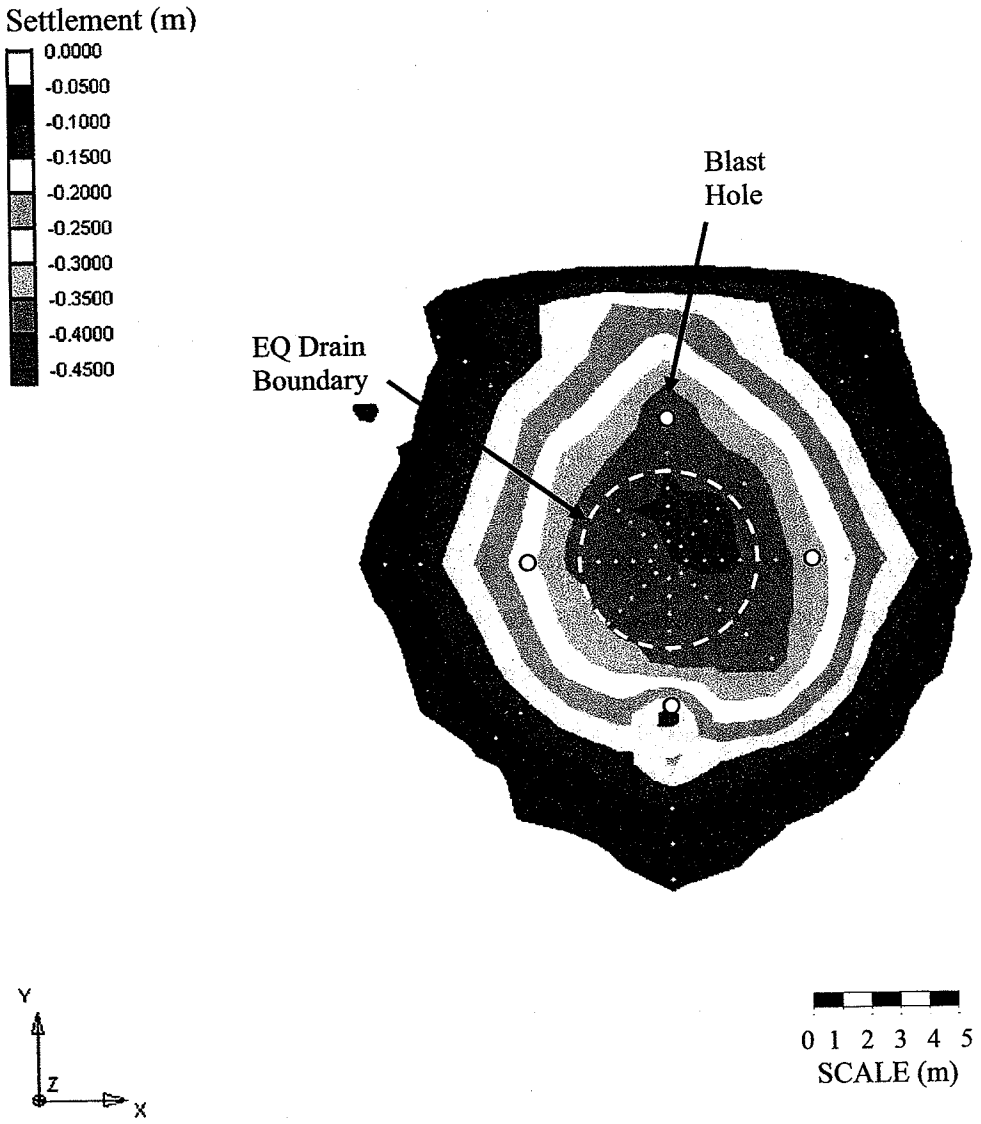

Figure 38 Contours of settlement induced by blast test at EQ Drain Test Area 1 with drains installed using pipe mandrel with low vibration. Blast hole locations, EQ Drain boundaries, and settlement stake locations are also shown

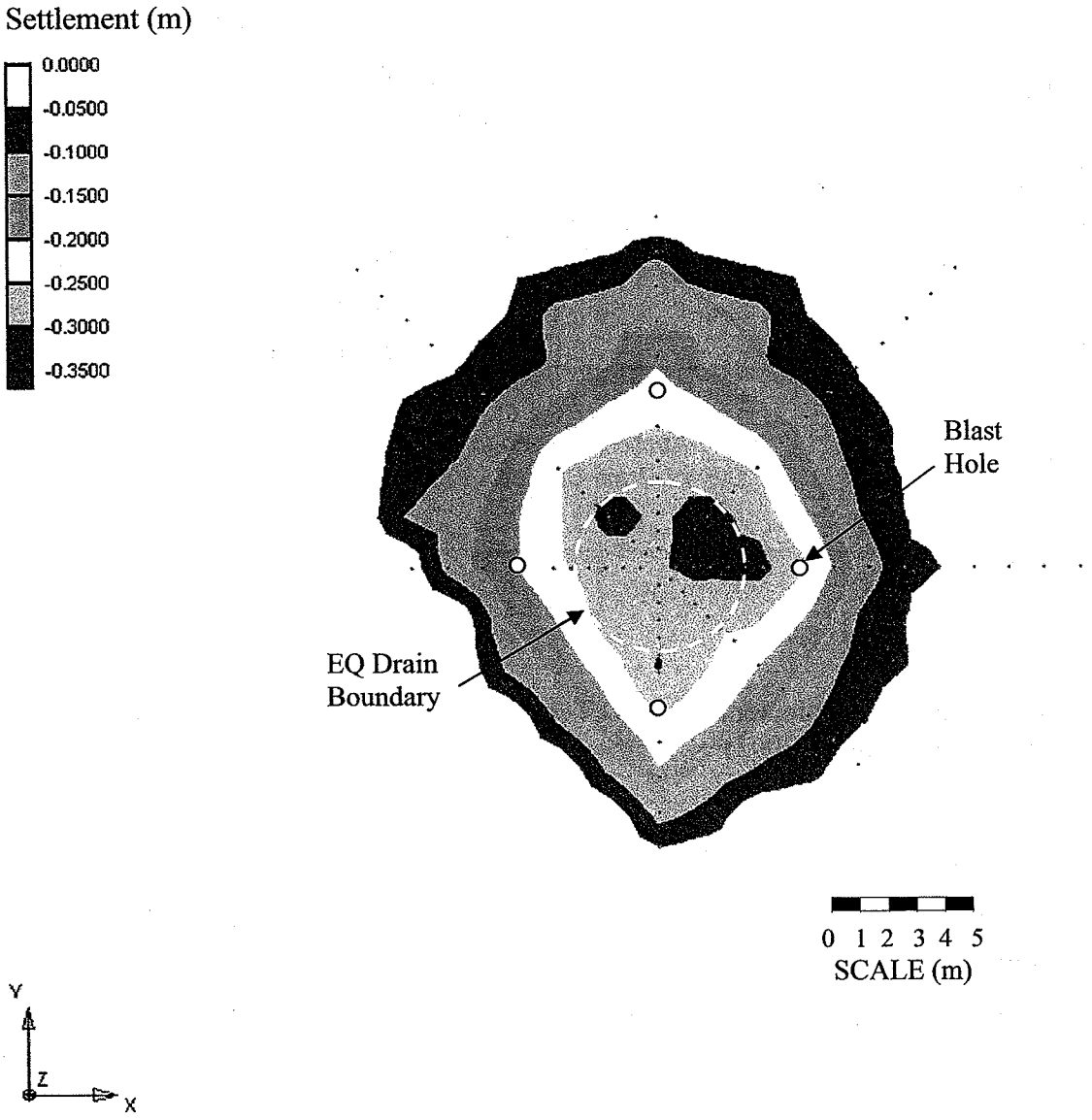

Figure 39 Contours of settlement induced by blast test at EQ Drain Test Area 2 with drains installed using finned mandrel and high vibration. Blast hole locations, EQ Drain boundaries, and settlement stake locations are also shown

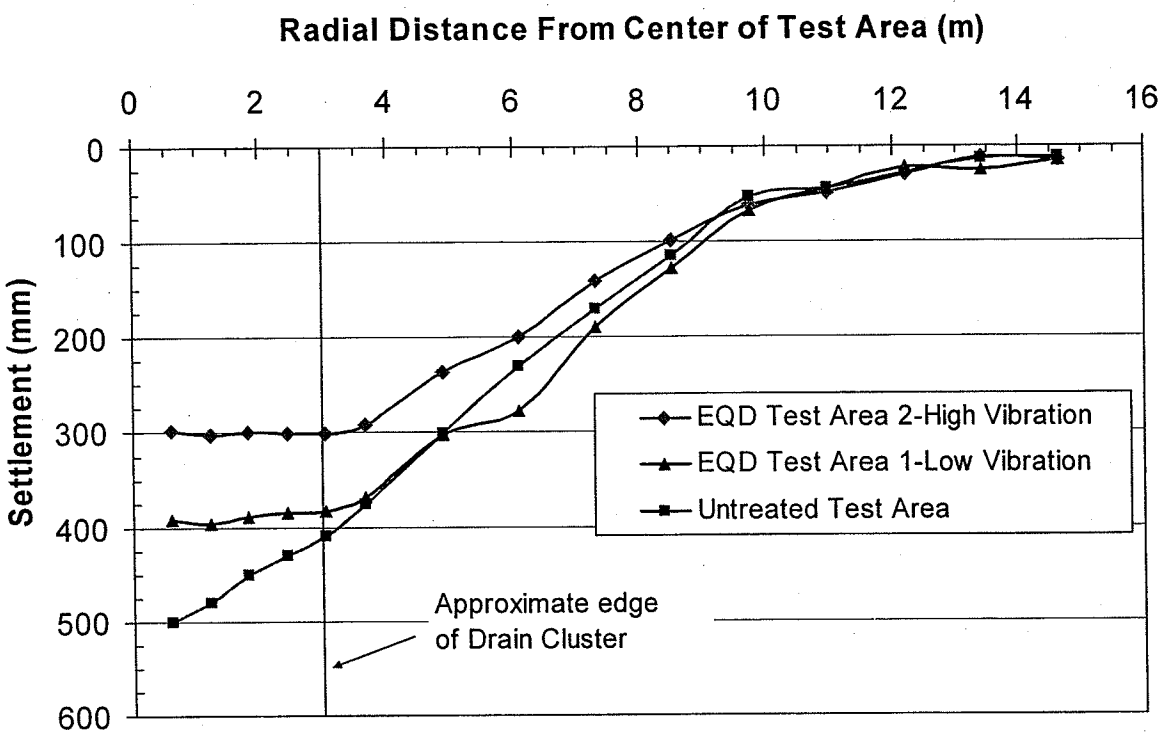

Figure 40 Blast induced settlement for EQD Test Areas 1 and 2 relative to untreated Test Area (Pacific Geodynamics, 2002).

settlement remains nearly constant with distance in the area treated with drains and then decreases with distance beyond this zone. In contrast, in the untreated test area the settlement consistently decreases with distance from the center.

If about half of the observed settlement is in the 7 m-thick clean sand zone from 6 to 13 m in depth, as was the case for the untreated case, then the volumetric strain in EQD Test Area 2 would be 2.1% while the volumetric strain in EQD Test Area 1 would be 2.9%. For comparison, volumetric strain in the untreated area was approximately 3.8%. This reduction in settlement occurred despite high R_u values.

Although the survey data provide the maximum settlement produced by the blast, they do not indicate the rate at which this settlement occurs. To obtain data on the rate of settlement, five string potentiometers were attached to a steel cable that was tensioned across the site between a fence pole and a front-end loader. The potentiometers were

shown in Figs. 10 and 11. Plots of the cone tip resistance as a function of depth are presented for each of the soundings at each test area in Figure 44. A review of the data indicates that there is no consistent increase in resistance with time at either of the sites. The differences appear to be due to natural variation in cone resistance following the blasts. Nevertheless, some trends between pre- and post-blast penetration resistance are apparent in the data. For example, Fig. 45 presents the average cone tip resistance profiles for each site following blasting along with profiles prior to drain installation and immediately after drain installation. At both test areas the post-blast penetration resistance in the clean sand is generally higher than the pre-installation resistance and considerably higher than the resistance immediately following installation. A comparison of the average post-blast CPT profiles at both test areas indicates that the resistance in the clean sand layer is considerably higher for EQD Test Area 2 where the finned mandrel was used with high vibration than for Test Area 1 where a pipe mandrel with low vibration was used. Since both test areas were subjected to the same blast induced stresses, the increased cone tip resistance must be attributed to the densification provided by the installation of the drains.

Profiles of the friction ratio versus depth for each EQD test area are presented in Fig. 46. Curves are provided for one sounding conducted prior to drain installation, one conducted a few days after drain installation and for the average of four soundings over a 56 day period after blasting. In contrast to the cone tip resistance, the friction ratio does not appear to be greatly affected by the drain installation or the blasting. At both sites the friction ratio drops slightly after drain installation and then increases slightly following blasting. The changes seem to be somewhat greater for EQD Test Area 1 but the changes are still quite small.

Based on the average post-blast CPT profile at each site, the relative density has been computed using equation 1. The post-blast relative density profile for each test area is presented in comparison with the profile at the untreated test area in Fig. 47. Because of the densification provided by the drain installation and the blasting, the relative density was increased from about 40% prior to treatment to about 50% in EQD Test Area 1 where low vibration was used and to about 60% in EQD Tests Area 2 where high vibration was used. Since both sites were subjected to the same blast densification, the

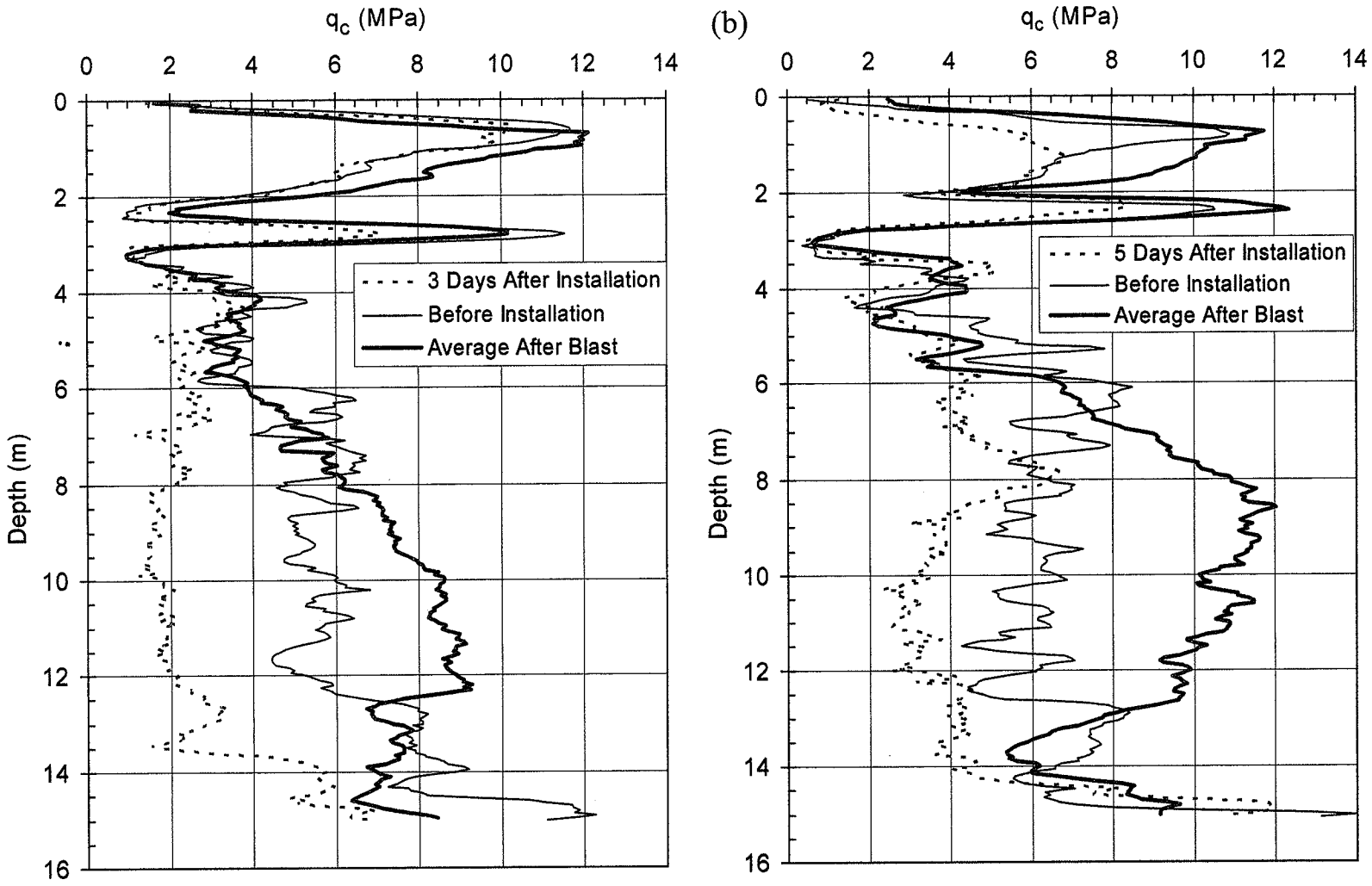

Figure 45 Comparison of cone tip resistance before drain installation, shortly after drain installation and after blasting for (a)EQ Drain Test Area 1 (Low Vibration) and (b) EQ Drain Test Area 2 (High Vibration).

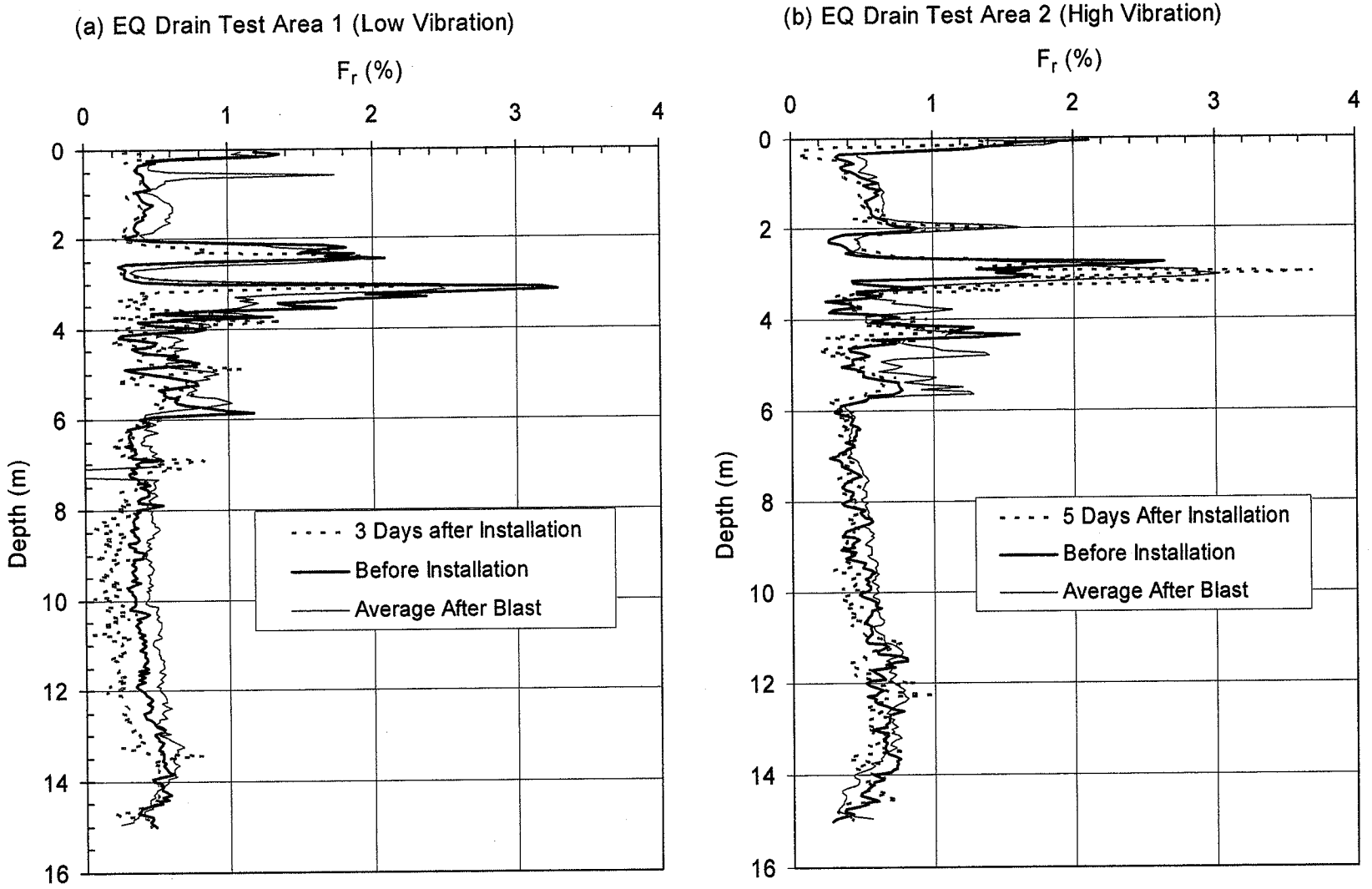

Figure 46 Comparison of friction ratio before drain installation, shortly after drain installation and after blasting for (a)EQ Drain Test Area 1 (Low Vibration) and (b) EQ Drain Test Area 2 (High Vibration).

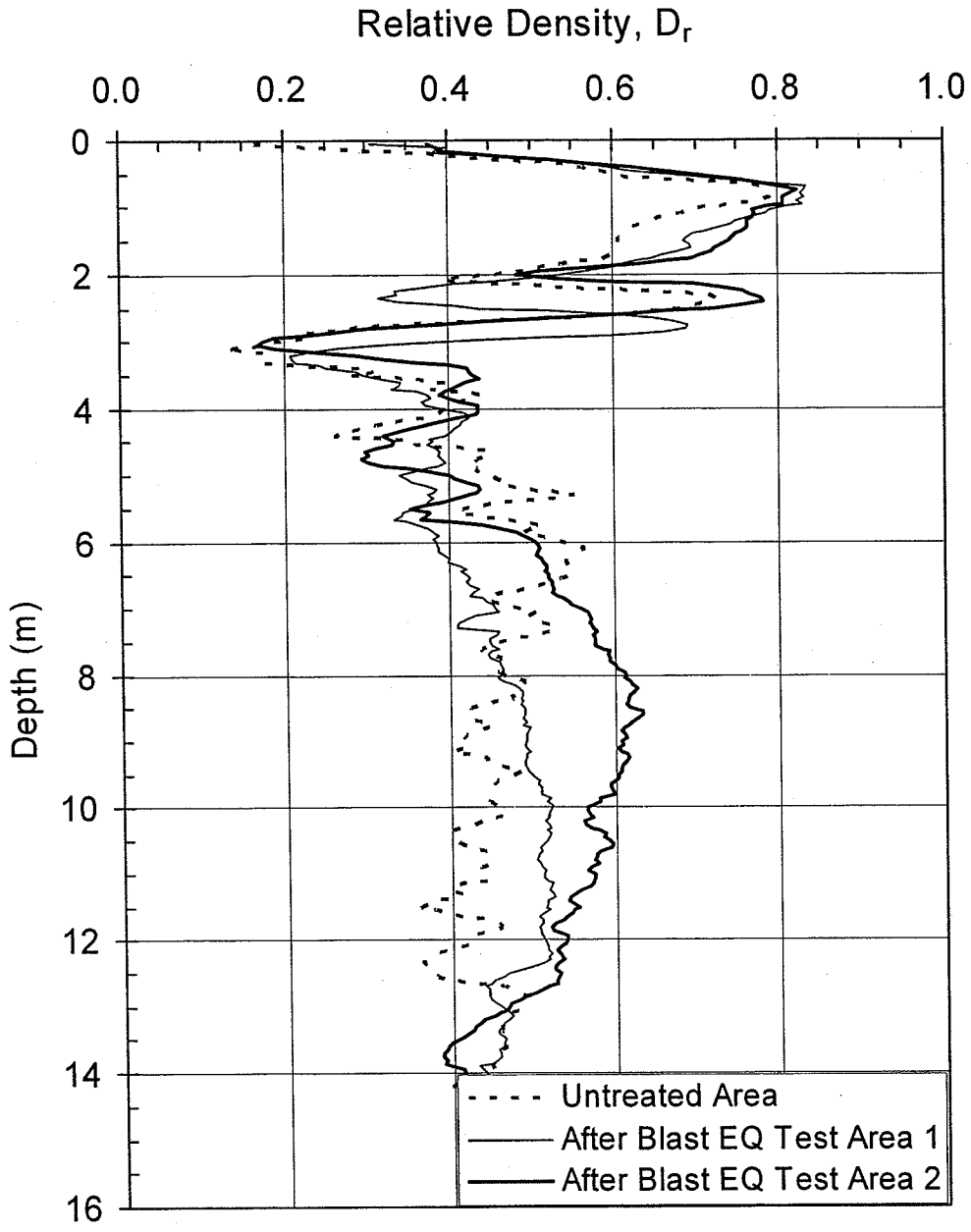

Figure 47 Comparison of relative density versus depth for EQ Drain Test Areas 1 (Low Vibration), and Test Area 2 (high vibration) and in untreated area.

additional 10 percentage point change in relative density at EQD Test Area 2 can be attributed to drain installation effects

6.0 ANALYSIS

Because the blast testing approach produces liquefaction much more rapidly than an earthquake, there is less time for pore pressure dissipation and the effectiveness of drains in an earthquake may be obscured. For example, the blast sequence at the Vancouver test site took only 2 or 3 seconds to produce liquefaction while destructive earthquakes might take 10 to 60 seconds to produce liquefaction. The longer time for pore pressure buildup allows the earthquake drains to operate more effectively in limiting pore pressure generation. That is, pore pressure dissipation through the drains, more easily keeps up with, or exceeds, pore pressure buildup from ground shaking

To provide increased understanding of the behavior of the drains in an earthquake, analyses were performed using the computer program FEQDrain (Pestana et al, 1997). FEQDrain uses an axi-symmetric finite element model of the soil profile and composite drain system. The program models an individual drain within a grid of drains using a "radius of influence" concept based on the drain spacing. The computer program calculates the excess pore pressure ratio in each soil layer within the radius of influence. This is done by accounting for the generation of pore pressure produced by the earthquake and the dissipation of pore pressure provided by flow to the drains.

The program is capable of accounting for head loss in the drain and storage in the drain as water levels change during pore pressure build-up. FEQDrain can also account for non-linear increases in the modulus of compressibility of the soil as the excess pore pressure ratio increases. In addition to computing pore pressure response, the program can compute the settlement due to the dissipation of excess pore pressures.

During this study, the computer model was first calibrated using the measured settlement and pore pressure response from the blast test. Then, the calibrated soil properties were held constant while the duration of shaking was increased to match typical earthquake durations.

6.1 CALIBRATION OF COMPUTER MODEL

6.1.1 Selection of Soil Input Parameters

The basic soil profile and layer thickness values used in the analysis of each EQ Drain tests area was based on the CPT profiles previously shown in Figs. 4 and 5. The

five most important soil properties in matching the pore pressure history and settlement are the horizontal hydraulic conductivity (k_h), vertical hydraulic conductivity (k_v), modulus of compressibility (M_v), relative density (Dr), and the number of cycles required to cause liquefaction (N_L).

Hydraulic Conductivity

The horizontal hydraulic conductivity is perhaps the most important factor governing the rate of dissipation. As k_h increases, the rate of dissipation increases. In general, the vertical hydraulic conductivity does not greatly influence the response since most of the drainage is radial or horizontal. For example, Seed and Booker (1977) used $k_v = 0$ in original computations for their design charts. In relatively uniform sands, k_v has little effect as shown by Pestana et al (1997); however, in layered soil strata, k_v can sometimes be important. Typical ranges of k_h as a function of soil type are provided by Pestana et al (1997) based on recommendations from Terzaghi and Peck (1948) in Table 3. A review of the data in the Table 3 indicates that significant variation can occur within a given soil type due to minor variations in fines content and density. Other investigators have indicated that the variation in k_h within a given soil type could be as much as two orders of magnitude (Freeze and Cherry, 1979)

Table 3 Typical values for horizontal hydraulic conductivity (k_h) from Pestana et al, 1997 (after Terzaghi and Peck, 1948).

Soil Type	Particle Size (mm)	Coefficient of hydraulic conductivity (cm/sec)
Very Fine Sand	0.05-0.10	0.001-0.005
Fine Sand	0.10-0.25	0.005-0.01
Medium Sand	0.25-0.50	0.01-0.1
Coarse Sand	0.50-1.00	0.1-1.0
Small Pebbles	1.00-5.00	1.0-5.0

Due to layering effects and soil structure orientation under stress, the horizontal hydraulic conductivity is typically higher than the vertical hydraulic conductivity. Typical ratios of the horizontal to vertical hydraulic conductivity for various soil conditions are given in Table 4.

Table 4 Relationship between k_h and k_v from Pestana et al (1997).

Description	k_h/k_v
Uniform (clean sands)	1.5-2.0
Moderately anisotropic (silt seams)	4.0-5.0
Highly anisotropic	10-100

The horizontal hydraulic conductivity used in this study was initially selected based on the measured in-situ by the packer tests as shown previously in Figure 8. The ratio of k_h/k_v was generally assumed to be between 2 and 3. In an iterative process, adjustments were made to the k values used in FEQ Drain to improve the match between the computed and measured pore pressure response in the various soil layers. The final profiles of k_h versus depth for the two EQ Drain Test Areas are shown in Fig. 48. Although the k values did increase somewhat from the initial values, the final values are still well within the ranges measured by the various in-situ test methods described previously. The back-calculated k_h values for EQ Drain Test Area 1 (low vibration) are higher than those for Area 2 (high vibration) as would be expected due to the density difference, but the difference decreases with depth.

Modulus of Compressibility

The modulus of compressibility (M_v) is a measure of the vertical strain produced by a change in vertical stress. This parameter is roughly equivalent to the inverse of the elastic or Young's modulus. Although M_v is often measured for clays while pore pressures dissipate, very few studies have made measurements of M_v for sands during pore pressure dissipation. Based on studies by Lee and Albeisa (1974), M_v for sand typically lies within a fairly narrow band ranging from 2.05×10^{-7} to 4.10×10^{-7} m^2/kN and is not sensitive to relative density. However, as the excess pore pressure ratio (R_u) increases beyond about 0.60, the M_v can increase significantly as shown in Fig. 49(a). In these cases, M_v is dependent on both the relative density and the excess pore pressure ratio. Seed et al (1974) developed a relationship to account for the variation in M_v with D_r and R_u as shown in Fig. 49 (b). This relationship is used in the computer model FEQDrain.

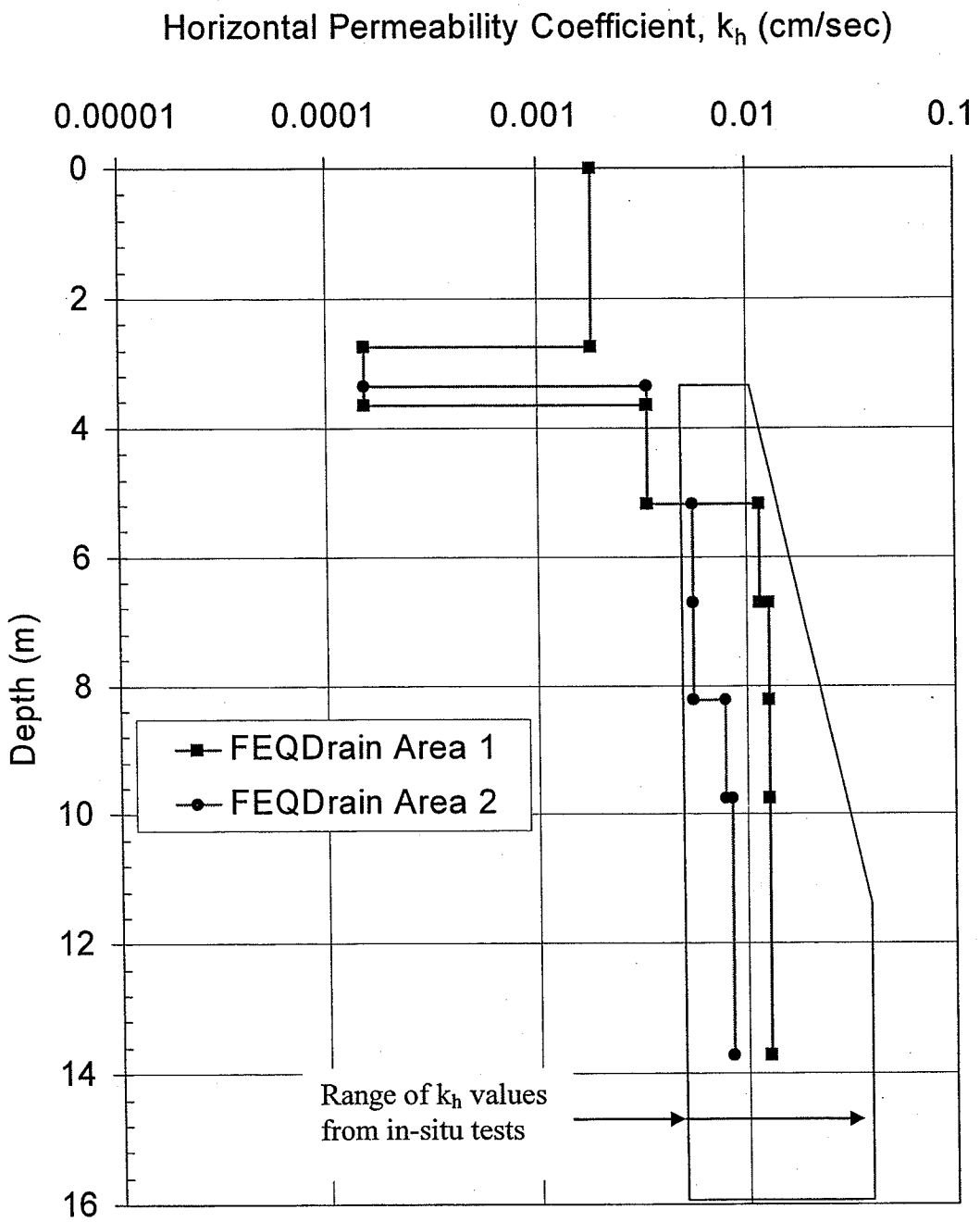

Figure 48 Comparison of measured horizontal hydraulic conductivity (k_h) versus depth with back-calculated values from FEQDrain for EQ Drain Test Areas 1 and 2.

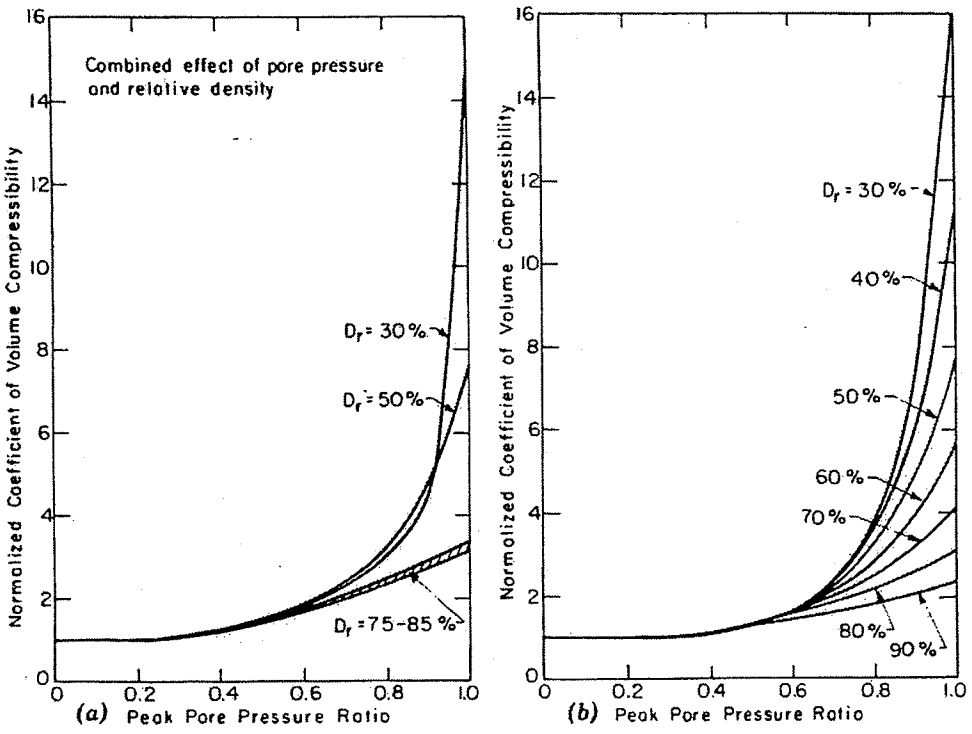

Figure 49 Variation in normalized coefficient of compressibility (M_v/M_{vi} versus) peak pore pressure ratio (R_u) for sands of various relative densities (D_r) from (a) laboratory tests, and (b) as modeled in FEQDrain (Seed et al, 1976).

The computed settlement is directly proportional to M_v; therefore, a simple check of the measured settlement against the computed settlement is usually enough to find the correct M_v. Once again, relatively small changes were sufficient to provide good agreement and the modified M_v values were at the high end of the acceptable range of values, which appears reasonable for the loose sand involved. Unfortunately, changing M_v also changed the time required for the pore pressures to dissipate. Therefore, if M_v was decreased to improve the match with settlement, k_h would have to be increased to maintain the match with the rate of dissipation.

Relative Density

The estimates of relative density were made based on the initial values provided by the CPT soundings. This parameter was not modified greatly during the investigation.

Number of Cycles to Cause Liquefaction

Another important characteristic of the soil is the number of cycles required to cause liquefaction (N_L). The N_L for the blast simulation was obtained by determining the

time at which liquefaction occurred using the pore pressure ratio versus time plot measured at the site as shown in Fig. 27. The soil was essentially liquefied just after the fourth detonation, suggesting that N_L for the liquefiable layers was four in this case.

Summary of Input Parameters

A summary of the initial estimates of the various soil input parameters used in the analysis is presented in Table 5.

Table 5 Initial estimates of soil properties used in FEQ Drain analysis.

Layer Number	k_h (cm/sec)	k_v (cm/sec)	M_v (m^2/kN)	D_r
1	$1.83x10^{-3}$	$5.49x10^{-3}$	$2.1x10^{-5}$	0.7
2	$1.52x10^{-4}$	$4.56x10^{-4}$	$4.2x10^{-5}$	0.6
3	$2.13x10^{-3}$	$6.10x10^{-3}$	$4.2x10^{-5}$	0.4
4	$3.05x10^{-3}$	$9.14x10^{-3}$	$4.2x10^{-5}$	0.4
5	$3.96x10^{-3}$	$1.22x10^{-2}$	$4.2x10^{-5}$	0.4
6	$3.96x10^{-3}$	$1.22x10^{-2}$	$4.2x10^{-5}$	0.4
7	$3.96x10^{-3}$	$1.22x10^{-2}$	$4.2x10^{-5}$	0.4

The final soil properties for each EQ Drain Test Area obtained by trial and error with FEQDrain are shown in Fig. 50. A comparison of the back-calculated parameters for the two test areas indicates that somewhat lower k and m_v values were obtained for the EQ Drain Test Area 2 where higher vibration was used relative to Area 1. This is an independent confirmation of the effectiveness of vibratory installation of the drains in improving soil properties.

6.2.1 Drain input properties

The radius of the drain was 6 cm which corresponded to a drain area of 114.3 cm^2. The radius of the area of influence was 0.64 m which represents a drain spacing of 1.22 m. The area of openings per unit length in the perforated pipe was 0.004 m^2/m and the constant associated with head loss through the perforations was taken as 1.0. The equation for head loss due to vertical resistance in the drain (H_{drain}) was given by

$$H_{drain} = 0.5\ (Q \cdot z)^2. \qquad (4)$$

where Q is flow rate and z is depth.

EQ Drain Test Area 1 (Low Vibration)			
	Layer Thickness	Depth to Sublayer	Description of soil and soil properties
Layer 1	2.134 m - 4 Sublayers	0.533 m 1.067 m 1.600 m 2.134 m	Silty Sand/Sand kh = 1.83E-03 cm/s kv = 0.92E-03 cm/s Mv = 2.1E-05 m^2/kN Dr = 0.7
Layer 2	1.524 m - 2 Sublayers	2.896 m 3.658 m	Clayey Silt kh = 1.52E-04 cm/s kv= 0.76E-04 cm/s Mv = 3.76E-05 m^2/kN Dr = 0.6
Layer 3	1.524 m - 6 Sublayers	3.912 m 4.166 m 4.420 m 4.674 m 4.928 m 5.182 m	Sandy Silt kh = 3.35E-03 cm/s kv = 1.68E-03 cm/s Mv = 4.2E-05 m^2/kN Dr = 0.4
Layer 4	1.524 m - 5 Sublayers	5.486 m 5.791 m 6.096 m 6.401 m 6.706 m	Silty Sand/Sand kh = 1.16E-02 cm/s kv = 0.58E-02 cm/s Mv = 4.4E-05 m^2/kN Dr = 0.4
Layer 5	1.524 m - 5 Sublayers	7.010 m 7.315 m 7.620 m 7.925 m 8.230 m	Silty Sand/Sand kh = 1.28E-02 cm/s kv = 0.64E-02 cm/s Mv = 4.4E-05 m2/kN Dr = 0.4
Layer 6	1.524 m - 5 Sublayers	8.535 m 8.839 m 9.144 m 9.449 m 9.754 m	Silty Sand/Sand kh = 1.28E-02 cm/s kv = 0.64E-02 cm/s Mv = 4.4E-05 m^2/kN Dr = 0.4
Layer 7	3.962 m - 9 Sublayers	10.193 m 10.631 m 11.070 m 11.509 m 11.948 m 12.387 m 12.826 m 13.265 m 13.716 m	Silty Sand/Sand kh = 1.28E-02 cm/s kv = 0.64E-02 cm/s Mv = 4.2E-05 m^2/kN Dr = 0.4

EQ Drain Test Area 2 (High Vibration)			
	Layer Thickness	Depth to Sublayer	Description of soil and soil properties
Layer 1	2.743 m - 4 Sublayers	0.6858 m 1.372 m 2.057 m 2.743 m	Silty Sand/Sand kh = 1.83E-03 cm/s kv = 0.92E-03 cm/s Mv = 2.10E-05 m^2/kN Dr = 0.7
Layer 2	0.61 m - 2 Sub-layers	3.048 m 3.353 m	Clayey Silt: kh=1.52E-04 cm/s kv=0.77E-04 cm/s Mv = 4.2E-05 m^2/kN Dr = 0.7
Layer 3	1.829 m - 6 sublayers	3.658 m 3.962 m 4.267 m 4.572m 4.877m 5.182 m	Sandy Silt kh = 3.35E-03 cm/s kv = 1.68E-03 cm/s Mv = 4.2E-05 m^2/kN Dr = 0.4
Layer 4	1.524 m - 5 sublayers	5.486 m 5.791 m 6.096 m 6.401 m 6.706 m	Silty Sand/Sand kh = 5.49E-03 cm/s kv = 2.75E-03 cm/s Mv = 4.1E-05 m^2/kN Dr = 0.4
Layer 5	1.524 m - 5 sublayers	7.010 m 7.315 m 7.620 m 7.925 m 8.230 m	Silty Sand/Sand kh = 5.49E-03 cm/s kv = 2.75E-02 cm/s Mv = 4.1E-05 m^2/kN Dr = 0.4
Layer 6	1.524 m - 5 sublayers	8.535 m 8.839 m 9.144 m 9.449 m 9.754 m	Silty Sand/Sand kh = 7.92E-03 cm/s kv = 3.96E-03 cm/s Mv = 4.1E-05 m^2/kN Dr = 0.4
Layer 7	3.962 m - 9 Sublayers	10.193 m 10.631 m 11.070 m 11.509 m 11.948 m 12.387 m 12.826 m 13.265 m 13.716 m	Silty Sand/Sand kh = 4.66E-03 cm/s kv = 1.83E-03 cm/s Mv = 4.1E-05 m2/kN Dr = 0.4

Figure 50 Summary of calibrated soil layers and final soil properties used in FEQDrain.

6.1.3 Other Required Input Parameters

To simulate the blast testing as an earthquake in FEQDrain, we had to determine the equivalent number of cycles (N_q) due to the "earthquake" loading that occurred as a result of the detonations and the duration of the "earthquake" event. This was accomplished by counting pulse peaks recorded by the blast accelerometers and piezometers. Sixteen detonations with a delay of 0.5 seconds between each detonation produced sixteen relatively distinct peaks. These were taken to be the cycles for the blast simulation in FEQDrain. The duration (t_d) of the explosions was pulled from the same plot of pore pressure generation. The event lasted approximately 8 seconds and this value was used for t_d.

Normally, the hydraulic head boundary at the top of the drain is set equal to the ground elevation because water can flow away from the drain above this level. However, in this case, the installation of the drains created a settlement basin around the drains. Therefore, the head boundary was set equal to the elevation above the ground surface at which water could flow out of the basin. The volume of water necessary to raise the water level above the ground surface was specified as a "reservoir". The reservoir volume was set equal to the equivalent diameter (d_e) of the tributary area around the drain multiplied by the height above the ground surface at which water flows out of the basin. For a triangular drain spacing, d_e is equal to 1.05 times the drain spacing.

6.1.4 Comparison of Measured and Computed Pore Pressure and Settlement

A comparison of the measured and computed excess pore pressure ratio time histories at depths of 9.1 and 11.6 m in EQ Drain Test Area 1 are presented in Figs. 51 and 52, respectively. Similar comparisons are provided in Figs. 53 and 54 for depths of 6.7 and 11.6 m, respectively, in EQ Drain Test Area 2. In general, the agreement between measured and computed pore pressure response is very good for both depths at EQD Test Area 2. The computed response does not account for the peaks and troughs in the time history produced by each blast detonation, but the average or residual pore pressure is reasonably well captured. In addition, there is good agreement with the measured dissipation rate out to a time of 100 seconds or more.

For EQD Test Area 1, the agreement is reasonably good for the dissipation portion of the curve but there are some discrepancies as pore pressure are being

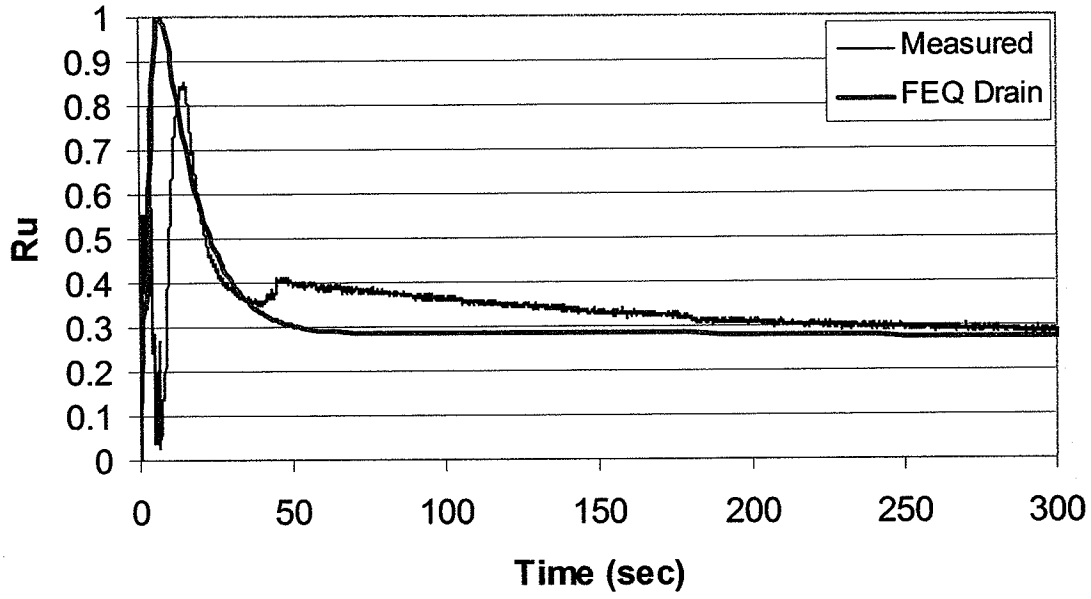

Figure 51 Comparison of measured R_u time history at EQD Test Area 1 (low vibration) with history computed by FEQDrain at 9.14 m depth.

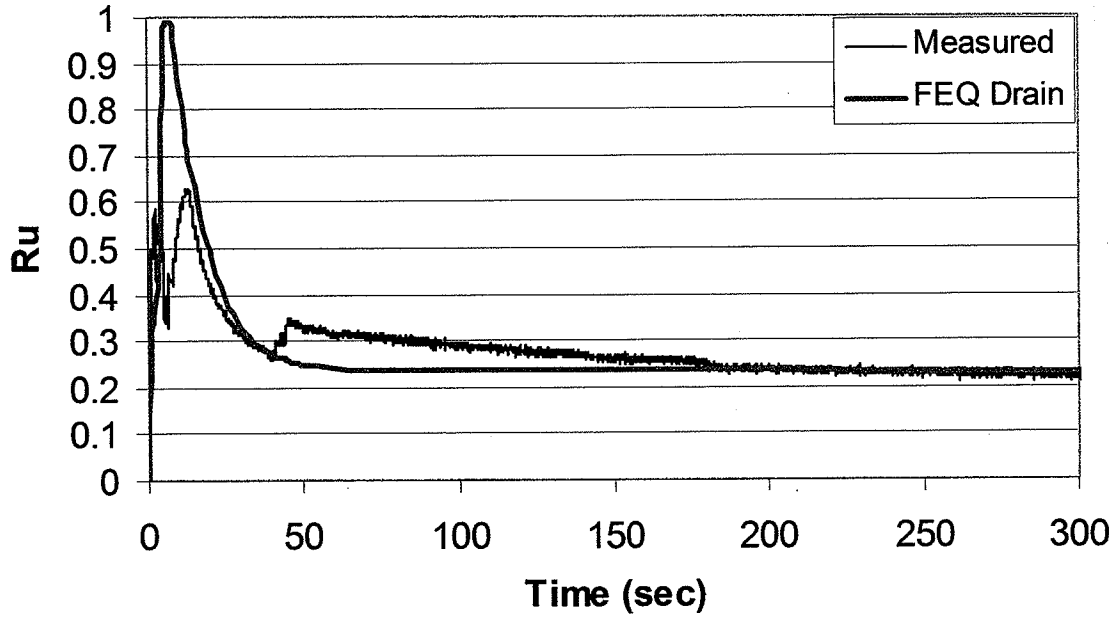

Figure 52 Comparison of measured R_u time history at EQD Test Area 1 (low vibration) with history computed by FEQ Drain at 11.6 m depth.

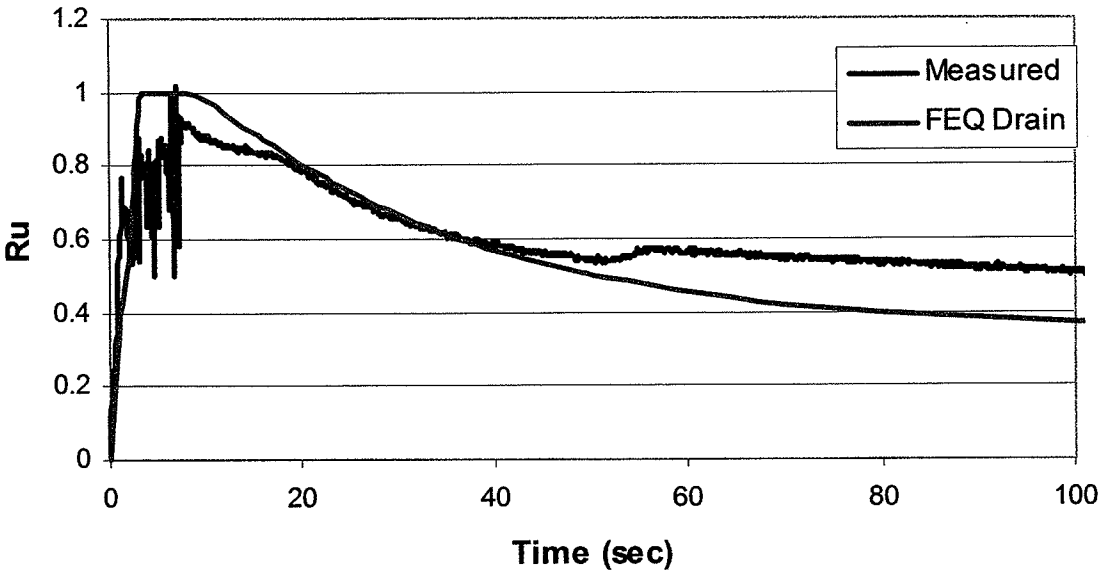

Figure 53 Comparison of measured R_u time history at EQ Drain Test Area 2 (high vibration) with history computed using FEQDrain at 6.71 m depth.

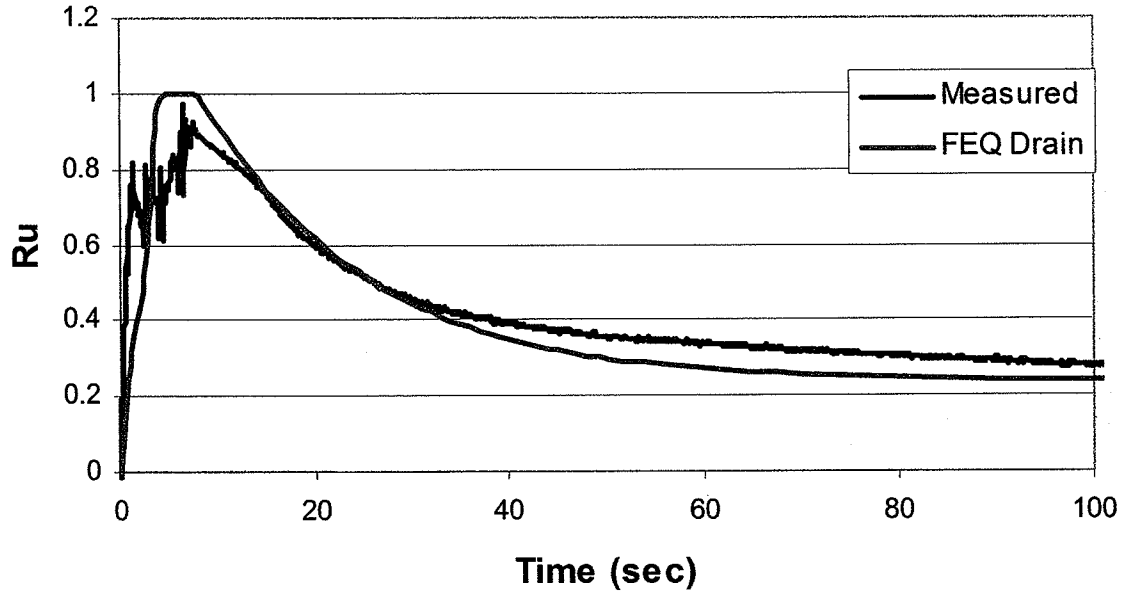

Figure 54 Comparison of measured R_u time history at EQ Drain Test Area 2 (high vibration) with history computed using FEQDrain at 11.6 m depth.

generated. The computed time histories show a parabolic curve reaching an R_u of 1.0 and then decreasing. In contrast, the measured response shows troughs in the R_u time history just as the peak in R_u would be expected. The measured response at 9.1 m appears to be less affected by this phenomenon and the agreement with the computed response overall is relatively good. However, the measured response at 11.6 m is more affected and the agreement in this time interval is poor. Since liquefaction clearly occurred at this test site, based on the flow coming from the drains, there is a strong likelihood that the measured response at 11.6 m does not represent the general behavior in this layer and that an R_u of 1.0 actually did occur as predicted by the computer model.

Comparisons of the measured settlement time histories with those computed using FEQDrain for EQ Drain Tests Areas 1 and 2 are provided in Figs. 55 and 56, respectively. The general shape of the computed settlement versus time curves is very similar to the measured shape, although somewhat smoother. In addition, the computed maximum settlement is close to the measured maximum settlement.

It was not possible to accurately model the pore pressure and settlement response at the untreated site using FEQ Drain because the program assumes an infinite area of liquefaction. If no drains are present, this prevents the horizontal hydraulic conductivity from having any effect on the rate of dissipation of pore water pressure in the computer model. In this case the dissipation is controlled almost exclusively by the vertical hydraulic conductivity. However, the blast testing only liquefies a circular area approximately 11 m in radius, which allows some of the water to dissipate horizontally into the surrounding soil. As a result, FEQ Drain consistently overestimates the time for pore pressure dissipation relative to the measured behavior when the calibrated k_h, k_v and M_v values are employed. In addition, FEQDrain cannot account for the presence of sand boils which would have the effect of partially draining the liquefied sand layer. Good agreement could potentially be obtained using fictitious values for k_v, but this exercise would not serve any useful purpose.

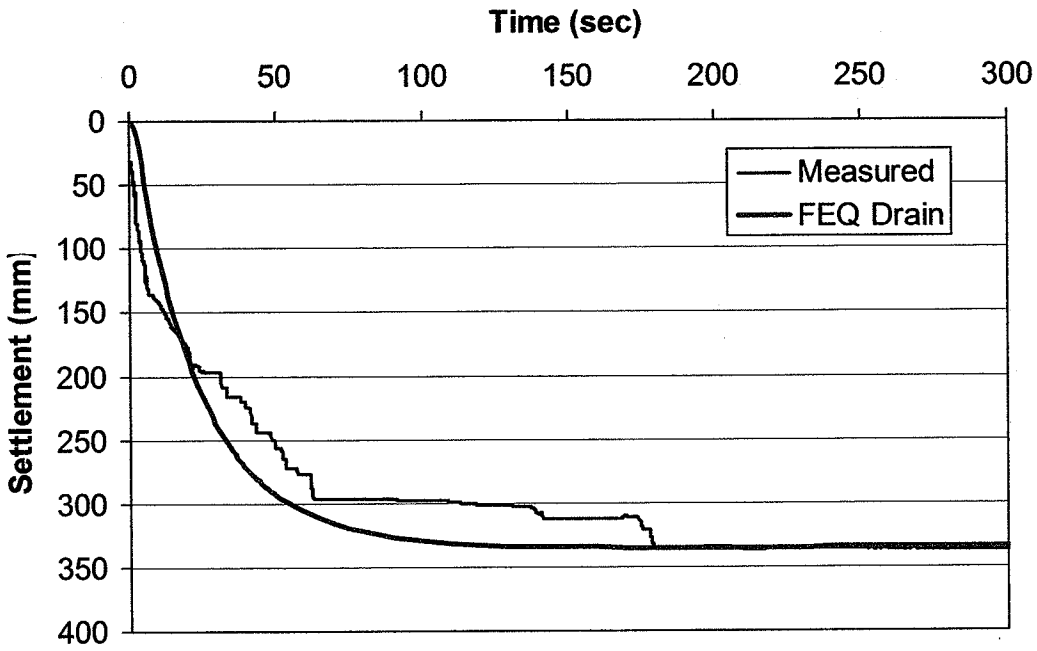

Figure 55 Comparison of measured and computed settlement versus time curves for EQ Drain Test Area 1 (Low Vibration).

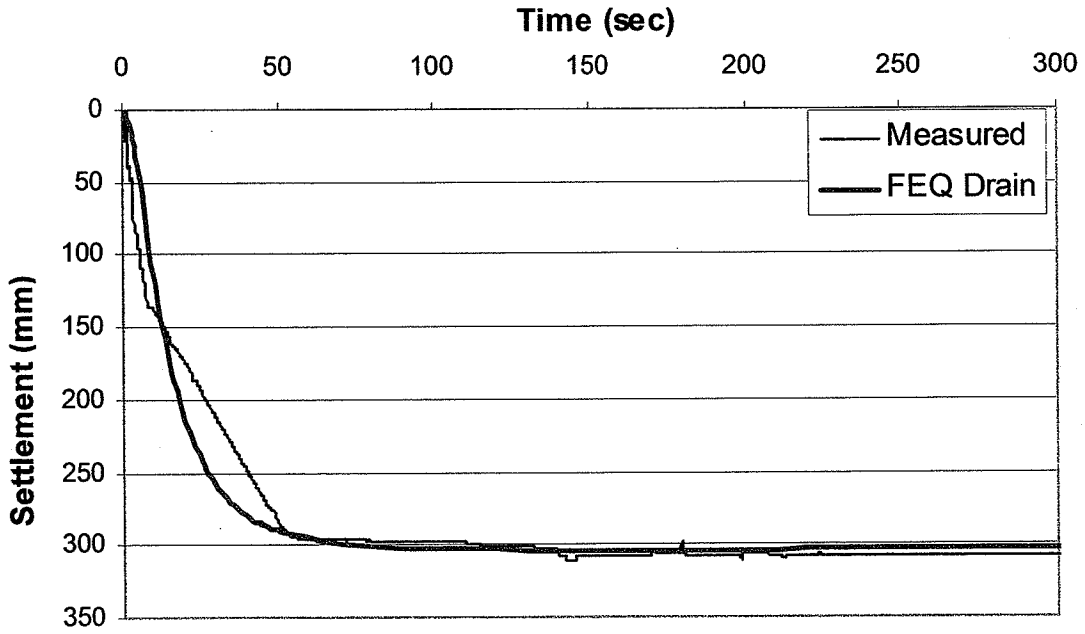

Figure 56 Comparison of measured and computed settlement versus time curves for EQ Drain Test Area 2 (High Vibration).

The excess pore pressure ratio (R_u) as a function of depth has been computed at a number of times for each EQD test area and the results are presented in Fig. 57. After 5 seconds, the entire zone from a depth of 3.5 to 12 m is liquefied and has an R_u ratio of 1.0. As time increases, the R_u values generally drop rapidly in the deeper sand layer, but remain relatively high near the top of the sand layer (around 3 m). This is likely due to upward flow of water in the sand which is restricted by the lower permeability silt layer located between 3 and 3.5 m. The R_u values in the zone from 0 to 3 m actually increase with time as the water eventually flows vertically through the silt layer and horizontally from the drains into the overlying partly saturated soil zones above the water table.

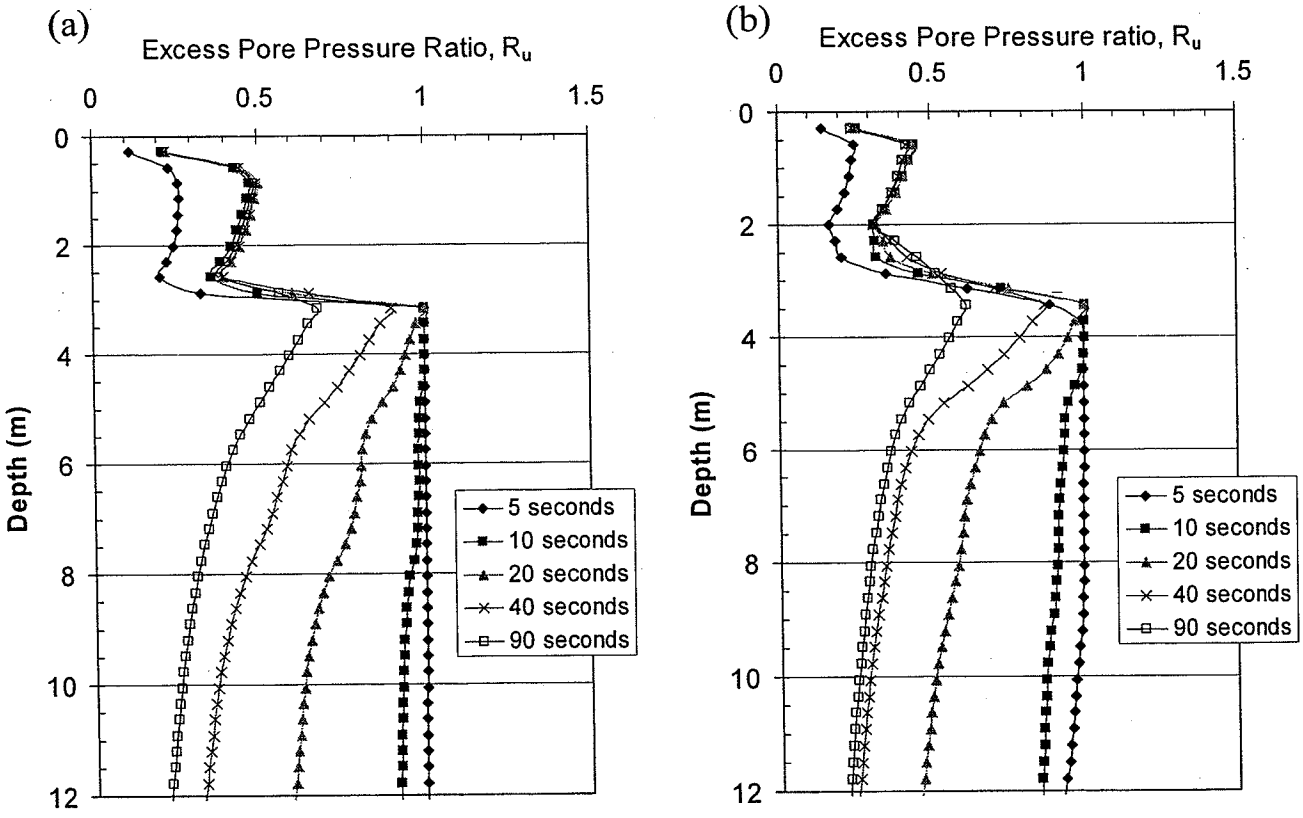

Figure 57 Pore pressure versus depth curves computed by FEQ Drain at various times for the test blasts at (a) EQD Test Area 1 (Low vibration) and (b) EQD Test Area 2 (High vibration).

6.2 EQ DRAIN PERFORMANCE IN SIMULATED EARTHQUAKE EVENTS

Once a reasonable match was obtained with the pore pressure and settlement response for the blast events using FEQDrain, earthquakes having less intense stress levels and slower load applications (longer durations) were simulated to measure the efficacy of the EQ Drains in preventing liquefaction.

6.2.1 Earthquake Input Parameters

Duration of Strong Motion

The duration of the strong ground motions (t_d) for various earthquake magnitudes used in the FEQDrain analyses were based on studies conducted by Seed et al (1975) and are summarized in Table 6. The duration is usually the time during which motions greater than a given minimum acceleration level (such as 0.05 g) are occurring. Although a M5.5 earthquake might have a duration similar to that produced by the test blasts, the duration of higher magnitude earthquake events are commonly two to eight times longer as shown in Table 6.

Table 6 Duration of earthquake strong motions (from Seed et al, 1975).

Magnitude	**Duration, t_d (sec)**
5.5-6.0	8
6.5	14
7.0	20
7.5	40
8	60

N_q/N_L Ratio

One measure of the severity of the motions imposed by an earthquake or blast event is the ratio of the number of equivalent stress cycles produced by the earthquake (N_q) to the number of cycles necessary to produce liquefaction (N_L). The more susceptible a site is to liquefaction, the higher the ratio will be. For a very loose sand or very strong ground motions, the ratio may be on the order of four or more, whereas for a denser sand or a weaker ground motion the ratio may be closer to one. For N_q/N_L ratios less than one, liquefaction would not be expected.

The N_q/N_L ratio is perhaps the most important factor controlling the ability of EQ Drains to mitigate liquefaction problems. For example, at low ratios, 75 to 100 mm diameter drains might be placed at spacings of 1 to 1.2 m to prevent liquefaction. At sites

with higher ratios, larger diameter drains and/or more closely spaced drains might be required in order to dissipate the water pressure quickly enough to prevent liquefaction. For very high ratios, the site may be too loose and liquefaction prone to treat with drainage techniques. In these cases, additional densification may be necessary to reduce the potential for liquefaction. In some cases the cost of densifying a very loose sand or a silty sand sufficiently to prevent liquefaction may be excessively high. In these cases, some cost savings might accrue by densifying with a moderate effort and then installing drains to prevent liquefaction.

Based on statistical studies conducted by Seed et al (1975), the N_q value can be correlated with the earthquake magnitude as summarized in Table 7.

Table 7 Equivalent number of cycles (N_q) produced by various magnitude earthquakes based on statistical studies by Seed et al (1975).

Magnitude	N_q
5.25	2
6	5
6.75	10
7.5	15
8.5	26

6.2.2 Calculated Response with EQ Drains Subjected to Earthquakes

In evaluating the response of the drains for various earthquake events, the duration and equivalent number of cycles for a given earthquake magnitude were selected. Computer runs were then made for various N_q/N_L ratios using FEQDrain.

Although the N_q/N_L is sufficient for use in the program, most liquefaction analyses typically use earthquake magnitude and peak ground acceleration (a_{max}) to quantify the severity of the ground motions. For a given N_q/N_L ratio, the a_{max} can be calculated using the following approach. First, for a given N_q/N_L ratio and earthquake magnitude, N_L can be determined. For example, in the case of a M7.5 earthquake with an N_q/N_L ratio of 2, N_q would be 15 and N_L would be 7.5. Based on an average $(N_1)_{60}$ of 10 in the clean sand layer at the test site, the cyclic resistance ratio (CRR) or liquefaction resistance for a M7.5 earthquake would be 0.105 using correlations recommended by Youd et al (2001). The CRR for 7.5 cycles would be significantly higher and can be computed using the Magnitude Scale Factor approach recommended by Youd et al

(2001). The recommended magnitude scaling factors have been plotted as a function of number of cycles in Fig. 58 based on the data in Table 7. Using Fig. 58, the MSF for 7.5 cycles would be about 1.55 and would increase the CRR to 0.163. If liquefaction occurred in 7.5 cycles, the CRR would be equal to the cyclic stress ratio (CSR) which is given by the equation

$$CSR = (\tau_{av}/\sigma'_o) = 0.65(a_{max}/g)(\sigma_{vo}/\sigma'_{vo})r_d \quad (5)$$

where a_{max} = peak horizontal acceleration at the ground surface generated by the earthquake; g = acceleration of gravity; σ_{vo} and σ'_{vo} are total and effective vertical overburden stresses, respectively; and r_d = stress reduction coefficient. Rearranging equation 5, a_{max} can be computed using the equation

$$a_{max} = CSR(\sigma'_{vo}/\sigma_{vo})(g/0.65)/r_d \quad (6)$$

Assuming liquefaction (CSR=0.163) at the top of the clean sand layer (6 m depth), with $r_d = 0.95$, and $\sigma'_{vo}/\sigma_{vo} = 0.70$ the computed a_{max} would be 0.19g.

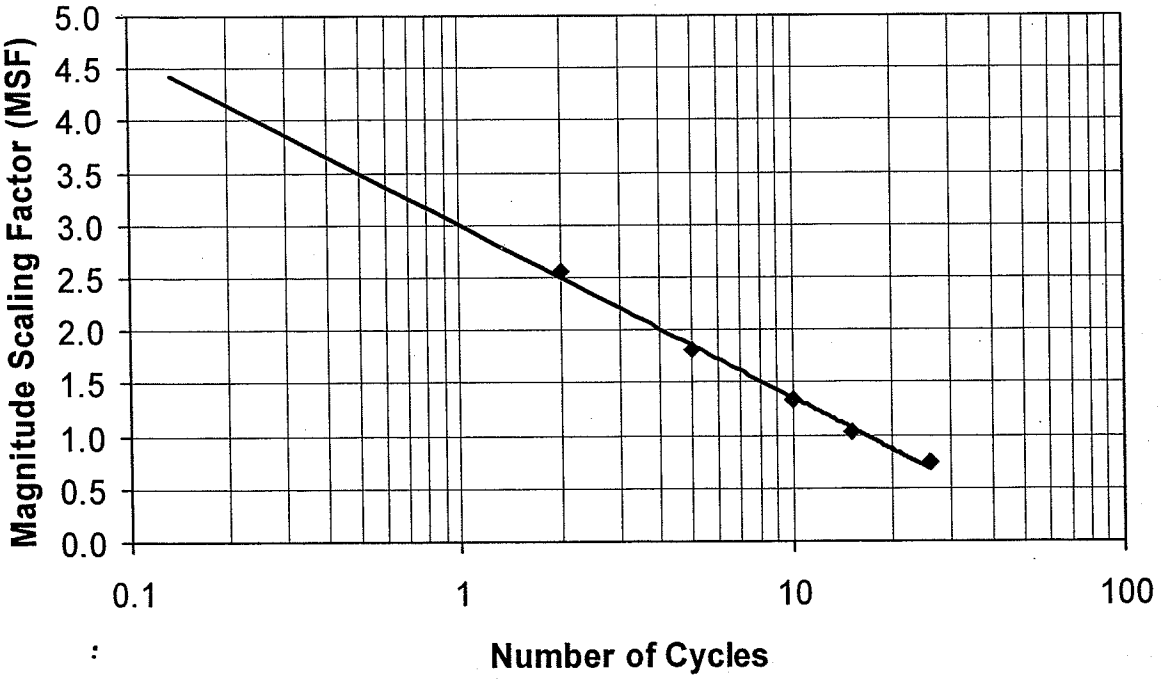

Figure 58 Magnitude scaling factor to account for variation in liquefaction resistance (CRR) relative to a M7.5 earthquake producing 15 stress cycles.

Using this procedure the a_{max} value has been computed for each M and N_q/N_L combination for which an FEQDrain analysis was performed.

With the soil properties back-calculated with the blast test data, FEQDrain was used to compute maximum Ru and settlement for a variety of potential earthquakes at the site and for a variety of drain configurations. Table 8 provides information on the magnitude, duration, N_q/N_L and, a_{max} values for each event along with the computed maximum pore pressure ratio and settlement for each event with drains spacing as indicated. The results summarized in Table 8 indicate that the EQ Drains can be effective in preventing liquefaction and the resulting settlement for significant earthquake events if drain diameter and drain spacing are appropriate selected. However, for large magnitude events with high N_q/N_L ratios, drains may be insufficient to prevent liquefaction from developing. As is the case with all mitigation measures, appropriate analysis and engineering expertise must be used in considering the use of EQ Drains

Table 8 Comparison of 10 cm drain performance for various earthquake events and drain spacings.

Magnitude	Duration (sec)	N_q/N_L	a_{max} (g)	Drain Spacing (m)	Maximum. R_u	Settlement (mm)
Blast	8	4.0	40	1.22	1.0	310
6.0	8	2.0	0.27	0.91	0.40	31
6.75	17	2.0	0.21	0.91	0.47	35
6.75	17	3.0	0.25	0.91	0.61	48
7.5	35	2.0	0.19	0.91	0.65	53

FEQDrain can provide significant insight in selecting appropriate drain features for a given soil profile and set of earthquake motions. For example, the effect of drain spacing on pore pressure and settlement can easily be analyzed. Figs. 59 and 60 show the variation in the computed R_u and settlement time histories, respectively, for various drain spacings due to a M6.75 earthquake event at the Vancouver test site. The results in Fig. 59 indicate that R_u decreases as the drain spacing decreases for a given magnitude earthquake and soil profile. The curves in Fig. 60 also indicate that settlement can be significantly reduced if drain spacing is small enough.

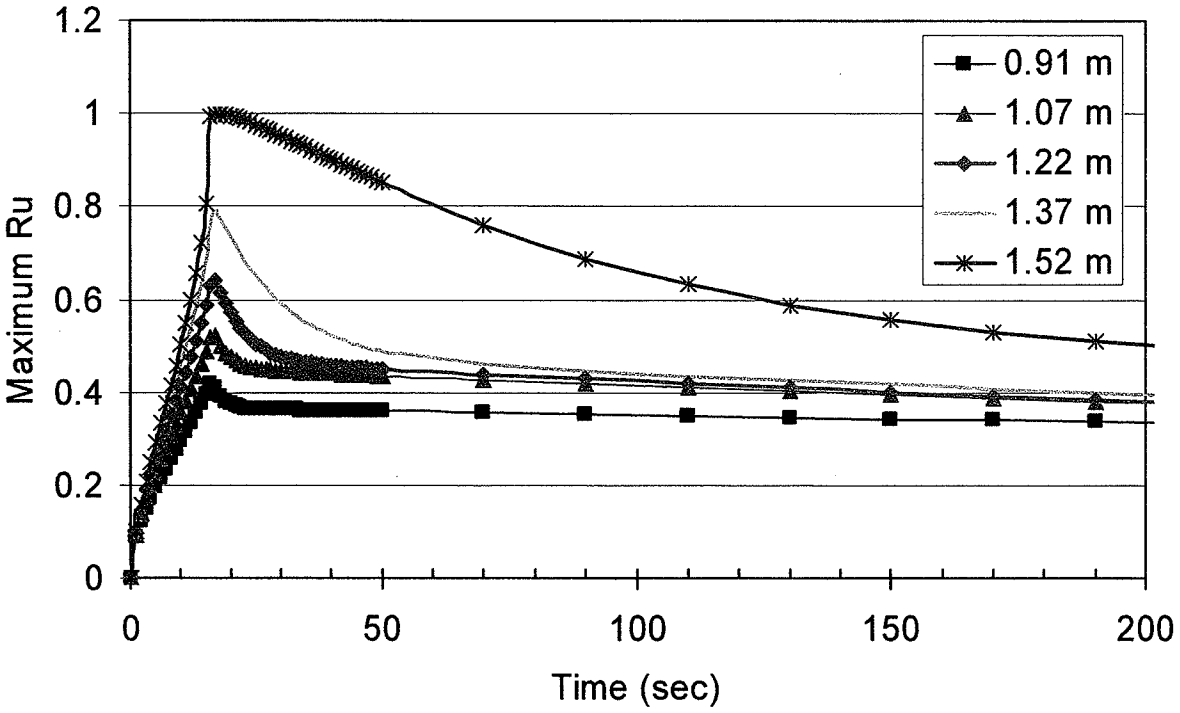

Figure 59 Maximum pore pressure versus time for various drain spacings computed by FEQ Drain for an M6.75 earthquake at the Vancouver test site.

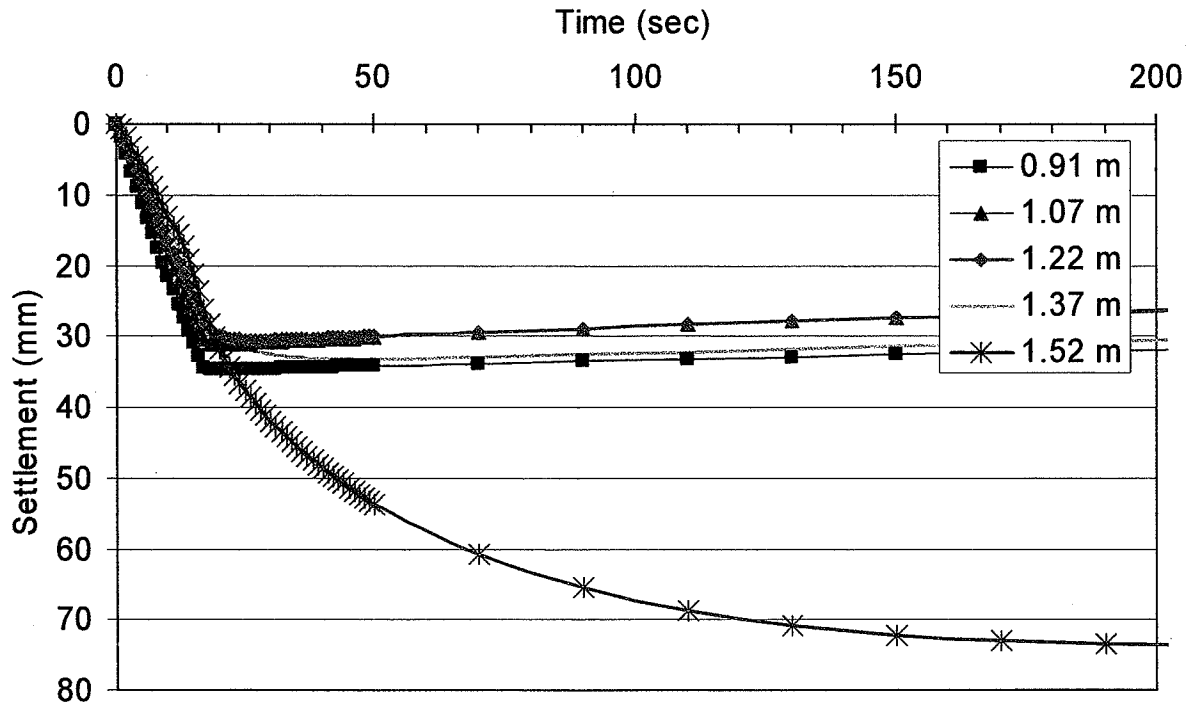

Figure 60 Settlement versus time curves for various drain spacings computed by FEQ Drain for a M6.75 earthquake at the Vancouver test site.

However, it appears that FEQ Drain may be limited in its ability to predict settlement for drain spacing less than 1.22 meters. Figure 60 shows a slight increase in settlement for drain spacing less than 1.22 m where intuition would say the settlement would decrease in a manner similar to that shown by the pore pressure. It is assumed that there is a computational error in the finite element program that occurs as the spacing becomes small.

7.0 ECONOMIC & CONSTRUCTION CONSIDERATIONS

7.1 COST CONSIDERATIONS

At present, a variety of methods are used to densify loose sand which may be susceptible to liquefaction; however, stone column treatment is perhaps the most common method and will serve as a benchmark for cost comparisons in this section. Stone column treatment typically involves the use of a vibratory mandrel to form a column with a diameter of 0.6 to 1 m in diameter composed of stone particles (≈20 mm diameter). Columns are typically installed in a triangular pattern in plan view with a center-to-center spacing ranging from 1.8 to 3 m. The cost of stone columns, including stone and installation cost, typically ranges from $82 to $115 per linear meter. Of course, these price estimates will vary depending on depth, spacing and quantity of columns.

The cost of EQ drains is roughly $6 to $12 per linear meter including the cost of the drains, the filter fabric and installation (Nilex, 2004; personal communication). Past experience with FEQDrain suggests that EQ drains must be spaced at about half the spacing of stone columns to provide an equivalent level of liquefaction protection. Based on this assumption, the cost per cubic meter would range from $10.2 to 14.3 for stone columns with a 3 m center-to-center spacing, while the cost per cubic meter for EQ drains would range from about $3 to $6 for a 1.5 m center-to-center spacing. Similarly, the cost per cubic meter would range from $15.9 to $22.3 for stone columns with a 2.44 m center-to-center spacing, while the cost per cubic meter for EQ drains would range from about $4.7 to $9.4 for a 1.22 m center-to-center spacing. Based on these comparisons, the EQ drains would be 30 to 40% of the cost of stone columns. Of course, these comparisons are based on price estimates and assumptions about required spacing which would

normally need to be validated with analyses. Nevertheless, they do suggest that significant cost savings could be achieved with earthquake drains.

The results of this testing program suggest that blasting in connection with drain installation could also provide a means of densifying loose sand to prevent liquefaction. Explosive compaction techniques have been employed at several sites in the past; however, general fears regarding explosives and concerns about vibration have often limited the use of this technique at many sites. Explosive compaction projects have generally employed larger charges and larger grid spacing than those in this study as well as multiple blasting passes. The cost for explosive compaction treatment on several recent Canadian projects has typically been about $3 to $3.5 per cubic meter of treated soil.

7.2 CONSTRUCTION TIME AND OTHER CONSIDERATIONS

Another important benefit provided by EQ drains is the reduction in time necessary for treatment. Assuming a liquefaction susceptible zone from 5 to 12 m thick, an EQ drain could be installed within 1 to 3 minutes per drain depending on depth and spacing. In contrast, treatment with stone columns would typically require 15 to 45 minutes per column depending on depth and spacing. For typical treatment spacing, this results in a reduction in treatment time of 50 to 75% when EQ drains are used.

Following treatment with stone columns or other densification methods, the improvement produced by the treatment is normally evaluated using some in-situ testing procedure such as the SPT or CPT test. Experience has shown that the penetration resistance obtained with these in-situ tests tends to increase with time after treatment; therefore, evaluation is normally performed a week or more after treatment. These test results must then be compared with minimum requirements in the specifications. If the treatment does not meet the minimum requirement, additional treatment and evaluation are normally required. This quality assurance procedure, while necessary, increases the construction time associated with densification methods. In contrast, the length of installed drain can be quickly measured during construction without any delay to the project. Although some densification will likely be achieved with the EQ drains, it is

generally unnecessary to evaluate this improvement. As a result, considerable time savings are provided by EQ drains when it comes to quality assurance issues.

The installation of stone columns generally requires considerably more truck traffic to haul the rock for the stone columns which may create more traffic and dust problems in and around the construction site. In addition, spoil material is often generated during the installation of stone columns. This may be as much as 1 to 3 cubic meters per column. This spoil is typically very soft soil, almost fluid, material mixed with rock. This spoil material must be stock-piled on site then either removed or spread out to dry prior to being used as fill material on-site. Although this cost does not normally show up in connection with stone columns it becomes a hidden cost that is borne by the general contractor or the earthwork subcontractor and increases the overall cost of the project. These problems are eliminated when EQ drains are employed.

8.0 CONCLUSIONS

1. Besides providing drainage, EQ Drains provide a side benefit of inducing significant settlement during installation. This leads to increased density and a lower compressibility which both reduce the amount of settlement and increase the rate of pore pressure dissipation relative to untreated sites. Installation using high vibration typically increased relative density by about 10 percentage points and produced volumetric strains of 2.5%.

2. Controlled blasting techniques have the potential for producing significant densification of liquefiable soils. Settlements of 2 to 4% of volume were produced for small charge masses and relative density was typically increase by 7 to 10 percentage points. Repeated blasting could, therefore, be used as an economically viable technique for liquefaction mitigation. However, vibration considerations might preclude its use at many sites.

3. The presence of earthquake drains significantly increased the rate of excess pore water pressure dissipation relative to untreated areas. Some of this increase can be attributed to

increased density but the increase was also observed when installation induced densification was not significant.

4. Settlement in areas where drains were installed using conventional procedures was reduced to only 60% of the settlement measured in untreated areas even though the drains did not prevent liquefaction for the high stress levels imposed by the blast tests.

5. Reasonable estimates of pore pressure dissipation rates and settlement can be obtained for the blast tests using FEQDrain. Further computer analyses, using soil properties calibrated with the blast test data, suggest that vertical drains can successfully limit pore pressure buildup and associated settlement for earthquake motions where the stress cycles are applied more slowly than during a blasting event.

9.0 REFERENCES

Andrus, R.D. and Stokoe, K.H., II (2000). "Liquefaction resistance of soils from shear-wave velocity." *J. Geotech. and Geoenvir. Engrg.,* ASCE, 126(11), 1015-1025.

Booker, J.R., Rahman, M.S. and Seed, H.B. (1976) "GADFLEA: A Computer Program for the Analysis of Pore Pressure Generation and Dissipation During Cyclic or Earthquake Loading" *Report No. EERC* 76-24, Univ. of California, Berkeley.

Boulanger, D.P., Hashish, Y. and Schmidt, B. (1997) Drainage Capacity of Stone Columns or Gravel Drains for Mitigating Liquefaction, *2nd Geotechnical Earthquake Engineering and Soil Dynamics Conference*, Seattle, Vol. I, 678-690.

Kulhawy, F. H. and Mayne, P. W. (1990) *Manual on Estimating Soil Properties for Foundation Design*, Electric Power Research Institute, Palo Alto, California, Research Report EERI EL-6800

EQE (1995) "The January 17, 1995 Kobe Earthquake" Summary Report, www.eqe.com/publications/kobe/economic.htm

Freeze, R.A. andCherry, J.A. (1979). Goundwater, Prentice-Hall, Inc., Englewood Cliffs, New Jersey.

Gohl, B. (2002). "Report on Gravel Drain Testing at South End of George Massey Tunnel", Prepared for Buckland & Taylor, Ltd. and British Columbia Ministry of Transportation, Pacific Geodynamics, Inc., Vancouver, BC, Canada

Goughnour, R.R. (2002). "Report on Earthquake Drain Testing at South End of George Massey Tunnel, Vancouver, B.C.", Prepared for Advanced Drainage Systems, Inc., Nilex, Inc., Denver, CO.

McCain, A.K. (2001). "Liquefaction Mitigation Through Composite Drainage", M.S. Thesis, Dept. of Civil & Environ. Engrg., Brigham Young Univ., Provo, UT, 248 p.

Monahan, P.A., Luternauers, J.L., and Barrie, J.V. (1995). "The geology of the CANLEX Phase II sites in Delta and Richmond, British Columbia" Procs, 48th Canadian Geotechnical Conference, Vancouver, 152-160.

Onoue, A. (1988), "Diagrams Considering Well Resistance for Designing Spacing Ratio of Gravel Drains," *Soils and Foundations*, Japanese Soc. of Soil Mechanics and Foundation Engineering, 28(No. 3), 160-168.

Pestana, J.M., Hunt, C.E. and Goughnour, R.R. (1997). "FEQDrain: A Finite Element Computer Program for the Analysis of the Earthquake Generation and Dissipation of Pore Water Pressure in Layered Sand Deposits with Vertical Drains," *Report No. EERC 97-17*, Earthquake Engineering Research Ctr., Univ. of Calif., Berkeley, CA

Robertson, P.K., Campanella, R.G., Gillespie, D., and Grieg, J. (1986). "Use of piezometer cone data". Procs., In-Situ '86, ASCE Specialty Conference, Blacksburg, VA, p. 1263-80.

Rollins, K.M., Ashford, S.A., Lane, J.D. and Hryciw, R.D. (2000) "Controlled Blasting to Simulate Liquefaction for Full-Scale Lateral Load Testing, Paper 1949, 12th World Conf. on Earthquake Engrg., New Zealand Soc. for Earthquake Engrg., 8 p.

Seed, H.B., Idriss, I.M., Makdisi, F., and Banerjee, J. (1975) "Representation of Irregular Stress Time Histories by Equivalent Uniform Stress Series in Liquefaction Analysis", *Report No. EERC 75-29,* Earthquake Engineering Research Ctr., Univ. of Calif., Berkeley, CA

Seed, H.B., Martin, P.P., and Lysmer, J. (1976). "Pore-Water Pressure Changes During Soil Liquefaction", *J. Geotech. Engrg. Div.,* ASCE, 102(GT4), pp. 323-346.

Seed, H.B., and Booker, J.R. (1977). "Stabilization of Potentially Liquefiable Sand Deposits Using Gravel Drains," *J. Geotech Engrg. Div.*, ASCE, 103(GT7), 757-768.

Terzaghi, K. and Peck, R.B. (1948). *Soil Mechanics in Engineering Practice*, John Wiley and Sons, New York.

Wride, C.E., Robertson, P.K., Biggar, K.W., Campanella, R.G., Hofmann, B.A., Hughes, J.M.G., Kuppper, A., and Woeller, D.J. (2000). "Interpretation of In-Situ Test Results from the CANLEX Sites", *Canadian Geotechnical Journal*, NRC, 37: 505-529.

Youd, T.L., Idriss, I.M., Andrus, R.D., Arango, I., Castro, G., Christian, J.T., Dobry, R., Finn, W.D.L., Harder, L.F., Hynes, M.E., Ishihara, K., Koester, J.P., Liao, S.S.C., Marcuson, W.F., Martin, G.R., Mitchell, J.K., Moriwaki, Y., Power, M.S., Robertson, P.K., Seed, R.B., and Stokoe, K.H. (2001). "Liquefaction Resistance of Soils: Summary Report from the 1996 NCEER and 1998 NCEER/NSF Workshops on Evaluation of Liquefaction Resistance of Soils, *J. Geotech. and Geoenvir.. Engrg.*, ASCE, 127(10), 817-833.

10.0 APPENDIX

Permeability Measurements.

In situ permeability tests were performed on one drain in each Earthquake Drain installation group. Both packer tests and pumping with draw down measurements were performed at drain BB in the group installed with compaction. Packer tests were performed at drain #2 in the group installed without compaction.

Packer Tests: Packer tests were performed in individual drains using equipment obtained from RST Instruments, LTD, consisting of a double Model PQ packer (see Figure A-1) and a flow meter/pressure gage assembly (see Figure A-2). A schematic representation of the packer test arrangement is shown in Figure A-3.

System head losses for the packer tests were determined by placing the outlet of the packer assembly at the same elevation as the pressure meter, and allowing water pumped through the assembly to exit freely from the system. For a flow of 1.534 cubic feet per minute, the pressure recorded was 11 psi, or 25.38 feet of water. System losses for other flow rates were assumed to be proportional to the flow rate (or velocity) squared.

Packer tests were performed by inserting the packer assembly into the test drain, taking care to place the central portion of the assembly at the desired level. The packers were then inflated to the manufacturer's recommended pressure by means of compressed nitrogen. GWT and H_m (Figure A-3) were carefully measured and recorded. Water was then pumped through the system. Flow rate was determined by measuring the time for a total water volume of 0.1 m^3 to flow through the system.

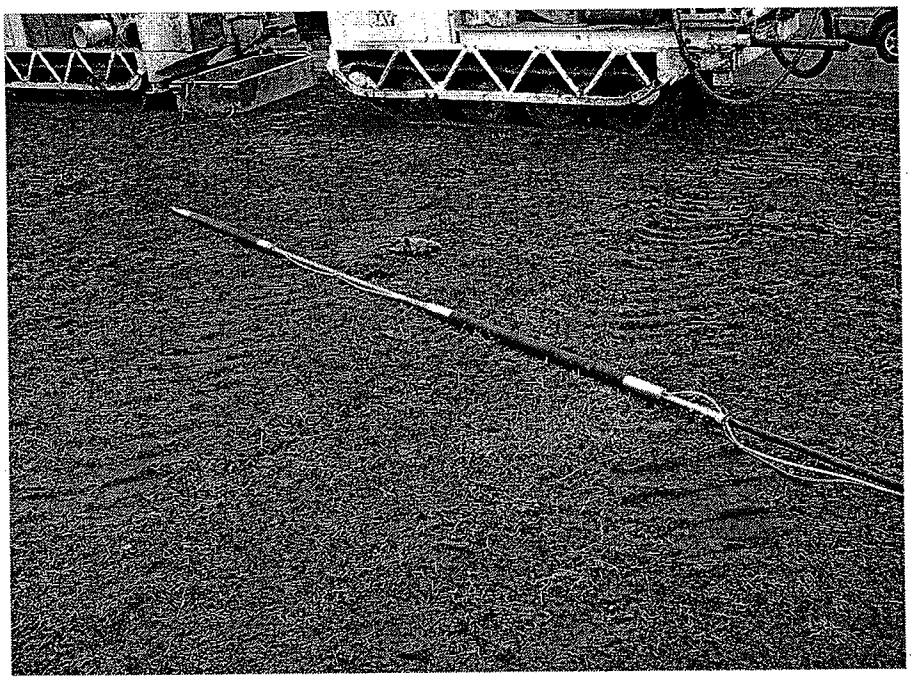

Figure A-1. Double Packer RST Model PQ.

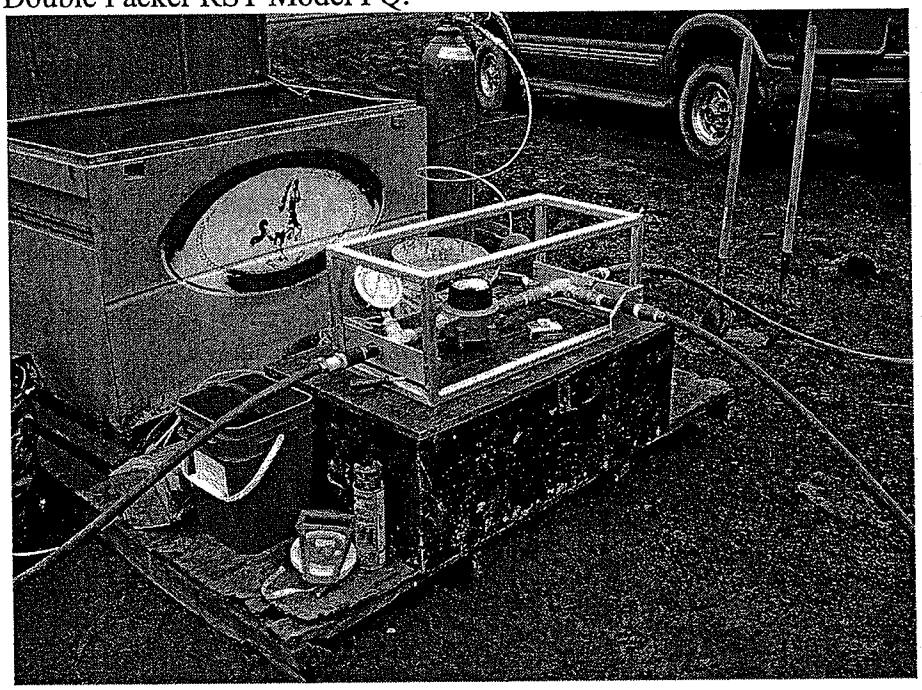

Figure A-2. Flow Meter and Pressure Gage for Permeability Test.

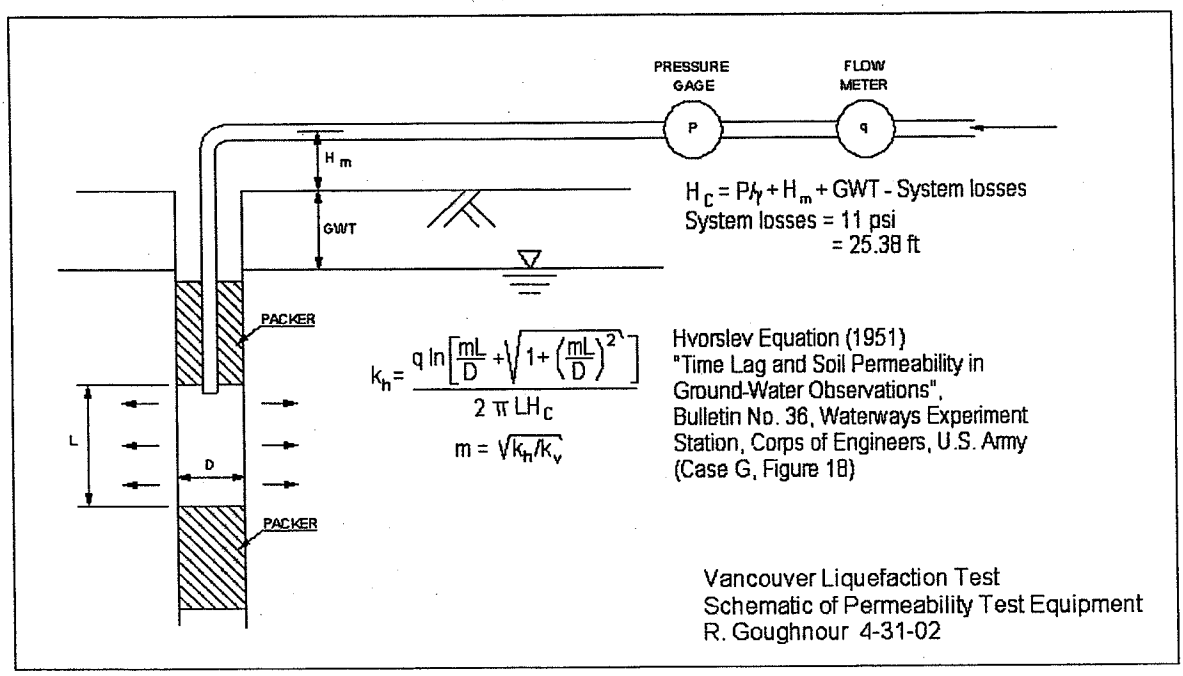

Figure A-3. Schematic Representation of Packer Test.

The pressure was read from a 4" dial meter with a range of 1 to 100 psi. Consequently readings could only be estimated to about 0.5 psi. The recorded pressure remained constant within these limits over the approximate 2 minutes required. Care was taken to keep water pressures within the ground below the effective overburden to prevent hydraulic fracturing of the soil.

There are two unknowns in the Hvorslev equation, k_h and m (or, k_h and k_v). The intention was to perform tests with two L-values and solve the equations simultaneously. Unfortunately, the equations are too ill-conditioned and actual measurements too variable for this scheme to work. However, k_h appears not to depend heavily on m, particularly for large L. The following calculations include a wide range of m-values. It appears that a value of $k_h/k_v = 1$ (m =1) produces the most consistent overall results.

Packer tests were performed in drain BB of the vibrated area with two different L-values; 6.26 ft and 2.167ft. A packer test was performed in drain #2 of the nonvibrated area with L = 6.26 feet only. Results follow:

PACKER TEST RESULTS:

Vibrated Area – Drain BB
3-24-02
$H_m = 36" = 3'$
GWT = 9.5'
L = 6.26'
D = 0.367'

Test Depth	Time for 0.1 m^3	q cfm	System loss psi	P psi	H_c ft
11'-17'	2.30 min	1.534	11	10	10.2
16'-22'	2.283	1.545	11.158	9.75	9.258
21'-27'	2.25	1.568	11.497	9.50	7.899
26'-32'	2.225	1.586	11.758	9	6.143
31'-37'	2.225	1.586	11.758	9	6.143

Solution to Hvorslev Eqn:
Permeability k_h in ft/min

	k_h/k_v					
	1	2	3	5	10	50
11'-17'	.0135	.0148	.0156	.0166	.0179	.0210
16'-22'	.0150	.0165	.0173	.0184	.0199	.0233
21'-27'	.0178	.0196	.0206	.0219	.0237	.0277
26'-32'	.0232	.0255	.0268	.0285	.0308	.0361
31'-37'	.0232	.0255	.0268	.0285	.0308	.0361

Vibrated Area – Drain BB
3-24-02
H_m = 36" = 3'
GWT = 9.5'
L = 2.167'
D = 0.367'

Test Depth	Time for 0.1 m^3	q cfm	System loss psi	P psi	H_c ft
14'-16'	2.30 min	1.534	11	10	10.2
19'-21'	2.317	1.523	10.84	10	10.57
24'-26'	2.292	1.540	11.080	9.5	8.86
29'-31'	2.25	1.568	11.493	9	6.76
34'-36'	2.267	1.557	11.328	9.5	8.29

Solution to Hvorslev Eqn:
Permeability k_h ft/min

	k_h/k_v					
	1	2	3	5	10	50
14'-16'	.0234	.0311	.0334	.0362	.0400	.0489

19'-21'	.0262	.0298	.0320	.0347	.0383	.0468
24'-26'	.0316	.0360	.0386	.0418	.0462	.0565
29'-31'	.0422	.0481	.0515	.0558	.0617	.0754
34'-36'	.0342	.0389	.0417	.0452	.0499	.0610

Drains Only (No vibration) – Drain #2
3-24-02
H_m = 15" = 1.25'
GWT = 10.25'
L = 6.26'
D = 0.367'

Test Depth	Time for 0.1 m^3	q cfm	System loss psi	P psi	H_c ft
11'-17'	2.367 min	1.491	10.392	8.25	6.55
16'-22'	2.500	1.412	9.313	10	13.08
21'-27'	2.383	1.481	10.250	8	6.30
26'-32'	2.350	1.502	10.540	7	3.32
31'-37'	2.250	1.568	11.498	7	1.11

Solution to Hvorslev Eqn:
Permeability k_h ft/min

			k_h/k_v			
	1	2	3	5	10	50
11'-17'	.0204	.0225	.0236	.0251	.0271	.0318
16'-22'	.0097	.0107	.0112	.0119	.0129	.0151
21'-27'	.0211	.0232	.0244	.0259	.0280	.0328
26'-32'	.0406	.0446	.0469	.0499	.0539	.0631
31'-37'	.1269	.1394	.1467	.1559	.1683	.1973

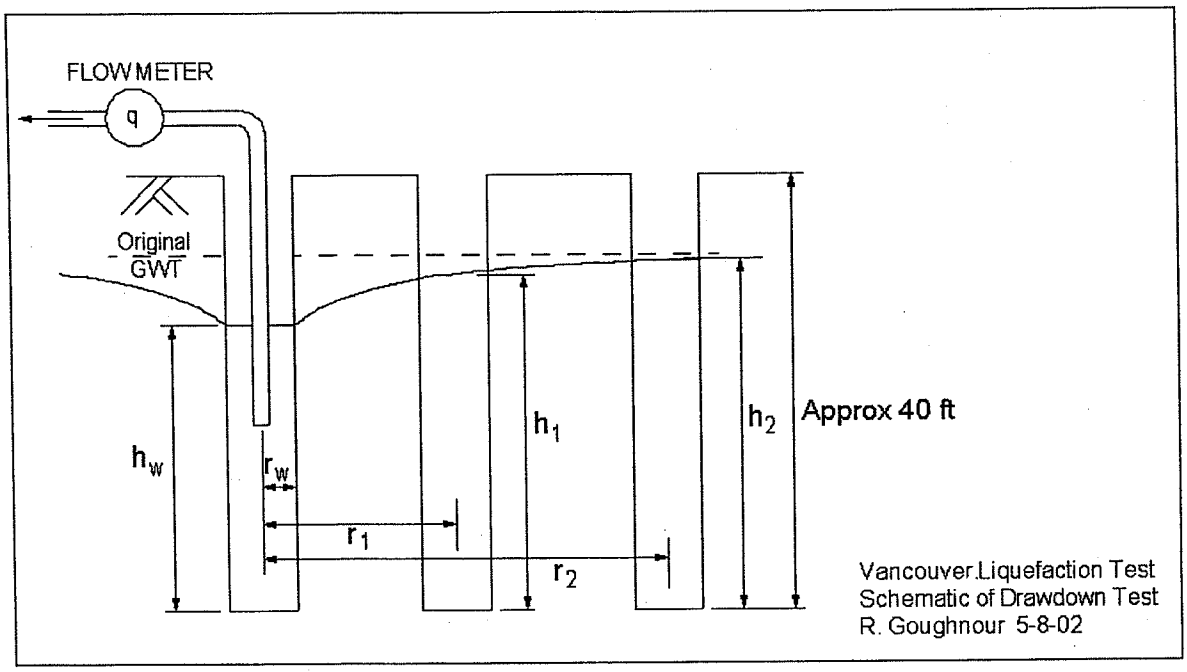

Figure A-4. Schematic of Draw Down Test at Drain #2 Uncompacted Drain Group.

Draw Down Tests

A draw down test was performed at drain BB of the drain group installed with compaction. This test, shown schematically in Figure A-4, was performed by pumping at a constant rate from the drain BB until equilibrium water levels were reached at drains BB, CC, and DD. Equilibrium appeared to be reached within 10 to 15 minutes.

Drawdown Test :

Water table initial 9.0 ft below ground
h_w = 28.5 ft
h_1 =30.0 ft
h_2 =30.42 ft
r_w = 0.1835 ft
r_1 = 4 ft
r_2 = 8 ft
Q at equilibrium = 1.568 ft^3/min
Pumped drain: BB of vibrated cluster
First drain: CC
Second drain: DD

Considering the drains to terminate at impermeable base:

$$k = \frac{Q}{\pi\left(h_1^2 - h_w^2\right)} \ln\left(\frac{r_1}{r_w}\right)$$

Well to 4 ft; k = 0.0175 ft/min
Well to 8 ft; k = 0.0167 ft/min
4 ft to 8 ft; k = 0.0137 ft/min

Considering Case F, Fig. 18 of Hvorslev with:

L = 30 ft
D = 0.367 ft
Q = 1.568 ft^3/min
H_c = 2.5 ft

m	k_h
1	.0170
2	.0204
3	.0211
5	.0219
10	.0231
50	.0258